PHAGE AT THE AIR – LIQUID INTERFACE FOR THE FABRICATION OF BIOSENSORS

Except where reference is made to the work of others, the work described in this dissertation is my own or was done in collaboration with my advisory committee. This dissertation does not include proprietary or classified information.

_____
Viswaprakash Nanduri

Certificate of Approval:

_____	_____
Valery A. Petrenko	Vitaly J. Vodyanoy, Chair
Professor	Professor
Department of Pathology	Anatomy, Physiology and Pharmacology
_____	_____
James M. Barbaree	Tatiana Samoylova
Professor	Research Assistant Professor
Biological Sciences	Scott Ritchey Research Centre

_____
Stephen L. McFarland
Dean
Graduate School

PHAGE AT THE AIR – LIQUID INTERFACE FOR THE FABRICATION OF BIOSENSORS

Viswaprakash Nanduri

A Dissertation

Submitted to

The Graduate Faculty of

Auburn University

In Partial Fulfillment of the

Requirements for the

Degree of

Doctor of Philosophy

Auburn, Alabama
December 16, 2005

PHAGE AT THE AIR – LIQUID INTERFACE FOR THE FABRICATION OF BIOSENSORS

Viswaprakash Nanduri

Permission is granted to Auburn University to ma ke copies of this dissertation at its discretion, upon request of individuals or institutions and at their expense. The author reserves all publication rights.

_____
Signature of Author

_____
Date of Graduation

VITA

Viswaprakash Nanduri, son of Shri Chinnam Raju Nanduri and Sheshamma Nanduri, was born on January 05, 1965. He attended University of Madras, India, and earned his Bachelor's Degree in Zoology in May, 1986. Viswaprakash earn ed his Masters in Marine Biology and Oceanography from the Centre of Advanced Study in Marine Biology and Oceanography, Annamalai University, India in May 1990. After working as a Fisheries Science teacher in the Republic of Maldives till December 1995, Viswaprakash migrated to New Zealand with his family. After working for one year as a teacher at De La Salle College, Mangere East, Auckland, he earned his diploma in Business Computing 1996 and was employed as a Manager and System Administrator for Visual Tech Systems till June 2001. Viswaprakash joined the Doctoral program in Biomedical Sciences, with an emphasis in Biophysics and Biosensor Research in the College of Veterinary Medicine, Auburn University in fall 2001.

Viswaprakash was born with 2 other siblings and has 2 older brothers, Aravind and Krishnanand Nanduri. Viswaprakash married Nilmini and has two sons, Ajitan and Ajay.

During his stay at Auburn University Viswaprakash was awarded the Presidential Scholarship 3 years in a row and also was awarded the Outstanding Graduate Student award for 2005.

DISSERTATION ABSTRACT

PHAGE AT THE AIR – LIQUID INTERFACE FOR THE FABRICATION OF BIOSENSORS

Viswaprakash Nanduri

Doctor of Philosophy, August 13, 2005
(M.S., Annamalai University, India, May 1990)
(B.S. University of Madras, India, May 1986)

144 Typed pages

Directed by Dr.Vitaly J. Vodyanoy

Food borne diseases cause an estimated 76 million illnesses, accounting for 325,000 hospitalizations and more than 5000 deaths in the United States each year. Currently, there are more than 250 known food borne diseases caused by different pathogenic microorganisms, including viruses, bacteria, fungi. Conventional methods of detecting pathogens entail a minimum of 24-48 hours of investigation, only after which results can be obtained. Apart from the urgent need of detection of food–borne pathogens, there is an even urgent need for the development of biosensors for the specific, sensitive and rapid detection of probable bio-terror agents. The general working principles of molecular recognition using thickness shear mode (TSM) sensors have been studied by employing different techniques such as formation of monolayer, and self assembled monolayers (SAM). But, the specific mechanisms of molecular interaction between the

probe-analyte that provides the sensitivity and specificity to the biosensor have not been thoroughly investigated.

As a part of a project for environmental monitoring of biothreat agents, this work was done to determine if filamentous phage could be used as a recognition molecule on a sensor. E.coli obtained from ß-galactosidase (ß-gal) was used as a model threat agent. Binding of ß–gal to the selected landscape phage was characterized by enzyme linked immunosorbent assay (ELISA), thickness shear mode (TSM) and a surface plasmon resonance (SPR-SPREETA ™) sensors and responses obtained were compared. The landscape phage was immobilized through physical adsorption. The characteristics of the gold surfaces of both the TSM and SPR sensors were investigated using an atomic force microscope (AFM). The orientation of phage on formvar, carbon coated copper grids was also studied using a transmission electron microscope (TEM).

Results obtained from 52 independent experiments showed a dose dependency in a range of 0.013 to 210 nM. The results of this work provided evidence that phage can be used as a recognition element on biosensors instead of antibodies and achieve detection in nanomolar ranges. Dose response curves indicated a stronger binding on a biosensor than that seen in ELISA. The sensitivity and specificity of phage peptide binding to an analyte envisages future applications of phage for the detection of bio-threat agents in bio-sensors. The sensitivity of both SPR and QCM sensor show similarities. The binding valences were 3.1 and 1.4 for the TSM and SPR sensor respectively. The apparent dissociation constants (K_d) are not significantly different It was observed that apparent K_d of the phage/ß-gal complex was 2.8 nM ± 1.1 (S.D.) in TSM quartz sensor. The affinity valences of 2.3 ± 0.8 (S.D.) were estimated. AFM studies were conducted using a *The*

SPM-100™ (Nanonics Imaging Ltd, Jerusalem Israel) NSOM & SPM System for studying the effect of the cleaning procedures used for both the TSM and SPR sensors. While the control set showed an R_q (average roughness) of 45.9 nm, the treated TSM samples showed an R_q of 31.2 nm. The values obtained from the SPR sensors on the other hand, showed a much smaller difference in R_q values.

Style manual used: Biosensors and Bioelectronics

Computer software used: Microsoft Word, Microsoft Excel, Microsoft Power Point, Microcal Origin 6.0, Adobe Photoshop, Macromedia Fireworks MX.

ACKNOWLEDGMENTS

First and foremost, I wish to thank my parents whose constant encouragement and belief in me coupled with the sacrifices they underwent to provide me with a sound education has enabled me to tread this of doctoral research. Thanks go to both my brothers for their presence through thick and thin. I owe my deepest gratitude to my wife Nilmini and my sons Ajitan and Ajay for their encouragement during my research years.

Much of my successful work would have never been possible without the persistent and gentle encouragement and guidance of Dr. Vitaly Vodyanoy. His simplicity of approach to research and the capacity to inspire the thirst for knowledge in his students make him a true mentor. I feel that I have been blessed for having been given an opportunity to work under his guidance. I wish to express my heartfelt thanks to Dr. Valery Petrenko, Dr. James Barbaree and Dr. Tatiana Samoylova for their endless support and guidance during my research. Special mention goes out to Dr. Valery Petrenko; Prof. Aleksandr Simonian for introducing me to optical biosensor research under his expert guidance. Special thanks go out to Dr. Alexander Samoylov for initial training, and assistance; Oleg Pustovyy, Dr Galina A Kouzmitcheva and Dr. Iryna B Sorokulova, Dr. Maria A. Toivio Kinnucan, Dr. Minseo Park and Dake Wang. Thanks to my in-laws, Mrs. Nagapooshany, Rajmanna and Thirumalini for their personal support during my research years. I dedicate this research to my parents, brothers, my wife and my sons.

TABLE OF CONTENTS

LIST OF FIGURES …….. xv

LIST OF TABLES …… xvii

1. INTRODUCTION ……. 1

1.1 Biosensor-definition and principles ……. 1

1.2 Bio-recognition layer…… 3

1.3 The physical transducer …… 4

1.3.1 Quartz Crystal Microbalance …… 4

1.3.2 Surface Plasmon Resonance …… 7

1.3.2a Overview of SPR based on Kretschmann geometry… 7

1.4 Atomic Force Microscopy…… 10

1.5 Transmission Electron Microscopy ……. 11

1.6 References …… 12

2 LITERATURE REVIEW ……... 15

2.1 Immunosensors …… 15

2.1.1 Antibodies ……. 15

2.2 Binding forces ……. 16

2.2.1. Kinetics of Binding ……. 17

2.2.2. Ligand Immobilization …….. 18

2.2.3. Mass Transfer …….. 18

2.3 Classical Sensor Platform …… 19

2.3.1 Electrochemical ……. 19

2.3.2 Piezoelectric Acoustic ……... 21

2.3.3 Evanescent wave optical sensing devices ……. 24

2.3.3.1 Surface Plasmon Resonance …….. 26

2.4 References ……..…….……. 28

3. OBJECTIVES AND CONTRIBUTIONS OF THIS STUDY TO THE EXISTING LITERATURE ……..……... 37

3.1 Validity of selected probe ß-galactosidase.…… 38

3.2 Physical micro/macro-environment-TSM sensor …… 38

3.3 Surface plasmon resonance sensor ……. 38

3.4 Compare binding studies using three platforms (ELISA, TSM, AND SPR)……. 38

3.5 Atomic force microscopy ……. 39

3.6 Transmission electron microscope ……... 39

4. OPTICAL PHAGE BIOSENSOR BASED ON SURFACE PLASMON RESONANCE SPECTROSCOPY…… 40

Abstract …….. 40

1. Introduction …… 40

2. Materials and Methods ……... 42

2.1 Phage ……... 42

2.2 *ß*-galactosidase …… 43

2.3 Solutions, reagents and tubing …… 43

2.4 Miniature two-channel SPR sensor.…….. 43

2.5 SPR sensor batch mode setup …….. 44

3. SPR sensor preparations …… 45

3.1 β-galactosidase binding measurements …… 45

3.1.1 Flow through mode ……... 46

3.1.2 Batch mode …… 46

3.2. Specificity of binding …….. 46

4. Results and discussion …… 47

4.1 Binding studies …… 47

4.2 Phage deposition and surface coverage …….. 48

4.3 Specificity of Binding ……. 50

5 Conclusions ……. 50

6 Acknowledgments …….. 51

7 References 65

5. PHAGE AS A MOLECULAR RECOGNITION ELEMENT IN BIOSENSORS IMMOBILIZED BY PHYSICAL ADSORPTION……... 69

Abstract ……..……. 69

1. Introduction …… 70

2. Materials and Methods ……... 71

2.1 Phage …… 71

2.2 ß-galactosidase …… 72

2.3 Solutions, reagents ……... 72

2.4 Phage Sensor preparation …… 72

2.5 ß-galactosidase binding measurements …… 73

2.5.1 Acoustic wave device……. 73

2.5.2 Binding measurements ……... 73

2.5.3 Specificity of binding …… 74

2.6 Enzyme Linked Immunosorbent Assay (ELISA) with ß-galactosidase ……... 74

2.7 Binding Equations……. 75

3. Results and Discussion ……... 78

3.1 Specificity and selectivity of ß-galactosidase binding …… 78

4. References……... 85

6. COMPARATIVE PHAGE BASED BIOSENSOR RESPONSES FROM ELISA, THICKNESS SHEAR MODE SENSOR AND A SURFACE PLASMON RESONACE SPREETA™ SENSOR 89

Abstract …….. 89

1. Introduction …… 90

2. Materials and Methods ……... 91

2.1 Phage……. 91

2.2 ß-galactosidase……... 92

2.3 Materials ……..... 92

2.3a ELISA, TSM and SPR sensor……. 92

2.3b Atomic force microscopy …… 93

2.3c Transmission electron microscopy ……. 93

3. Phage immobilization on sensors…… 93

3.1 TSM sensor preparation ……... 93

3.2 SPR sensor preparation ……. 94

4. ß-galactosidase binding measurements …….. 94
4.1 Enzyme-linked immunosorbent assay (ELISA)…… 94
4.2 Acoustic wave device……..…….. 95
4.2.1 Binding measurements ……... 95
4.3 Surface plasmon resonance (SPREETA™) sensor.……... 96
4.3.1 SPR binding measurements…… 96
4.4 Atomic force microscopy……. 96
4.4.1 AFM Imaging…… 96
4.4.2 Surface roughness calculation ……... 97
4.4.3 Preparations of samples for AFM imaging ……... 97
4.5 Transmission electron microscopy…… 97
4.5.1 Negative staining …….. 97
4.5.2 Phage loading procedures ……. 98
5. Results and discussion……..…….. 98
5.1 ELISA and TSM sensor ……..…….. 98
5.2 SPR and TSM sensor.……..……... 99
5.3 Atomic force microscopy ……. 99
5.4 Transmission electron microscopy …….. 100
6. Conclusions.……..…….……... 101
7. References……..…….. 119
7. CONCLUSIONS……..…… 123

LIST OF FIGURES

1.1	Working principle of a biosensor……..	2
1.2	Schematic representation of the various components of the phage used in this study……..……..	4
1.3	Piezoelectricity……..…….	5
1.4	A TSM sensor setup on an anti vibration chamber……...	6
1.5	Surface Plasmon Resonance-Principle…….	7
1.6	Surface Plasmon Resonance-angle shift……...	8
1.7	Schematic of the miniature SPREETA™ sensor……...	9
1.8	Scanner head of the Atomic Force Microscope……	10
4.1	Schematic of the flow through mode setup ……..	52
4.2	The batch mode setup……..……..	53
4.3.A.a	A full range dose response curve for a SPR sensor……..	54
4.3.A.b	Hill plots of binding isotherms from SPR sensors……	55
4.3.B.a	A low range dose response curve.……	56
4.3.B.b	Hill plots of binding isotherms from SPR sensors……	57
4.3.C.a	A high range dose response curve.……...	58
4.3.C.b	Hill plots of binding isotherms from SPR sensors……	59
4.4	Graph shows a typical example of addition of 1G40 phage……..	60
4.5 A	A full range dose response curve……..	61
4.5 B	Hill plots of binding from SPR sensors……	62

4.6	Typical binding mean responses from SPR sensors……	63
4.7	Specificity of phage using SPR sensor…….	64
5.1	Dose Dependent binding of ß-galactosidase to the phage……	81
5.2A	Dose dependency binding of ß-galactosidase to TSM sensor and ELISA...	82
5.2B	Hill Plots from binding isotherms of a TSM sensor and ELISA……..	83
5.3	Specificity of ß-galactosidase binding in TSM sensor…….	84
6.1	Dose responses from ELISA and TSM sensor…….	102
6.2	Hill plots of binding isotherms for ELISA and TSM sensor……	103
6.3	Dose responses from SPR and TSM sensors……	104
6.4	Hill plots of binding isotherms for SPR and TSM sensors……..	105
6.5a(I)	Surface Topography of a TSM sensor surface before cleaning……	106
6.5a(II)	Three dimensional features of a TSM sensor surface before cleaning…….	107
6.5b(I)	Surface Topography of a TSM sensor surface after cleaning……...	108
6.5b(II)	Three dimensional features of a TSM sensor surface after cleaning……	109
6.6a(I)	Surface Topography of a SPR sensor surface before cleaning…….	110
6.6a(II)	Three dimensional features of a SPR sensor surface before cleaning……..	111
6.6b(I)	Surface Topography of a SPR sensor surface after cleaning……	112
6.6b(II)	Three dimensional features of a SPR sensor surface after cleaning……	113
6.7a	TEM image of phage on formvar, carbon coated grid……..	115
6.7b	TEM image of phage on formvar, without using a wetting agent……	116
6.8	TEM image of phage on gold gilded grids, without using a wetting agent..	117
6.9	TEM image of phage diluted in Millipore water……..	118

LIST OF TABLES

6 T. 1 Mean surface roughness of sensor surface samples…….. 114

6 T.2 Comparative EC_{50} and effective K_d values of an SPR and a TSM sensor… 114

1. INTRODUCTION

1.1 Biosensors -definition and principles

A biosensor is a device that integrates a biological sensing element with a physical transducer to provide us a signal for a specific target analyte. Biosensors are nowadays used in a wide range of fields from the detection of pollutants in the environment to the detection of pathogens in the food industry. More recently, the use of biosensors for the detection of bio-terrorist agents has seen an increased wave of research in this field. Classifications of biosensors are based upon either the type of biomolecules employed or on the type of physical transducer that is coupled with the biological element. Biomolecules ranging from enzymes, antibodies, receptors, tissues, whole cells, DNA and phage have been employed. Further classification of biosensors is based upon the type of action that is involved viz., biocatalytic sensors use enzymes, microorganisms, and tissue elements that are involved in the catalytic activity of a specific biological reaction; and bioaffinity sensors that revolve on molecular recognition by antibodies, receptors, binding proteins and phage. Biosensors are also classified based upon the physical transducer that is involved such as acoustic wave sensors (Quartz crystal microbalance/ Thickness Shear Mode (TSM), surface acoustic wave device) and optical sensors (surface plasmon resonance, fibreoptic and waveguides). A successful biosensor is one which fulfills high selectivity and sensitivity. Selectivity of the sensor is a function

of the sensing element and its ability to interact with its target analyte. Efficient detection of the interaction between the sensing element and the target analyte results in a highly

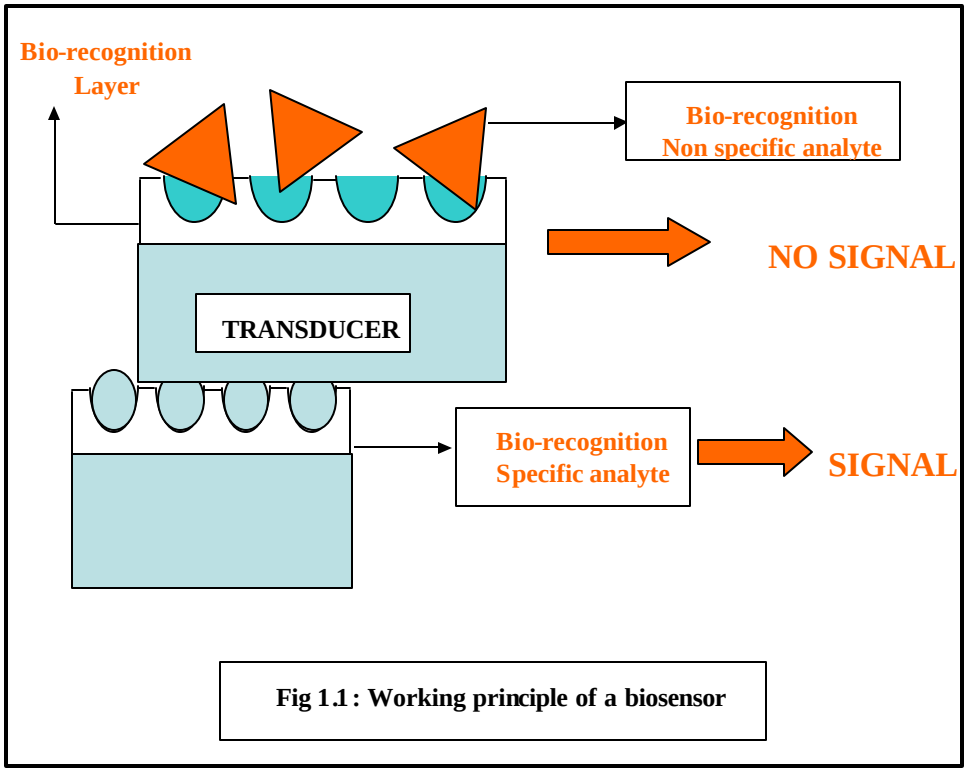

Fig 1.1 : Working principle of a biosensor

sensitive biosensor. High specificity of a biosensor is defined by the degree of interaction between the sensing element and the target analyte, even in the presence of interferents. Many biosensors directly detect the presence of the target analyte doing away with the cumbersome process of addition of different reagents and thus adding cost and time to the detection process. The prevalent use of biosensors for the detection of bacteria[1-5], African swine virus[6] and even screening of phage libraries[7] has proved the versatility of biosensors in a wide arena of detection . Diagnostic kits for the detection of small

amounts of drugs are assisting both doctors and law enforcement officers in assessing drug abuse.

1.2 Bio-recognition layer

For the development of an ideal biosensor, it is essential that both the essential components of the biosensor, the bio-recognition layer and the physical transducer be selected appropriately. In this study, we use filamentous phage as the bio-recognition layer. Phages are viruses that infect bacterial cells. Many phages are vectors used in recombinant DNA research and the standard recombinant DNA host is E. coli. Filamentous phage M13, f1 and fd are thread-shaped bacterial viruses. By inserting random peptides into their major coat protein (PVIII), a landscape library with billions of variations on the outer coat peptides is constructed. The library has been exploited for selection of phage that binds to the target analyte, ß-galactosidase (ß-gal). Fig 1.2 shows a schematic of both the wild type (no modification to the outer coat) filamentous phage and a modified phage. The various major and minor coat proteins are shown. The phages selected in this study are flexible rods about 1.3µm long and 10nm in diameter and composed mainly of a tube of helically arranged molecules of the major coat protein pVIII. There is a single-stranded viral DNA inside the tube. Five copies each of the 4 minor coat proteins-pIII, pVI, pVII, pIX close off the ends of the sheath.

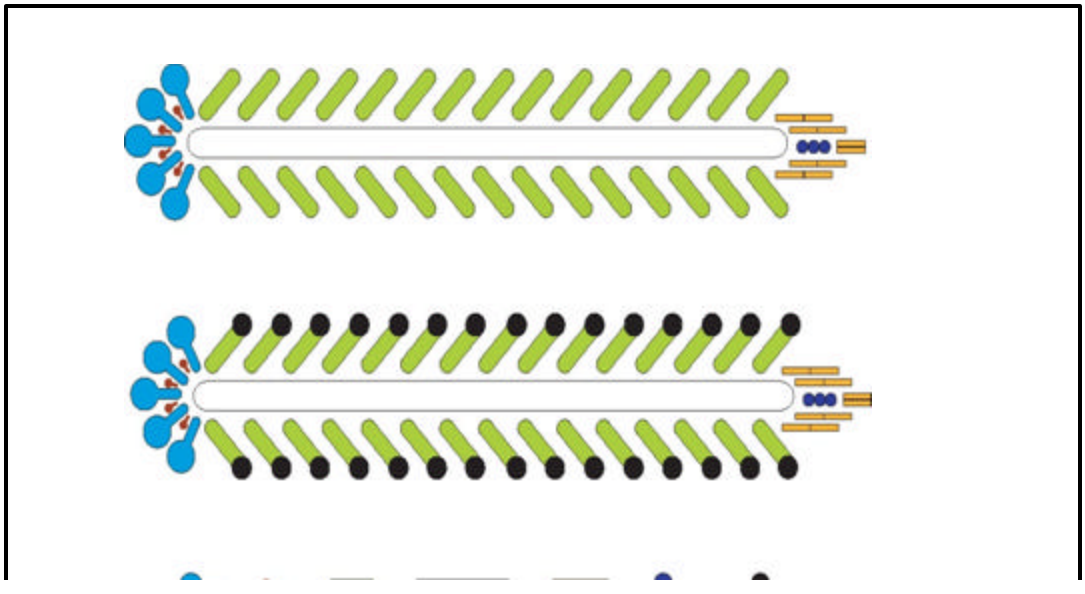

Fig1.2: Schematic representation of the various components of the phage used in this study

1.3 The physical transducer

1.3.1 Quartz Crystal Microbalance/Thickness Shear Mode (TSM) sensor

The direct piezoelectric effect was discovered by the Curie brothers in 1880. When a weight was placed on a quartz crystal, charges appeared on the surface of the crystal that was proportional to the weight. When a voltage is applied to the crystal, deformation occurs due to lattice strains. This is reverse piezoelectricity and this effect was demonstrated in 1881. Piezoelectric crystals lack a center of symmetry. When a force deforms the lattice, the centers of gravity of the positive and negative charges in the crystal can be separated so as to produce surface charges. When a crystal has a center of

symmetry, i.e., when the properties of the crystal are the same in both directions along any line in the crystal, no p iezoelectric effect can occur.

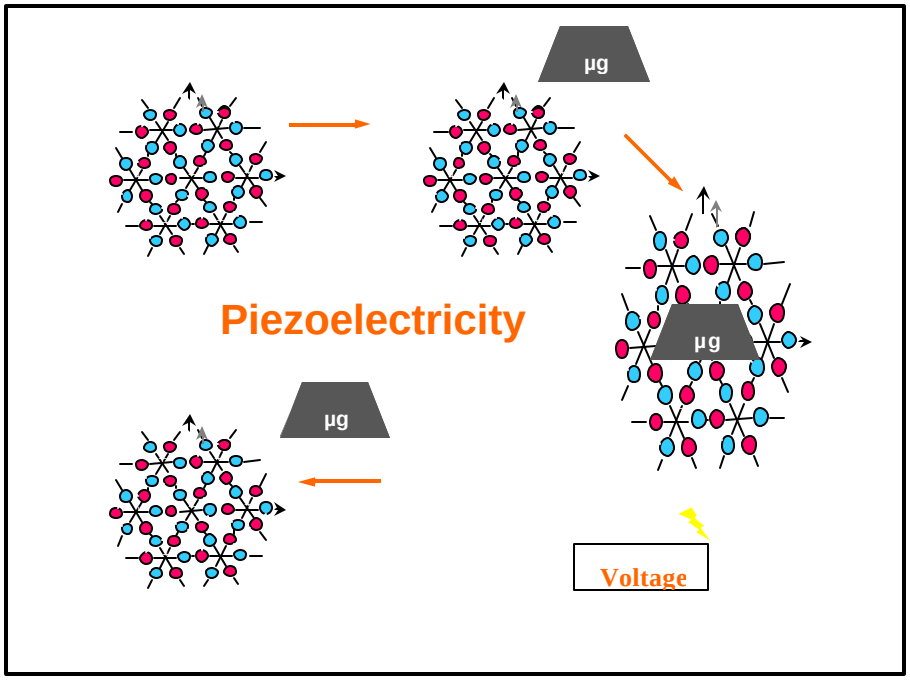

Fig 1.3: ***Piezoelectricity*** The figure shows one example of the effect in quartz. Each silicon atom is represented by the blue spheres, and each oxygen atom by the red spheres. When a strain is applied so as to elongate the crystal along the Y-axis, there are net movements of negative charges to the left and positive charges to the right (along the X-axis). *(**Adapted from**: R. A. Heising; Quartz Crystals for Electrical Circuits - Their Design and Manufacture, D. Van Nostrand Co., New York, pp. 16-20. 1946.)*

The quartz crystal microbalance (QCM) also popularly called the thickness shear mode (TSM) sensoruses reverse piezoelectricity viz., when voltage is applied to the quartz substrate, it induces motion in thickness-shear mode. When mass on the crystal is

increased, due to binding of the probe to the analyte of interest, there is a decrease in frequency which is corresponds to an increase in output voltage. The TSM sensor's characteristics of being small; rugged and entailing low costs offer significant advantages over other detection technologies. When TSM sensors are used with antibodies specific for the antigen under study, their sensitivity compares with techniques such as ELISA[8, 9] and the use of TSM sensors for the detection of different pathogens have been well documented [10].

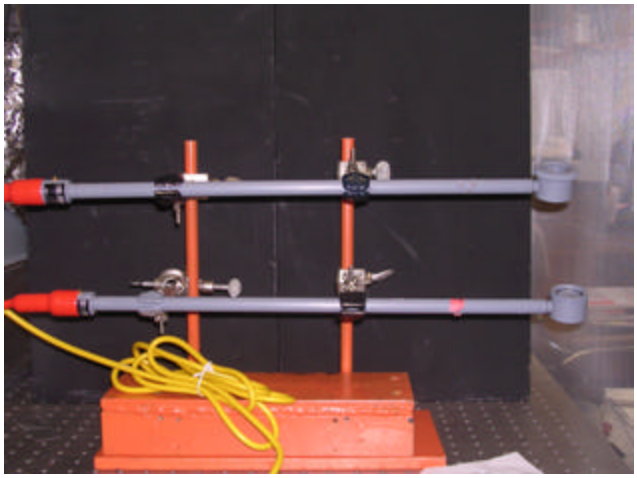

Fig 1.4: A TSM sensor setup on an anti vibration platform.

1.3.2 Surface Plasmon Resonance

Surface Plasmon Resonance (SPR) has become a well established tool for the characterization of biorecognition. Rapid, real time monitoring of the association and dissociation processes without the added chore of complex preparation of the sample is

possible using the SPR technique. Recent years have seen the use of SPR for the detection and characterization of various molecular reactions. Through this platform, the sample to be investigated can be studied without any labeling; provide continuous real time monitoring; regeneration of the sensor's surface using low pH wash and can be used for the detection of both chemical and biological warfare agents [11].

1.3.2a Overview of SPR based on Kretschmann geometry

Surface plasmon resonance (SPR) is a phenomenon that occurs at metal surfaces (usually gold or silver) when an incident p-polarized light beam strikes the surface at a particular angle, greater than the total internal reflection (TIR) angle.

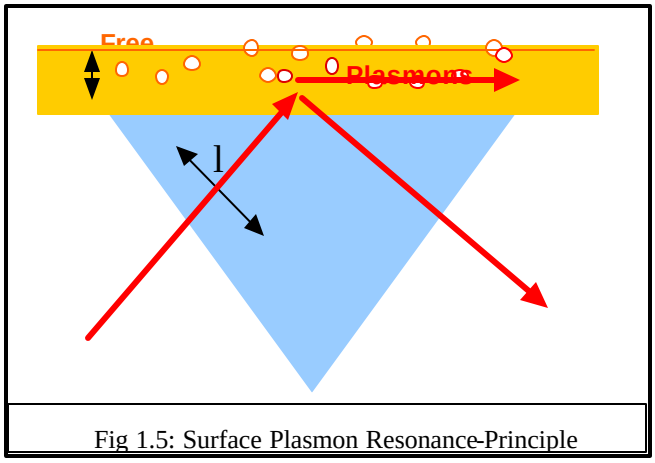

Fig 1.5: Surface Plasmon Resonance-Principle

In our experiments, we use the *Kretschmann* geometry, where the metal (gold) surface is exposed to light transmitted via a transparent prism. As molecules bind to immobilized targets on the gold surface, the optical properties of the medium closest to the surface change (fig 1.6 a). This causes a proportionate shift in the SPR angle, (fig 1.6 b) which provides a quantitative measurement of the amount of mass binding. This in turn, can be used to determine a bio-molecular interaction in real time. In our experiments we used

SPREETA™ sensors produced by Texas Instruments. This inexpensive dual channel, miniature sensors are very suitable for fundamental investigations.

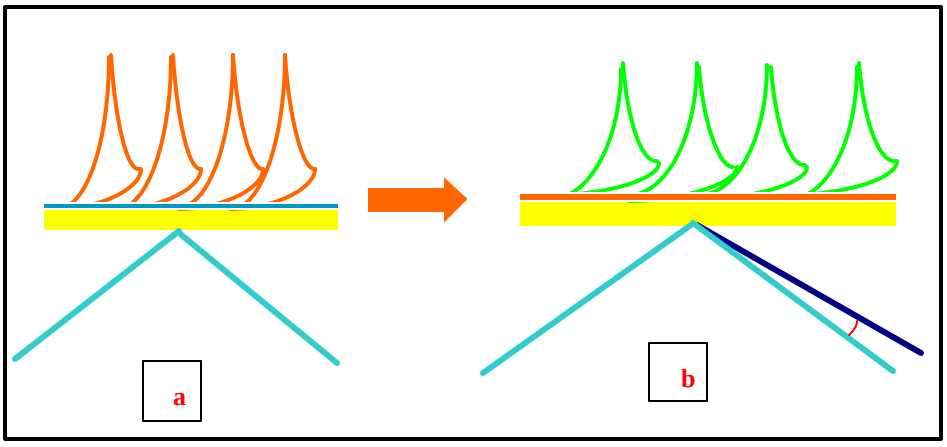

Fig 1.6: Surface Plasmon Resonance-angle shift

The **SPREETA**™ is a highly integrated SPR sensor that uses the *Kretschmann* geometry and detects binding at the gold surface using the principle of angle interrogation. Fig1.7 depicts a schematic of the typical components of the device. **SPREETA**™ mainly consists of light emitting diode, polarizer, temperature sensor, 2 photodiode arrays, reflecting mirror and an optical plastic substrate. An AlGaAs light emitting diode (LED) with a wavelength of 830nm is enclosed within an absorbing apertured box[12] . The LED light, after passing through a polarizer illuminates the gold coated glass slide with a wide range of angles.

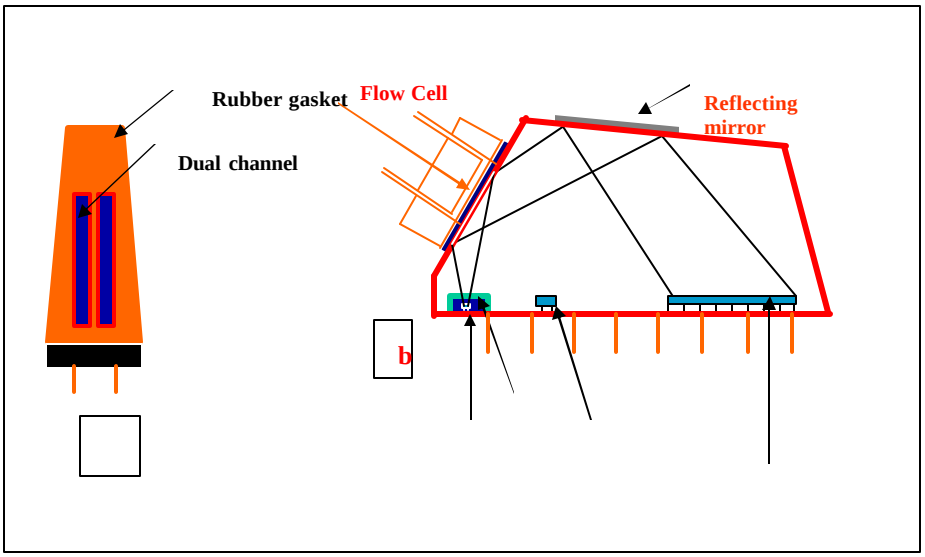

Fig 1.7: Schematic of the miniature SPREETA™ sensor. 1.7 a shows the frontal view of the two channels, showing the gasket that makes it possible. 1.7 b shows the various components of the sensor and the detachable flow cell.

The polarizer filters and helps in the emission of only the transverse magnetic (TM) component as the transverse electric component cannot produce surface plasmon oscillations. The glass slide is positioned to get an appropriate SPR signal. The light from the gold surface strikes the mirror on top of the sensor and reaches the photodiode arrays. Protective encapsulation of all the components is provided by the optical substrate[12]. Moreover, this encapsulation also does away with the chore of optical alignment[13].

1.4 Atomic Force Microscope

AFM studies were conducted using a *The SPM-100*™ (Nanonics Imaging Ltd, Jerusalem Israel) NSOM & SPM System. The system essentially consists of

a) The NSOM/AFM 100™ scan head which contains (i) a 9 pin outlet controlling the stepper motor that enables the scanning;(ii) a 15 pin outlet to a position sensitive detector and laser (iii) and lastly a 9 pin outlet that is connected to the scanner controller. **(fig. 1.8)**

b) The Topaz controller which controls the scan and feedback mechanism.

c) The DT box which interfaces the computer to the controller through a 50 pin flat band cable

d) A NSOM Topaz interface box that interfaces the controller to the scan head.

e) And a personal computer with Quartz and data translation software that aids in data acquisition and image processing. Fig 1.8 shows the scan head with the different components

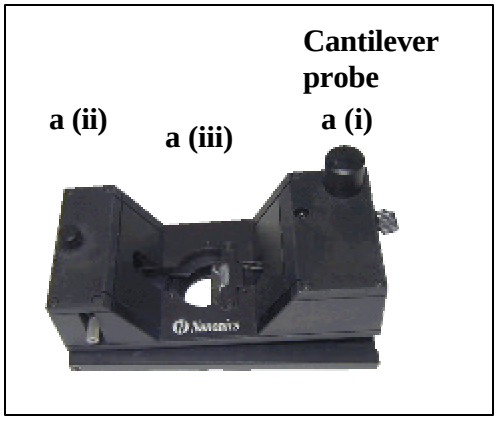

Fig 1.8: The scanner head of the AFM with the different components

The system uses a piezoelectric flat scanner (thickness 7 mm) with a scan range of 70 µm Z-range and 70 µm XY-range. Fiberglass cantilevered probes of 20 nm tips size were used for all our experiments, which were conducted at room temperature. The average surface roughness, R_q of the samples was calculated using the Quartz software (provided by the manufacturer) and is derived from the equation

$$Rq = \sqrt{\frac{1}{N\Sigma(Z_n - Z)^{-2}}}$$

Where N is the number of points in the defined area; z_n, is the z values within the scanned area and z, the current z value.

1.5 Transmission Electron Microscope

Transmission electron microscopy studies were carried out using the Philips 301 Transmission Electron Microscope (TEM) [FEI Company Hillsboro, Oregon]. This study was conducted as a prelude to understanding the orientation of phage. Formvar carbon coated /copper grids/formvar carbon gold guilder grids were incubated on 20 µl drops of 3.18×10^{11} vir/mL of phage solution for 20 minutes, membrane side down. The grids were then rinsed in a drop of 2% PTA so as to aid in the removal of excess non-adhered material and then placed in a second drop of the same stain preparation for 2 minutes. The grids were dried before examination under a Philips 301 TEM at 60 Kv. Representative fields were photographed at an original magnification of 71,000, magnified 2.75 times giving us a final magnification of 195,250.

1.6 References:

1. Carter, R.M., Mekalanos, J.J., Jacobs, M.B., Lubrano, G.J. & Guilbault, G.G., *Quartz crystal microbalance detection of Vibrio cholerae O139 serotype*. Journal of Immunological Methods, 1995. **187**: p. 121-125.
2. Pathirana, S. T.,Barbaree, J.,Chin, B. A.,Hartell, M. G.,Neely, W. C.,Vodyanoy, V. *Rapid and sensitive biosensor for Salmonella*. Biosensors and Bioelectronics, 2000. **15**(3-4): p. 135-141.
3. He, Fengjiao.,Zhang, Liude.,Zhao, Jianwen.,Hu, Biaolong.,Lei, Jingtian., *A TSM immunosensor for detection of M. tuberculosis with a new membrane material*. Sensors and Actuators B: Chemical, 2002. **85**(3): p. 284-290.
4. Naimushin., Alexei N.Soelberg., Scott D.Nguyen., Di K.Dunlap., Lucinda Bartholomew., Dwight Elkind., Jerry Melendez., Jose and Furlong, Clement E. *Detection of Staphylococcus aureus enterotoxin B at femtomolar levels with a miniature integrated two-channel surface plasmon resonance (SPR) sensor*. Biosensors and Bioelectronics, 2002. **17**(6-7): p. 573-584.
5. Olsen, E. V.,Pathirana, S. T.,Samoylov, A. M.,Barbaree, J. M.,Chin, B. A.,Neely, W. C.,Vodyanoy, V. et al., *Specific and selective biosensor for Salmonella and its detection in the environment*. Journal of Microbiological Methods, 2003. **53**(2): p. 273-285.
6. Abad, J. M.,Pariente, F.,Hernandez, L.,Lorenzo, E. *A quartz crystal microbalance assay for detection of antibodies against the recombinant African swine fever*

virus attachment protein p12 in swine serum. Analytica Chimica Acta, 1998. **368**(3): p. 183-189.

7. Hengerer, Arne.,Decker, Jochen.,Prohaska, Elke.,Hauck, Sabine.,Ko[ss]linger, Conrad.,Wolf, Hans *Quartz crystal microbalance (QCM) as a device for the screening of phage libraries.* Biosensors and Bioelectronics, 1999. **14**(2): p. 139-144.

8. Park I.S., Kim N., *Thiolated Salmonella antibody immobilization onto the gold surface of piezoelectric quartz crystal*. Biosensors and Bioelectronics, 1998. **13**(10): p. 1091-1097.

9. Park, I.-S. and N. Kim, *Thiolated Salmonella antibody immobilization onto the gold surface of piezoelectric quartz crystal*. Biosensors and Bioelectronics, 1998. **13**(10): p. 1091-1097.

10. Pyun J.C., B.H., Meyer J.U., Ruf H.H., *Development of a biosensor for E. coli based on a flexural plate wave (FPW) transducer.* Biosensors and Bioelectronics, 1998. **13**(7): p. 839-845.

11. Alexei N. Naimushin., Charles B. Spinelli., Scott D. Soelberg., Tobias Mann., Richard C. Stevens., Timothy Chinowsky., Peter Kauffman., Sinclair Yee.,Clement E. Furlong. *Airborne analyte detection with an aircraft-adapted surface plasmon resonance sensor system.* Sensors and Actuators B: Chemical.

12. Naimushin., Alexei N.Soelberg., Scott D.Nguyen., Di K.Dunlap., Lucinda Bartholomew., Dwight Elkind., Jerry Melendez., Jose and Furlong, Clement E., *Detection of Staphylococcus aureus enterotoxin B at femtomolar levels with a*

miniature integrated two-channel surface plasmon resonance (SPR) sensor. Biosensors and Bioelectronics, 2002. **17**(6-7): p. 573-584.

13. Kari Kukanskis., J.E., Jose Melendez., Tiffany Murphy., Gregory Miller., Harold Garner., *Detection of DNA Hybridization Using the TISPR-1 Surface Plasmon Resonance Biosensor*. Analytical Biochemistry, 1999. **274,**: p. 7–17.

2. REVIEW OF LITERATURE

2.1 Immunosensors

Immunosensors are biosensors that use antibodies as the recognition element. Spurred by the multi-million dollar industry of immunodiagnostics, interest in immunosensors has increased by leaps and bounds. Modern immunosensors are able to provide precise measurements of myriad analytes in complex mixtures. The convenience of not having to accurately pipette various reagents in a multitude of steps, rapidity of testing, portability, and simultaneous multi-analyte measurement are some of the distinct advantages of modern day immunosensors over the conventional methods.

2.1.1 Antibodies

Immunosensors work on the principle of highly selective molecular recognition systems in order to determine the presence/absence and the amount of antigen. An antigen is any molecular species that is seen and identified by the body as foreign and triggers an immune response. The different classes of immunoglobulins (IgG, IgA, IgM, IgD, and IgE) are structurally related glycoproteins that differ in size, charge, amino acid composition, and carbohydrate content. Although antibodies are often chosen as the biological recognition element, this study uses filamentous phage designed for specific binding to the model antigen, ß-galactosidase (ß-gal). While molecular recognition

between antibody and the antigen is through epitope interaction, the specific method of molecular interaction between phage and ß-galactosidase is not clearly understood. Upon antigen challenge, a variety of antibodies are generated that, although they respond to the same antigen, bind to different sites on the antigen and have different affinities for that antigen. They belong to different subclasses and have differences in epitope specificity.

2.2 Binding Forces

A number of forces that are present in the biomolecular reaction are responsible for the stabilization of the interaction between the antibody and antigen. These are forces such as electrostatic, Van der Walls, and hydrophobic interactions. Hydrogen bonding also plays a major part and along with the other forces make up for the affinity interactions between antibody and antigen [1].

Electrostatic interactions can be of two types:

i) Repulsive or attractive forces between charged molecules

ii) Diole-dipole interactions between highly polar molecules.

Hydrogen bonds are considered as a type of electrostatic interactions. Dipoles that are weaker than those seen in electrostatic interactions exhibit Van der Waals forces. The temporary dipoles that are responsible for these forces are a direct result of the electric fields of nearby molecules. Although when taken singly, each of the forces is weak, the collective force from the several interactions can contribute up to 50% of the total binding strength [2]. Repulsive forces such as those seen between nonpolar molecules and water are called hydrophobic interaction. Existence of nonpolar regions at reaction sites, mainly as a result of entropy driven water exclusion and attainment of low favorable energy levels leads to intermolecular stabilization and increased binding strength [1].

Other forces beside electrostatic interactions hydrogen bonding are also responsible for intermolecular stabilization and these other forces add on to the attractive forces in the interaction [1]. Repulsions between interpenetrating electron clouds of non-bonded atoms are a result of steric hindrances. The effect of these repulsive forces become minimal as the complement between the reactants increases [3].

2.2.1 Kinetics of Binding

Based on the basic thermodynamic principle governing antibody/phage-antigen/ß-gal interactions in solution can be expressed by:

$$Ph + bg \underset{k_d}{\overset{k_a}{\Leftrightarrow}} Phbg \qquad (2.1)$$

Where, *Ph* represents free phage, and *ßg* represents free ß-gal, *Phßg* is the Phage-ß-gal complex, and k_a and k_d are the association and dissociation rate constants, respectively. The equilibrium constant, or the affinity, is given by:

$$K = \frac{k_a}{k_d} = \frac{[Phbg]}{[Ph]\ [bg]} \qquad (2.2)$$

Both the association and dissociation are relatively quicker in solution and while the former is mostly affected by the diffusion of the reactants, the latter is mainly determined by the strength of the phage-ß-gal bond. Whatever maybe the immobilization technique employed, immobilization can alter the properties of the antibody (or antigen), thus affects the binding kinetics [1].

2.2.2 Ligand Immobilization

The physical and chemical environment of the antibody-antigen complex is crucial for determining the sensitivity of the biosensor, be it TSM or SPR. Factors such the position of the antigen (ß-gal) capturing areas of the antibody (Phage), after the latter has been immobilized on the surface of the sensor plays a vital role in understanding the conformational freedom of the immobilized phage. This is largely dependant on the immobilization techniques that have been employed such as Langmuir-Blodgett (LB) method [4],[5],[6] and molecular self-assembling of phage layer using biotin/streptavidin [7] This will in turn, determine the stability of the complex. Attachment of affinity ligands to the hydrogel matrix is also accomplished through well-known methods [8]. The most elementary method of ligand immobilization is nonspecific adsorption. This method has been employed successfully for the detection of African swine fever virus protein [9], IgG [10], anti-vibro cholera [11] and recombinant protein fragments of HIV specific antibodies [12]

2.2.3 Mass Transfer

Transport of the target through the bulk solution such as that occurs in the Surface Plasmon Resonance (SPR) experiments, is governed by active transport and the kinetics of binding that govern ligand-target interactions. The bulk flow rate will affect the macroscopic transport through the system to the sensor surface[13]. Secondly, diffusion through the non-stirred boundary layer depends on bulk flow rate, geometry of the flow cell, and the diffusion coefficient of the target in solution[13]. Interactions between antibody and antigen in solution have been well understood. The binding of an antibody in solution to antigen immobilized on a surface has been described as a two-step

process[14]. Lateral interactions between macromolecules are thought to stabilize the adsorbed protein and antigen -antibody complexes on the surface, leading to an increase rate of binding and an increase in the antibody concentration near the surface[14].

2.3. Classical Sensor Platforms

Based on the measuring principle that is used, immunosensors can be classified as electrochemical, piezoelectric/acoustic and thermometric. Furthermore, all types can be categorized as either direct or indirect. Direct sensors are designed so that formation of the probe-analyte complex induces physical changes such as changes in frequency, mass electrode potential, membrane potential or the optical properties allowing for target measurement[15]. Materials such as electrodes, membranes, piezoelectric material, or optically active material surfaces are used to construct direct immunosensors. Indirect sensors rely on labels conjugated to either the antibody or antigen to visualize the binding event. Increased sensitivity can be achieved by the inclusion of enzymes, catalysts, fluorophores, electrochemically active molecules, and liposomes as labels[15]. The final step must include incorporation of a label, which is then determined by optical, potentiometric or amperometric, measurements. The principles of the classical sensing platforms, including electrochemical, piezoelectric/acoustic, and optical immunosensors based on evanescent wave phenomenon will be discussed.

2.3.1 Electrochemical

Potentiometric and amperometric are the two basic electrochemical sensors. The changes in potential at an ion selective electrode are measured in a potentiometric sensor. These changes are with reference to the *reference* electrode. The electrodes are either submerged into a sample or separated from the sample by a membrane and placed into a

defined electrolyte solution. The measured potential difference taken with respect to the reference electrode is dependent on all potential differences that appear at the various phase boundaries, including that of the reference electrode and differences between electrolytes[16]. The most common potentiometric devices are pH electrodes and other ion-selective electrodes. The chief drawback of this system is that changes in potential due to antibody-antigen binding are very small (1-5 mV) and, consequently, limitations on the reliability and sensitivity due to background effects is present [17]. Amperometric devices function by measuring the current produced by the oxidation/reduction of an electro active compound at an electrode while a constant potential is applied to this electrode with respect to the second electrode. The glucose biosensor, which makes use of the electrochemical detection of the species produced (hydrogen peroxide) or consumed (oxygen) by the enzyme glucose oxidase, which is immobilized on an electrode surface is a typical example. Results from potentiometric immunosensors for syphilis and blood typing have been reported by [15, 18, 19], human chorionic gonadotropin (hCG) in solution by coating the electrode surface with anti-hCG[15]. Another type of potentiometric immunosensor is the ion-selective field effect transistor (ISFET) immunosensor. The ISFET is based on the field effect transistor (FET) used in electronics to detect voltage variations with minimal current drain. Detection of Heparin in the range of 0.3 to 2.0 units/mL by coating the sensor with a protamine (an affinity ligand) immobilized membrane has been reported [20]. The FET devices have practical problems associated with membrane performance [21]. Furthermore, FET drift, lack of selectivity and difficulty in making a stable, miniaturized reference electrode has made commercial development of these sensors difficult[20]. These potentiometric

immunosensors demonstrate insufficient sensitivity. A low charge density compared with background interferences such as ions of most biological molecules is responsible for the low signal-to-noise ratios. They also show a marked dependence of signal response on sample conditions such as pH and ionic strength [21].

2.3 .2 Piezoelectric/ Acoustic devices

Piezoelectric biosensors such as Quartz Crystal Microbalance (QCM) or Thickness Shear Mode (TSM) resonators have found a wide range of biosensing applications. Metal transducers (e.g. gold) on the surface of the crystal send acoustic waves into the material at ultrasonic frequencies. The potential of QCM/TSM devices in sensor applications was made possible after the derivation of the frequency to mass relationship by Sauerbrey [22]

$$\Delta f = \frac{-2.3\times10^{-6} f^2 \Delta m}{A} \qquad (2.3)$$

where ?f is the change in fundamental frequency of the coated crystal in Hz, f is the fundamental frequency of the crystal(Hz), A is the resonator active area in cm^2 and ?m is the mass deposited on the crystal in grams. The crystal orientation, thickness of the piezoelectric material, and geometry of the metal transducer determine the type of acoustic wave generated and the resonance frequency [23]. A change in weight on the crystal can be determined by measuring the shift in resonating frequency, wave velocity, or amplitude. The frequency shift of the piezoelectric crystal is proportional to mass change. Changes in acoustic wave propagation are then correlated to the amount of analyte captured on the crystal surface. TSM sensors have been used for the detection of immunoglobulins [24], antibodies for African swine virus [25], and *S. typhimurium* [5].

The characteristics of the TSM sensor being small, rugged and entailing low costs offer significant advantages over other detection technologies. When TSM sensors are used with antibodies specific for the antigen in study, their sensitivity compares with techniques such as ELISA[26] and the use of TSM sensors for the detection of different pathogens have been well documented [27]. A bulk wave sensor was used to observe antibody in liquid phase[28]. The sensor surface was coated with goat anti-human immunoglobulin (IgG) either by attachment to a polyacrylamide gel with glutaraldehyde or by silylation onto the surface, then exposed to human IgG in solution. The advantage of the indirect method over the direct is that for a given amount of analyte bound, the mass of precipitate is much greater than that of the original bound analyte, hence sensor response is amplified. Variations of the acoustic wave sensor include the use of bulk acoustic waves, surface acoustic waves, and acoustic plate waves [15]. The influence of compressional wave generation on a TSM response in a fluid was investigated and it was shown that it does not affect the frequency shift [29]. By analyzing the frequency sifts and bandwidths of quartz coated resonators, a method to calculate the viscoelastic coefficients was derived [30]. A functional relationship between the frequency shift and the density and viscosity of the solution using a QCM was shown [31]. It was also shown that the changes in the oscillation frequency of a QCM in contact with a fluid is dependent on the material parameters of the fluid and quartz[32]. Use of QCM for the detection of gases [33-35], herbicide[36], polar and non polar halogenated organic chemicals [37], cell adhesion [38], endothelial cell adhesion [39], detection of microtubule alteration in living cells at nM nocodazole concentrations[40, 41], detection of M13 phages in liquids[42] and genetically modified organisms [43] have been reported.

The physical and chemical environment of the probe-analyte complex is crucial for determining the sensitivity of the biosensor[44], be it TSM or SPR. Factors such the position of the analyte (ß-gal) capturing areas of the probe (Phage), after the latter has been immobilized on the surface of the sensor plays a vital role in understanding the conformational freedom of the immobilized phage. This will in turn, determine the stability of the complex. The stability, consistence and sensitivity of detection using the TSM sensor is limited by the type of immobilization that is being used. A myriad of immobilization methods have been tried and the optimal method one can employ relies mainly on the nature of the biological compound that needs to be immobilized. Immobilization techniques that have been employed are the Langmuir-Blodgett (LB) method[4-6], molecular self-assembling of phage layer using biotin/streptavidin [7], functionalized self assembled monolayers [45], surface modifications using Protein A[46-48], Protein G[49] and enzymatic immobilization[50]. In our study, we propose to use a significantly simpler method of immobilization viz., ***physical adsorption***. The strict relationship between the frequency change and the mass of BSA adsorbed was determined[51]. Physical adsorption technique has been employed successfully for the detection of African swine fever virus protein [9], IgG [10], anti-vibro cholera [11] and recombinant protein fragments of HIV specific antibodies [12]. The major criteria for an ideal active surface is that it should be chemically stable, contain a high surface coverage of the active sites of the immobilized material the coating should be as thin and uniform as possible[52]. All the above traits determine the sensitivity of the biosensor, as higher sensitivity and stable signals can be obtained by active, thin and rigid layers[53].The

importance of uniform coating of the immobilized layer in order to obtain accurate measurements using the QCM was also shown [54].

2.3.3 Evanescent Wave Optical Sensing Devices

The improvement of optoelectronics, availability of better fabrication materials and improved methods of signal generation and detection [15] has led to the rapid growth of optical immunosensors. Several types of optical transducers that are currently popular are Surface Plasmon Resonance (SPR) sensors, planar waveguides or fiber optic sensors. Detection of the probe-analyte binding by the optical immunosensors is achieved through changes in absorption, rotation, bio/chemi-luminescence, fluorescence or refractive index. Optical immunosensors can also be classified as direct, which depend solely on the binding of the probe-analyte binding to change the signal whereas the indirect optical immunosensors use labels to detect the binding events. Immunosensors that use evanescent waves detect target binding by measuring parameters such as absorbance, fluorescence, or refractive index. Surface plasmon resonance (SPR) is a phenomenon resulting from the presence of evanescent waves. Optical biosensors based on the evanescent wave (EW) use the principle of attenuated total reflection (ATR) spectroscopy and surface plasmon resonance (SPR) to measure real-time interaction between biomolecules. The basis of ATR is the reflection of light inside the core of a waveguide when the angle of incidence is less than the critical angle. Waveguides can be slab guides, planar integrated optics or optical fibers. Light waves are propagated along fibers by the law of total internal reflection (TIR). This law states that incident light striking nearly parallel to the interface between two media of differing refractive indices,

entering through the media of higher refractive index will be reflected or refracted according to Snell's Law:

$$n_1 \sin \Theta_1 = n_2 \sin \Theta_2 \tag{2.4}$$

where n_1 is the higher refractive index (core), Θ_1 is the incident ray angle through the core, n_2 is the lower refractive index (cladding), and Θ_2 is the angle of either internal reflection back into the core or refraction into the cladding. TIR occurs when the angle of incidence is greater than the critical angle. The critical angle is defined as:

$$\Theta_c = \sin -1 \frac{n_2}{n_1} \tag{2.5}$$

Although TIR occurs, the intensity does not suddenly fall to zero at the interface. The intensity exponentially decays with distance, starting at the interface and extending into the medium of lower refractive index. The EW is the electromagnetic field created in the second medium, which is characterized by the penetration depth. The penetration depth is defined as the distance from the interface at which it decays to 1/e of its value at the interface [55]. The wavelength of light, ratio of the refractive indices,

and angle of the light at the interface determine the penetration depth [56]. The penetration depth (dp) is related to these factors by:

$$d_p = \frac{l}{2p\,(n_1^2 \sin^2 \Theta_1 - n_2^2)^{1/2}} \tag{2.6}$$

where T1 represents the incident ray angle with the normal to the n_1/n_2 (core/cladding) interface, and ? represents the wavelength of light[57]. Typical penetration depths range from 50 to 1000 nm for visible light (dp<?), thus the EW is able to interact with many monolayers at the surface of the probe[58]. If the cladding is removed and a ligand is immobilized on the core, the EW travels through this layer into the sample medium. Perturbations of the EW occur due to reactions occurring very close to the interface and these perturbations (signal) can be related to the amount of binding between the analyte and the probe that has been immobilized at the interface. This measured signal can be in the form of absorbance, fluorescence, or refractive index.

2.3.3.1 Surface Plasmon Resonance

SPR is the result of total internal reflection (TIR) at the thin metal-liquid interface. When an incident p-polarized light strikes a very thin metal (gold/silver) surface at a particular angle (greater than TIR), the evanescent wave will interact with free oscillating electrons (plasmons) in the metal film[23]. Energy from the incident light is lost to the metal, resulting in a decrease of reflected light intensity. This reflectance minimum appears in the reflected light at an acutely defined incident angle (resonance angle), which is dependent on the refractive index of the medium close to the metal film surface. Any change in the refractive index within the evanescent field results is reflected as a change in the resonance angle. The extent of this surface plasmon is dependent on the wavelength of the incident light. In our experiments, we use the *Kretschmann* geometry, where the metal (gold) surface is exposed to light transmitted via a glass prism. As molecules bind to immobilized targets on the gold surface, the optical properties of the

medium closest to the surface change. This causes a proportionate shift in the SPR angle, which provides a quantitative measurement of the amount of mass binding. This in turn, can be used to determine in real time a bio-molecular interaction. In our experiments use SPREETA™ sensors produced by Texas Instruments. This inexpensive dual channel and miniature sensors are very suitable for fundamental investigations. SPREETA™ has been used for the detection of analysis of biomolecular interactions with biomaterials [59]; *E. coli* enterotoxin [60]; structural analysis of human endothelin-1 [61] and characterization of thin film assembly [62]. Sample investigation through this platform can be achieved without any labeling; unlike other devices uses comparatively low volumes of reagents and can be used for the detection of biological warfare agents[63]. The simpler method of immobilization through physical adsorption was successfully employed for the immobilization of a wide range of biological elements ranging from anti-vibro cholera[11], African swine fever virus protein [9] and IgG [64]. Evidence of irreversible adsorption of protein molecules to gold surfaces due to hydrophobic actions was previously reported [65]. The viability of both TSM and SPR sensors for use a biosensors have been compared for the study of whole blood and plasma coagulation[66], in the structural analysis of human endothelin-1[61] and study of DNA assembly and hybridization [67].

2.4 References:

1. Rabbany, S.Y., Donner, B.L. and Ligler, F.S., *Optical Immunosensors.* Critical Reviews in Biomedical Engineering, 1994. **22**(5-6): p. 307-346.
2. Roitt, I., *Essential Immunology, 5th ed.* 1984, Oxford: Blackwell Scientific: St. Louis, MO.
3. Steward, M.W., *Affinity of the Antibody-Antigen Reaction and Its Biological Significance.*, in *Immunochemistry-An Advanced Textbook (Glynn, L.E. and Steward, M.W., ed.)*. 1977, John Wiley and Sons: New York. p. 233-262.
4. Samoylov, A.M., et al., *Recognition of cell-specific binding of phage display derived peptides using an acoustic wave sensor.* Biomolecular Engineering, 2002. **18**(6): p. 269-272.
5. Pathirana, S.T., et al., *Rapid and sensitive biosensor for Salmonella.* Biosensors and Bioelectronics, 2000. **15**(3-4): p. 135-141.
6. Pathirana, S., et al., *Assembly of cadmium stearate and valinomycin molecules assists complexing of K+ in mixed Langmuir-Blodgett films.* Supramolecular Science, 1995. **2**(3-4): p. 149-154.
7. Sukhorukov, G.B., et al., *Multilayer films containing immobilized nucleic acids. Their structure and possibilities in biosensor applications.* Biosensors and Bioelectronics, 1996. **11**(9): p. 913-922.
8. Hermanson, G.T., Mallia, A.K. and Smith, P.K.:, *Immobilized Affinity Ligand Techniques.* Academic Press, San Diego, CA,, 1992.

9. Uttenthaler, E., C. Ko[ss]linger, and S. Drost, *Characterization of immobilization methods for African swine fever virus protein and antibodies with a piezoelectric immunosensor*. Biosensors and Bioelectronics, 1998. **13**(12): p. 1279-1286.

10. Caruso, F., E. Rodda, and D.N. Furlong, *Orientational Aspects of Antibody Immobilization and Immunological Activity on Quartz Crystal Microbalance Electrodes.* Journal of Colloid and Interface Science, 1996. **178**(1): p. 104-115.

11. Carter, R.M., Mekalanos, J.J., Jacobs, M.B., Lubrano, G.J. & Guilbault, G.G., *Quartz crystal microbalance detection of Vibrio cholerae O139 serotype.* Journal of Immunological Methods, 1995. **187**: p. 121-125.

12. Aberl, F., et al., *HIV serology using piezoelectric immunosensors.* Sensors and Actuators B: Chemical, 1994. **18**(1-3): p. 271-275.

13. Glaser, R.W., *Antigen-Antibody Binding and Mass Transport by Convection and Diffusion to a Surface:A Two-Dimensional Computer Model of Binding and Dissociation Kinetics.* Analytical Biochemistry, 1993. **213**: p. 152-161.

14. Sadana, A.a.M., A., *Binding Kinetics of Antigen by Immobilized Antibody or of Antibody by Immobilized Antigen.* Influence of Lateral Interactions and Variable Rate Coefficients. Biotechnology Progress, 1993. **9**: p. 259-266.

15. Aizawa, M., *Immunosensors for Chemical Analysis.* Advances in Clinical Chemistry, 1994. **31**: p. 247-275.

16. Liu, Y.a.Y., T., *Polymers and Enzyme Biosensors.* Journal of Macromolecular Science, Reviews in Macromolecular Chemistry and Physics, 1997. **C37**(3): p. 459-500.

17. Marco, M.-P.a.B., D., *Environmental Applications of Analytical Biosensors.* Measurement Science & Technology., 1996. **7**(11): p. 1547-1562.

18. Aizawa, M., Kato, S. and Suzuki, S., *Immunoresponsive Membrane I. Membrane Potential Change Associated with an Immunochemical Reaction Between Membrane-Bound Antigen and Free Antibody.* Journal of Membrane Science. :, 1977a. **2**: p. 125-132.

19. Aizawa, M., Kato, S. and Suzuki, S., *Electrochemical Typing of Blood Using Affinity Membranes.* Journal of Membrane Science. :, 1980a. **7**: p. 1-10.

20. Pearson, J.E., Gill, A. and Vadgama, P., *Analytical Aspects of Biosensors.* Annals of Clinical Biochemistry, 2000. **37**: p. 119-145.

21. North, J.R., *Immunosensors: Antibody-Based Biosensors.* Trends in Biotechnology, 1985. **3**(7): p. 180-186.

22. Sauerbrey, G., *The Use of Quartz Oscillators for Weighing Thin Layers and for Microweighing.* Journal of Physics, 1959. **155**: p. 206-222.

23. Paddle, B.M., *Biosensors for Chemical and Biological Agents in Defence Interest.* Biosensors & Bioelectronics, 1996. **11**(11): p. 1079-1113.

24. Muramatsu, H., E. Tamiya, and I. Karube, *Determination of microbes and immunoglobulins using a piezoelectric biosensor.* Journal of Membrane Science, 1989. **41**: p. 281-290.

25. Abad, J.M.P., F. Hernandez, L. and Lorenzo, E., *A quartz crystal microbalance assay for detection of antibodies against the recombinant African swine fever virus attachment protein p12 in swine serum.* Analytica Chimica Acta, 1998. **368**(3): p. 183-189.

26. Park, I.-S. and N. Kim, *Thiolated Salmonella antibody immobilization onto the gold surface of piezoelectric quartz crystal.* Biosensors and Bioelectronics, 1998. **13**(10): p. 1091-1097.

27. Pyun, J.C., et al., *Development of a biosensor for E. coli based on a flexural plate wave (FPW) transducer.* Biosensors and Bioelectronics, 1998. **13**(7-8): p. 839-845.

28. Thompson, M., Dhaliwal, G.K., Arthur, C.L. and Calabrese, G.S., *The Potential of the Bulk Acoustic Wave Device as a Liquid-Phase Immunosensor*. IEEE Transactions on Ultrasonics, Ferroelectrics, and Frequency Control, 1987. **UFFC-34**(2): p. 127-135.

29. Martin, T.W.S.a.S.J., *Influence of compressional wave generation on a thickness shear mode resonator response in a fluid.* Anal. Chem, 1995. **67**: p. 3324.

30. Johannsmann, D., *Viscoelastic Analysis of Organic Thin Films on Quartz Resonators.* Macromol. Chem. Phys, 1999. **200**: p. 501.

31. Bruckenstein S. and Shay M., *Experimental aspects of use of the quartz crystal microbalance in solution.* Electrochim. Acta, 1985. **30**: p. 1295.

32. K. K. Kanazawa and J. G. Gordon, *The oscillation frequency of a quartz resonator in contact with a liquid.* Anal. Chim. Acta, 1985. **175**: p. 99-105.

33. G.G. Guilbault., N.-N., *Use of protein coatings on piezoelectric crystals for assay of gaseous pollutants.* Analytical Uses of Immobilized Biological Compounds for Detection, Medical and Industrial Uses. NATO reference series. Riedel.

34. Bodenhofer, K., *Performances of Mass-Sensitive Devices for Gas Sensing: Thickness Shear Mode and Surface Acoustic Wave Transducers.* Anal. Chem, 1996. **68**: p. 2210.

35. Nanto, H., *Novel gas sensor using polymer-film-coated quartz resonator for environmental monitoring.* Materials Science and Engineering, 2000. **C 12**: p. 43.

36. Liang, C., *Bulk Acoustic wave sensor for herbicide assay based on molecularly imprinted polymer*. Frsenius J. Anal. Chem, 2000. **367**: p. 551.

37. Rupa Patel, R.Z., K. Zinszer, F. Josse, and R. Cernozek, *Real-time Detection of Organic Compounds in Liquid Environments Using Polymer-coated Thickness Shear Mode Quartz Resonators.* Anal. Chem, 2000. **72**: p. 4888.

38. C. Fredriksson, S.K., M. Rodahl and B. Kasemo, *The Piezoelectric Quartz Crystal Mass and Dissipation Sensor: A means of Studying Cell Adhesion.* Langmuir, 1998. **14**: p. 248.

39. Zhou, T., K.A. Marx, M. Warren, H. Schulze and S.J. Braunhut, *The Quartz Crystal Microbalance as a Continuous Monitoring Tool for the Study of Endothelial Cell Attachment and Growth.* Biotechnology Progress, 2000. **16**: p. 268-277.

40. Marx, K., Zhou, T., Montrone A., Shultze, H. and S.J. Braunhut, *A quartz crystal microbalance cell biosensor: detection of microtubule alterations in living cells at nM nocodazole concentrations.* Biosensors and Bioelectronics, 2001. **16**: p. 773-782.

41. Marx, K.A., T. Zhou, A. Montrone and S.J. Braunhut. *A quartz Crystal Microbalance Cell Biosensor: Detecting Nocodazole-Dependent Microtuble*

Disruption Dynamics in Living Cells. in *Proceedings MRS: Advanced BiomaterialsCharacterization, Tissue Engineering and Complexity, Materials Research Society*. 2002. Pittsburgh, PA.

42. Uttenhaler, E., *Ultrasesnitive QCM Sesnors for detection of M13-Phages in liquids.* Biosensors and Bioelectronics, 2001. **16**: p. 735-743.

43. Ilaria Mannelli, M.M., , Sara Tombelli and Marco Mascini, *Quartz crystal microbalance (QCM) affinity biosensor for genetically modified organisms (GMOs) detection.* Biosensors and Biotechnology, 2003. **18**: p. 129.

44. F. Höök, M.R., B. Kasemo and P. Brzezinski, *Structural changes in hemoglobin during adsorption to solid surfaces: Effects of pH, ionic strength and ligand Binding*. Proc. Natl. Acad. Sci, 1998. **95**: p. 12271.

45. Spangler, B.D.a.T., B, *Capture Agents for a Quartz Crystal Microbalance - Continuous Flow Biosensor: Functionalized Self-assembled Monolayers on Gold*. Anal. Chim. Acta, 1999. **399**: p. 51-62.

46. Welsh, W., Klein. C.,Schickfus Von.M.,Hunklinger.S, *Development of a surface acoustic wave immunosensor.* Anal.Chem, 1996. **68**: p. 2000-2004.

47. Konig, B., Gratzel.M, *A novel immunosensor for herpes virus.* Anal.Chem, 1994. **66**: p. 341-344.

48. Konig, B., Gratzel.M, *A piezoelectric immunosensor for hepatitis viruses.* Analytica Chimica Acta, 1995. **309**: p. 19-25.

49. Minnunni.M., M.M., Carter.M.,Jacobs.M.B.,Lubrano.G.L.,Guibault.G, *A quartz crystal microbalance displacement assay for Listeria monocytogenes.* Anal.Chim.Acta, 1996. **325**: p. 169-175.

50. Santos.A.F, *Development of a piezoelectric biosensor for the determination of toxic amines in seafood*. 1994, Univesity of Rhode Island.

51. Muratsugu, M., *Quartz Crystal Microbalance for the Detection of microgram quantities of Human Serum Albumin: Relationship between the frequency change and the mass of protein adsorbed.* Anal. Chem, 1993. **65**: p. 2933.

52. Babacan.S., P.P., Lecher.S.,Rand.A.G., *Evaluation of antibody immobilization methods for piezoelectric biosensor application.* Biosensors and Bioelectronics, 2000. **15**: p. 615-621.

53. Luong JH, G.G., *Analytical applications of piezoelectric crystal biosensors.* Bioprocess Technol, 1991. **15**: p. 107-138.

54. Ward M. D. and Delawski E. J., *Radial Mass Sensitivity of the Quartz Crystal Microbalance in Liquid Media.* Anal. Chem, 1991. **63**: p. 886.

55. Squillante III, E., *Applications of Fiber-Optic Evanescent Wave Spectroscopy*. Drug Development and Industrial Pharmacy, 1998. **24**(12): p. 1163-1175.

56. Thompson, R.B.a.L., F.S., *Chemistry and Technology of Evanescent Wave Biosensors*, in *Biosensors with Fiberoptics (Wise, D.L. and Wingard, L.B., ed.)*. 1991, Humana Press: Clifton, NJ. p. 111-138.

57. Place, J.F., Sutherland, R.M. and Dahne, C., *Opto-Electronic Immunosensors: A Review of Optical Immunoassays at Continuous Surfaces.* Biosensors & Bioelectronics, 1985. **1**: p. 321- 354.

58. Lave, W.F., Button, L.J. and Slovacek, R.E.:, *Optical Characteristics of Fiberoptic Evanescent Wave Sensors: Theory and Experiment.* Biosensors With

Fibreoptics (Wise, D.L. and Wingard, L.B., ed.). 1991, Clifton,NJ: Humana Press. 139-180.

59. Green R.J., F.R.A., Shakesheff K.M., Davies M.C., Roberts C.J., Tendler S.J.B., *Surface plasmon resonance analysis of dynamic biological interactions with biomaterials.* Biomaterials, 2000. **21**: p. 1823-1835.

60. Spangler, B.D., Wilkinson, Elisabeth A.,Murphy, Jesse T. and Tyler, Bonnie J., *Comparison of the Spreeta(R) surface plasmon resonance sensor and a quartz crystal microbalance for detection of Escherichia coli heat-labile enterotoxin.* Analytica Chimica Acta, 2001. **444**(1): p. 149-161.

61. Laricchia-Robbio, L. and R.P. Revoltella, *Comparison between the surface plasmon resonance (SPR) and the quartz crystal microbalance (QCM) method in a structural analysis of human endothelin-1*. Biosensors and Bioelectronics, 2004. **19**(12): p. 1753-1758.

62. Aleksandr L. Simonian, A.R., Jamers R. Wild, Jerry Elkind and Michael V. Pishko, *Characterization of oxidoreductase-redox polymer electrostatic film assembly on gtold by surface plasmon resonance spectroscopy and Fourier transform infrared -external reflection spectroscopy.* Analytica Chimica Acta, 2002. **466**: p. 201-212.

63. Alexei N. Naimushin, C.B.S., Scott D. Soelberg, Tobias Mann, Richard C. Stevens, Timothy Chinowsky, Peter Kauffman, Sinclair Yee and Clement E. Furlong, *Airborne analyte detection with an aircraft-adapted surface plasmon resonance sensor system.* Sensors and Actuators B: Chemical, 2005. **104**(2): p. 237-248.

64. Minunni, M., Skladal, P. & Mascini, M., *A Piezoelectric Quartz-Crystal Biosensor as a Direct Affinity Sensor.* Analytical Letters, 1994. **27**: p. 1475-1487.

65. Horisberger, M.a.V., M., *Labeling of colloidal gold with protein.* Histochemistry, 1984. **80**: p. 13-18.

66. Vikinge, T.P., et al., *Comparison of surface plasmon resonance and quartz crystal microbalance in the study of whole blood and plasma coagulation.* Biosensors and Bioelectronics, 2000. **15**(11-12): p. 605-613.

67. Su, X., Y.-J. Wu, and W. Knoll, *Comparison of surface plasmon resonance spectroscopy and quartz crystal microbalance techniques for studying DNA assembly and hybridization.* Biosensors and Bioelectronics, 2005.

3. OBJECTIVES AND CONTRIBUTIONS OF THIS STUDY TO THE EXISTING LITERATURE

Obviously, there is a need for the development of an immunosensor that is able to detect large size molecules. Investigations into such immunosensors will provide us with a fundamental understanding so as to enable us to design efficient biosensors. Although sufficient literature exists for the characterization of each of the different types of biosensors, there is a dearth for comparative study literature. This research was conducted in order to expand the existing knowledge on immunosensor, especially immunosensors for large molecules that could mimic the large protein molecules that are used to detect pathogenic species. The objective of this work is to determine and characterize the interaction between analyte [phage(1G40)]- antigen [ß-galactosidase(ß-gal)] on different platforms such as ELISA , TSM and SPR sensor platforms, that leads to development of a sensitive, specific and rapid biosensor. The *rationale* that underlies this objective is that the interactive properties of the probe-analyte play a crucial role on the sensitivity and specificity of the biosensor. Hence, for the development of an effective biosensor, it is very important to understand the intricacies of the binding properties of probe-analyte system. This current research explores the use of *phage* as opposed to the conventional

antibody and *ß-galactosidase* as the test antigen. To accomplish the objective, the research was organized under four research directions.

3.1(A) validity of selected probe for ß -galactosidase

- Define the validity of phage recognition to the target antigen, ß-galactosidase using Enzyme Linked Immunosorbent Assay (ELISA)
- Characterize specificity and selectivity of the selected phage to ß-galactosidase by ELISA.

3.2(B) Physical micro/macro -environment-TSM sensor

- Define the conditions for immobilization of probe by physical adsorption on gold surface.
- Determine parameters of binding of ß-gal to selected phage on a surface of a Thickness Shear Mode (TSM) sensor.
- Determine and characterize specificity and selectivity of binding.

3.3 (C) Surface plasmon resonance sensor

- Determine and optimize binding parameters of phage-ß-gal molecular interactions using the Surface Plasmon Resonance (**SPR**) platform.
- Characterize selectivity and specificity of binding using the Surface Plasmon Resonance (**SPR**) platform.
- Define binding parameters in both flow mode and batch mode of sensing.

3.4(D) Compare binding studies using three platforms (ELISA, TSM, ANDSPR).

- Compare the binding parameters such as K_d and binding valences on the three different platforms.

3.5(E) Atomic force microscopy

- Determine changes in surface topography due to the different cleaning processes on both the gold surface of both the TSM and SPR sensors.

3.6(F) Transmission Electron Microscope

- Determine the visualization of phage on formavar/Cu grids using a Transmission Electron Microscope.

4. OPTICAL PHAGE BIOSENSOR BASED ON SURFACE PLASMON RESONANCE SPECTROSCOPY

Abstract

SPREETA ™, a compact, dual channel and scaled down version of surface plasmon resonance sensor (SPR) was used to study the binding of ß-galactosidase (ß-gal) to phage immobilized to the gold surface through physical adsorption [1]. Landscape ß-gal binding phage [2] and ß-gal derived from *E.coli* were used as a probe/analyte system. Apart from a flow through mode used to deliver the solutions to the surface for the SPR sensor, batch mode sensing was also employed to study the binding of ß-gal to immobilized phage. Specificity of the phage selected for binding to ß-gal was also studied. Effective dissociation constants (K_d) obtained from SPR sensors indicate their ability to detect binding of ß-gal up to 13 pM. Experiments using a flow through mode of delivery provided more consistent results in the full dose range and showed higher sensitivity as opposed to the batch mode studies. The binding valences, on the other hand however, were higher for the batch mode sensing indicating more of a divalent interaction as opposed to a more monovalent interaction of phage and ß-gal.

1. Introduction

Food borne diseases cause an estimated 76 million illnesses, accounting for 325,000 hospitalizations and more than 5000 deaths in the United States each year [3].

Currently, there are more than 250 known food borne diseases caused by different pathogenic microorganisms, including viruses, bacteria, fungi. Conventional methods of detecting pathogens entail a minimum of 24-48 hours of investigation, only after which results can be obtained. Apart from the urgent need of detection of food-borne pathogens, there is an even urgent need for the development of biosensors for the specific, sensitive and rapid detection of probable bio-terror agents.

The filamentous bacteriophages used as probes in this study are viruses that possess a single stranded DNA encapsulated in a protein sheath. The protein sheath is made up of both major and minor coat proteins. The target for designing the probe is the major coat protein, pVIII, of which there several thousand copies. The probe selected in this study, 1G40, was designed for specific action with the target analyte, viz., ß-gal from a library of filamentous phages [4]. *Escherichia coli* ß-galactosidase was selected for these studies as a typical protein.

SPR has become a well established tool for the characterization of biorecognition. Recent years have seen the use of SPR for the detection and characterization of various molecular reactions. SPR has been used for the detection of *E. coli* enterotoxin [5]; screening of compounds interacting with HIV-1 proteinase [6]; analysis of biomolecular interactions with biomaterials{Green R.J., 2000 #18}; quantification of human IgE [8]; structural analysis of human endothelin-1 [9] and characterization of thin film assembly [10]. Through this platform, the sample to be investigated can be studied without any labeling; provides continuous real time monitoring; sensor's surface can be regenerated

using low pH wash; consumes low volumes of reagents unlike other methods and can be used for the detection of biological warfare agents [11]. SPREETA™, described in details earlier [12, 13] has been successfully employed for the detection of mutant DNA [14], [15]; immobilization of DNA probes [16], [17] and detection of Hg^{2+} [18]. The compactness of the SPREETA™ provides a distinct advantage over other platforms for deployment in the field. The fact that the SPR sensor surface can be reused by employing simple regeneration reagents and techniques adds on to the advantages of the SPR platform over other contemporary biosensor platforms in use today.

2. Materials and methods

2.1 Phage

The phage (phage 1G40) used for binding to ß-Gal was affinity selected from a landscape library as described [19]. The total number of viral particles present in phage preparations was determined by spectrophotometer using the formula [20]:

$$\text{Virions (vir) /ml} = (A_{269} \times 6 \times 10^{16}) \text{ /number of nucleotides in the phage genome}$$

Where, A_{269} is absorbance at 269 nm. For the recombinant phages used in this work (9198 nucleotides), the formula:

$$\text{Absorbance unit (AU)}_{269} = 6.5 \times 10^{12} \text{ vir/ml}$$

was used to determine the concentration of phage particles in a solution.

2.2 ß-galactosidase

Escherichia coli ß-galactosidase was obtained from Sigma Chemical Co. (G5635) as a lyophilized powder and was dissolved in Dulbecco's phosphate buffered saline (DPBS) at final concentration of 2.4 mg/ml.

2.3 Solutions, reagents and tubing

Dulbecco's phosphate buffered saline solution [DPBS] was obtained from BioWhittaker Inc., (17-512F). Tris-buffered saline (TBS) was prepared from Tris crystallized free base; Fisher Scientific, BP 152-1; TBS-Tween [TBS containing 0.5% (v/v) Tween]. Bovine serum albumin (BSA) Fraction V; Sigma Chemical Co. A2153; 50 mg/ml stock dissolved in Millipore water was filter-sterilized and stored at 4°C. O.64 mm (inner diameter) silicone tubing (Cole Parmer, cat #: 07625-22), 3mL latex syringes (Becton and Dickinson) and 2 mL polypropylene cryogenic, round bottomed tubes cylinder (Corning, cat #: EW-44351-15)

2.4 Miniature two-channel SPR sensor

In our experiments we use SPREETA™, a dual channel miniature sensor (Texas instruments) that belongs to the class of SPR sensors that use angle interrogation. The various components of the device and the flow cell and their different functions are as described [21]. The wavelength of the light employed for interrogation of the angle change is 830 nM. The approximate flow rate was set at 150 µl/min. It should be mentioned that all the experiments were conducted at room temperature, which did not fluctuate significantly at any point during the duration of study.

2.5 SPR sensor batch mode setup

Apart from the flow through mode setup [21] that was employed to deliver all solutions to the gold surface, a batch mode setup (*Fig4.2*) was also designed and tested. A Teflon block was milled to smoothness using a Microlux milling machine to dimensions of 26.13× 24.95mm with a thickness of 11.16 mm. Four holes were drilled in the corners of the Teflon block to match those on the front edges of the black anodized side plates that were used to sandwich the SPEEETA™ sensor in between them. The screws were used to hold the Teflon block to the sensor/side plates, and the whole setup was clamped. A reservoir of 9.62× 4.95 mm, the bottom of which aligned with the gold surface of the sensor also was cut into the Teflon block and formed a measurement cell. A rubber gasket of similar dimensions was shaped and applied between the Teflon block and the sensor to provide a tight seal for prevention of any leakage. A small inlet of 2.95 mm (inner diameter) was drilled near the bottom of one side of the reservoir to facilitate delivery of different solutions in a plane parallel to the gold surface of the sensor. This type of delivery was found to be most effective for stability of the sensing (phage) layer. A latex syringe of 3 ml capacity (Becton and Dickinson) was used to deliver the solutions. Separate syringes were employed for the delivery of different solutions. The whole setup was then housed in a black box so as to prevent interference from background light.

3 SPR sensor preparations

SPREETA ™, a scaled down, highly integrated surface plasmon resonance (SPR) sensor was used to study the binding of the selected phage to ß-gal. All SPR sensors were plasma cleaned in Argon using Plasmod ™ system (Manchester Inc) at 1 torr for 5 minutes prior to being employed in any tests. Immobilization of the phage to the gold surfaces was through physical adsorption for both flow through and batch mode of investigations [1]. In the flow through mode, both the inlet and outlet silicone tubing were of uniform internal diameter (0.64 mm). Both inflow and collection solution tubes were round bottomed, polypropylene cryogenic tubes of 2 ml capacity [Corning]. Both of the above conditions were consistently maintained so as to ensure absence of any air bubbles in the system.

3.1 b-galactosidase binding measurements

The photodiode array response changes as a measure of refractive indices/units were recorded and transferred to a personal computer via an RS 232 interface card. All the data were observed in real-time using the "Multispr" (version 10.68) software which also enables us to store the data that can be analyzed offline. The software also provides us with such information of the signal as either refractive index or refractive units vs. time; thickness and coverage of adlayer (adsorbate) and angle. All binding was determined and quantified using the Hill plot, [22] and all results such as Hill coefficient, EC 50 , and effective dissociation constant K_d and the binding valences were determined as described [2].

3.1.1Flow through mode

Two methods of delivery of solutions to the gold surface of the sensors were employed. In the flow through mode, a cleaned, gold surface of the sensor was exposed to a phage suspension at a concentration of $3.2x10^{11}$ virions/mL till saturation was achieved (approximately 3 hours) and followed by washing with Dulbecco's phosphate buffered saline (DPBS). Bovine serum albumin (BSA) 2mg/mL was used to block the sensor surface. The sensor was then exposed to graded concentrations of ß-gal solutions (0.0032-210 nM) with intermediate washes of DPBS, and the changes in the refractive units were recorded as described [1]. The flow through mode had the added advantage of a dual channel, so that while one channel served as the working one, the second one was used as a control.

3.1.2 Batch mode

In the batch mode method, the SPR sensors samples were subjected to plasma cleaning as described and then the gold surfaces of cleaned SPR sensors were exposed to a phage suspension containing 2.3×10^{11} virions/mL for 1 hour. After incubation with the phage solution, the sensor surface was treated with DPBS and then was placed in a humidified chamber at 4 °C for 24 hours. The next day, the sensor surface was blocked as described [1] before tests with sequential concentrations of β-gal (0.0032-210 nM) began.

3.2 Specificity of binding

Specificity of phage binding to β-gal was examined thus. First, free phage suspensions (2.2×10^{12}-3.36×10^{7} vir/ml) was incubated with 22nM ß-gal for 1 hour. The phage sensor was prepared as described in section 3.1.1 and then treated with BSA (2mg/mL),

following which the sensor was exposed to the phage suspensions, pre-incubated with ß-gal, as described above.

4. Results and discussion

4.1 Binding studies

It was observed that the dose responses of binding experiments using the flow through mode, showed three distinct types, which probably depended on the orientation and the rigor of binding of phage to the sensor surface. While 81% [Type: S] of the sensors tested showed a full range of a typical dose response curve (*fig. 4.3Aa*) 9.6% [Type: L] showed us responses in the lower range (*fig 4.3Ba*) and 9.4 % [Type: M] showed a response curve in the maximum range (*fig 4.3Ca*). The effective K_d of the "S", "L", and "M" types were 1.3nM, 0.1µM and 3.2 nM. Binding of ß-gal to immobilized phage showed variations depending upon the condition of the surface of the sensors and the different experimental conditions under which binding studies were conducted. The two major experimental setups, flow mode and batch mode that were used to study binding produced different results. Binding studies conducted using both the flow through and batch mode system was repeated six times under similar conditions. The mean effective K_d and binding valences for the flow through mode studies was 1.3nM and 1.5 respectively, in comparison to 26nM and 2.4 for the batch mode studies. This shows that flow through mode is more effective in alleviating the sensitivity of the SPR sensors. The higher binding valency in the batch mode studies could be attributed to a higher availability of binding sites on the phage layer, as a result of the comparatively thinner deposition of the phage adlayer. Another possible explanation could be a different

packaging and orientation of the phage on the surface in course of flow and batch deposition.

A possibility to re-use sensors was investigated. A sensor that has been utilized several times for the same binding experiments described herein the paper is termed as a 'reused sensor'. It should be noted that the reused and new sensors are cleaned in the same manner as described above prior to being used in a new experiment. The term 'new sensor' denotes those that are 'out of the box' that have never been used and cleaned as described above. Out of ten new sensors that underwent cleaning procedures as described above, before which binding studies were carried out, 50% showed a full range response curves as opposed to 69% full range response curves given by reused sensors that underwent the same cleaning procedures as described before. The mean effective K_d was seven times greater for reused sensors than that for new sensors, while the binding valences between the categories did not show any significant differences. To summarize, out of a total of twenty experiments conducted using the SPREETA sensor, the mean effective K_d was 1.9 nM and the mean binding valences and Hill constants being 1.6 and 0.66 respectively.

4.2 Phage deposition and surface coverage

The thickness, the orientation, and the surface coverage of the phage layer through physical adsorption play a vital role in increasing the efficiency of the sensitivity of the sensor and also on the manner of interaction with the target analyte (ß-gal). Jung et al provided a mathematical formalism for understanding the SPR signals from adsorbed layers using a variety of structures [23]. Leidberg et al proved the exponential decay of SPR response with distance from the surface [24]. Lukosz proved linear and nonlinear

relationships between variations in effective refractive indices and thin and thick adlayer thickness respectively. [25, 26] Using the functions of the *MultiSPR* software, the thickness of the adlayer (nM) were calculated for the adsorbed phage layer and the variations and relationships between the thicknesses of the adlayer and the respective responses in refractive indices were investigated. *Fig. 4.4* shows a typical increase in the adlayer thickness for the two working channels of the SPR sensor in flow mode. The average thickness of phage 1G40 adlayer deposited through flow through mode was 3nM and the corresponding mean responses of ß-gal binding to the phage shows a sigmoidal dose response, as seen in *Figure. 4.5 (A)*. The smooth curve representing phage binding is the sigmoid fit to the mean of twenty experimental data (? - χ^2=3815 RU, R^2=0.99) repeated under similar conditions. The average phage adlayer thickness for the experiments, where batch mode was employed was 0.66nM and the corresponding mean responses showed a linear relationship (slope=$2.6\times10^{-4}\pm1.5\times10^{-5}$; R=0.99) as can be seen in *Figure.4.6* . Such differences between adlayer thicknesses for two modes may be due to very different manner of phage supply to the surface of the sensor, and thus, very different pattern of the page layer. The continuous flow mode with flow turbulences allows an "active" distribution of the phage rod-shaped molecules along with flow direction. Meanwhile, in batch mode distribution the phage binding occurs in "static" conditions, when rod-shape phage is lefts to its own and binding is take place chaotically, with more diffusional problems and in longer period of time. This leads to different shaping/orientation of the page on the surface, and therefore, to different kinetic characteristics of the binding. The lower value of the adlayer in the batch mode

experiments where the responses show a linear relationship in comparison to those where flow through mode was employed agrees well with earlier studies. [25, 26]

4.3 Specificity of Binding

Specificity studies showed that the phage 1G40 was specific to the ß-gal. As can be seen (F*igure.4.7*), at higher concentrations of free phage, pre-incubated with ß-gal, low binding is observed as a result of low availability of ß-gal (due to cross interaction with free phage in solution) to interact with the phage immobilized on the sensor surface. However, as opposed to that, a higher signal is observed at lower concentrations, where more ß-gal is available to interact with phage immobilized on the sensor surface (F*igure. 4.7*). The smooth curve is the sigmoid fit to the experimental data ($\chi^2=3.5\times10^{-9}$, $R^2=0.97$). For these specificity experiments, the lower end of detection of ß-gal binding was chosen, so as to avoid any possibility of external noise signal that may occur at higher concentrations.

5 Conclusions

The studies show that phage can be used as the sensing layer for the specific and sensitive detection of ß-gal. Employing the flow through mode gives us a sensor of higher sensitivity in comparison to that obtained through batch mode studies. On the other hand, the binding valences however, were higher in the batch mode studies as opposed to the flow through mode. This was possibly due to divalent interaction of phage-ß-gal which could be as a result of

a) The thin nature of the phage adlayer which could in turn, increase the flexibility of the phage layer making more binding sites available to ß-gal
b) Due to the stabilization of the phage layer prior to being interacted with ß-gal

c) Or the combination of both the above factors.

6 Acknowledgments

Support for this work comes from NSF Grant (CTS-0330189 to ALS), DAADOJ-02-C-0016, Aetos technologies Inc, and from Auburn University Detection and Food Safety Center. Help from Dr. Jerry Elkind and Dr. Dwight Bartholomew are greatly appreciated.

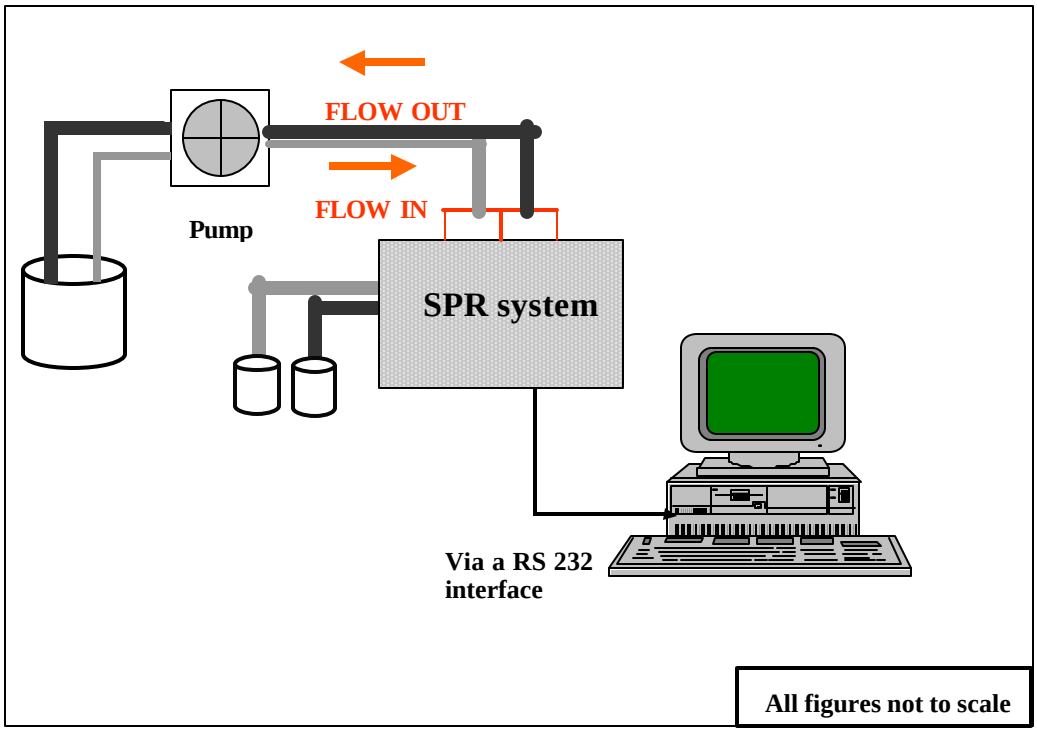

Fig 4.1: Schematic of the flow through mode setup

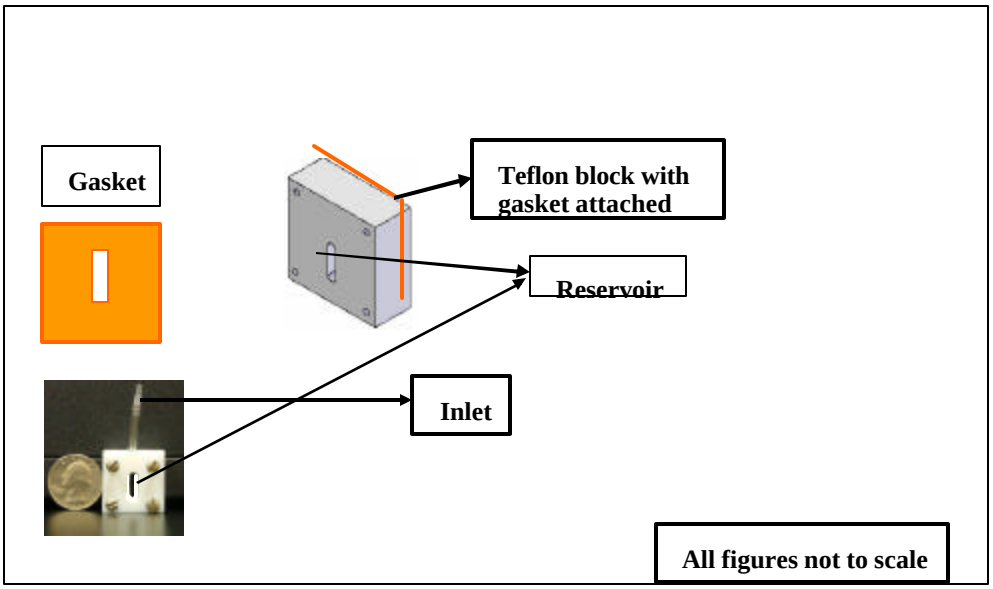

Fig 4.2: The batch mode setup

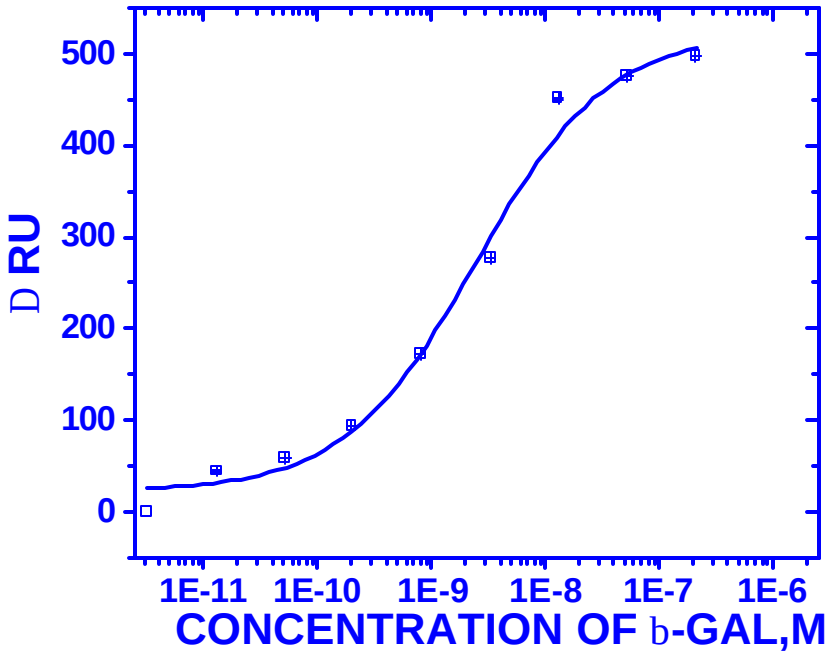

Fig 4.3 A (a): A full range dose response curve. The smooth curve **(a)** representing phage binding is the sigmoid fit to the experimental data (□- χ^2=3157.5 RU, R^2=0.99). Each experiment was replicated twenty times. Experimental values were obtained by averaging of about 120 data points of each steady-state level of response-time curves.

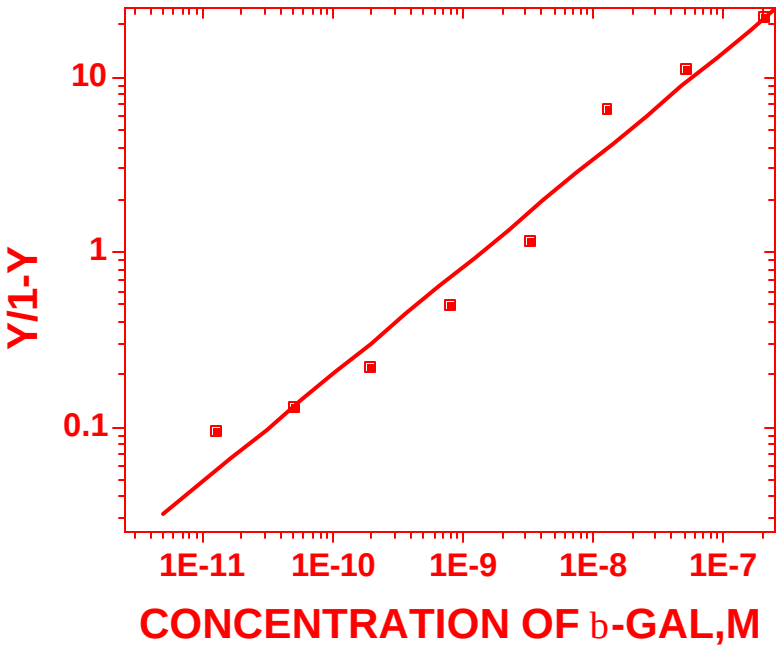

Fig 4.3 A (b): Hill plots of binding isotherms showing the ratio of occupied and free phages as a function of ß-galactosidase concentrations. The straight line is the linear least squares fit to the data (slope=0.61 ±0.04; R=0.98)

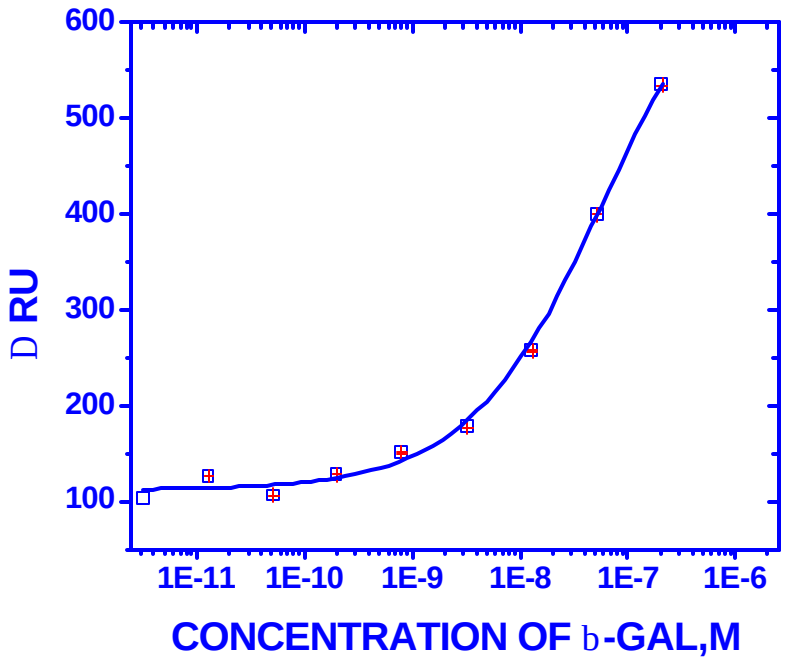

Fig 4.3 B (a): A low range dose response curve. The smooth curve representing phage binding is the sigmoid fit to the experimental data (▫- χ^2=904.7 RU, R^2=0.99). Each experiment was replicated seven times. Experimental values were obtained by averaging of about 120 data points of each steady-state level of response-time curves.

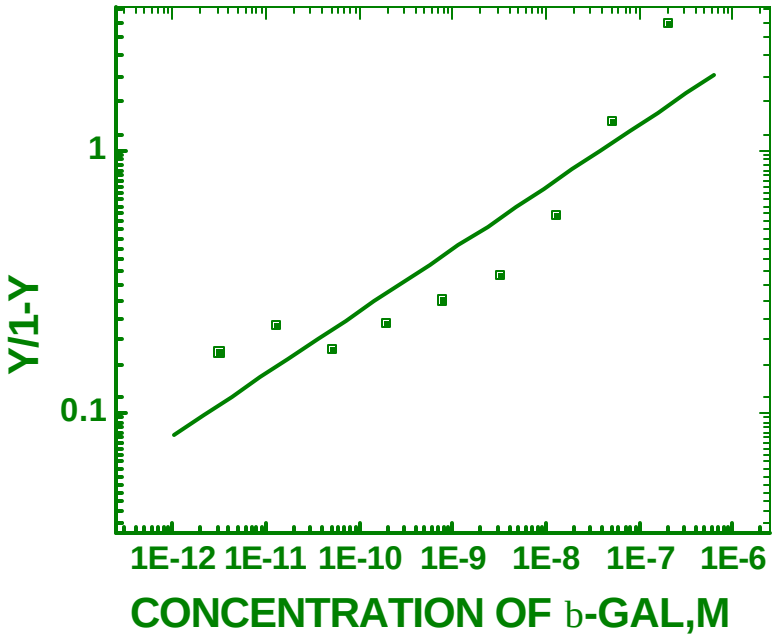

Fig 4.3 B (b): Hill plots of binding isotherms showing the ratio of occupied and free phages as a function of ß-galactosidase concentrations. The Straight line is the linear least squares fit to the data (slope=0.24 ±0.04; R=0.90)

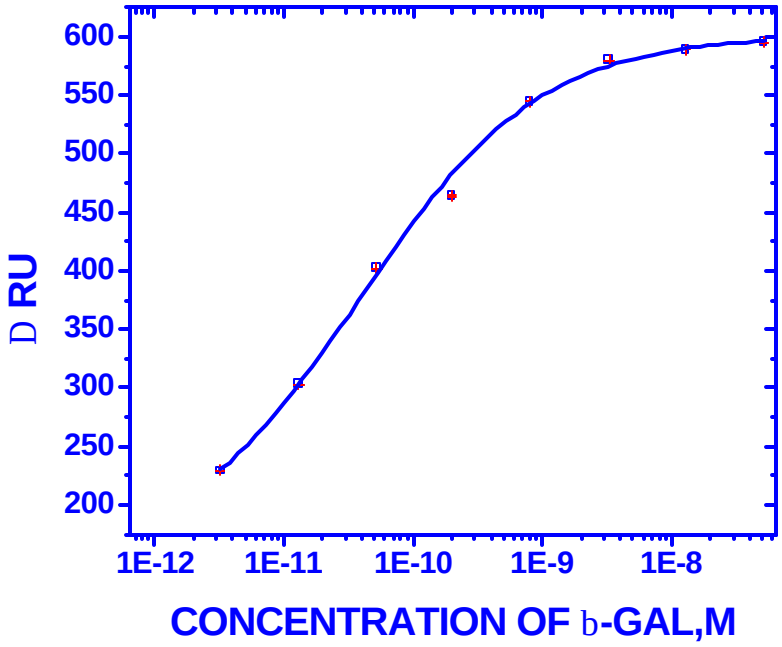

Fig 4.3 C (a): A high range dose response curve. The smooth curve representing phage binding is the sigmoid fit to the experimental data (□- c^2=454.4 RU, R^2=0.99). Each experiment was replicated five times. Experimental values were obtained by averaging of about 120 data points of each steady-state level of response-time curves.

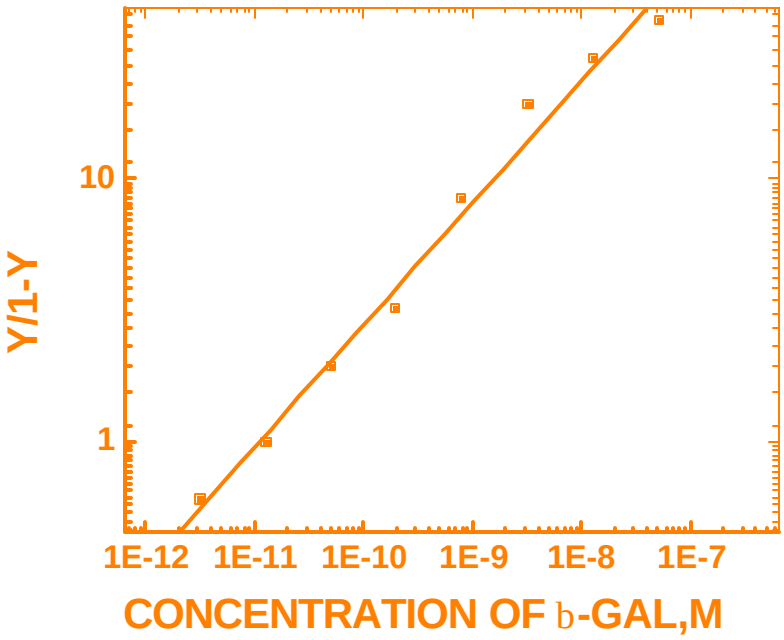

Fig 4.3 C (b): Hill plots of binding isotherms showing the ratio of occupied and free phages as a function of ß-galactosidase concentrations. The Straight line is the linear least square fit to the data (slope=0.46 ±0.02; R=0.99)

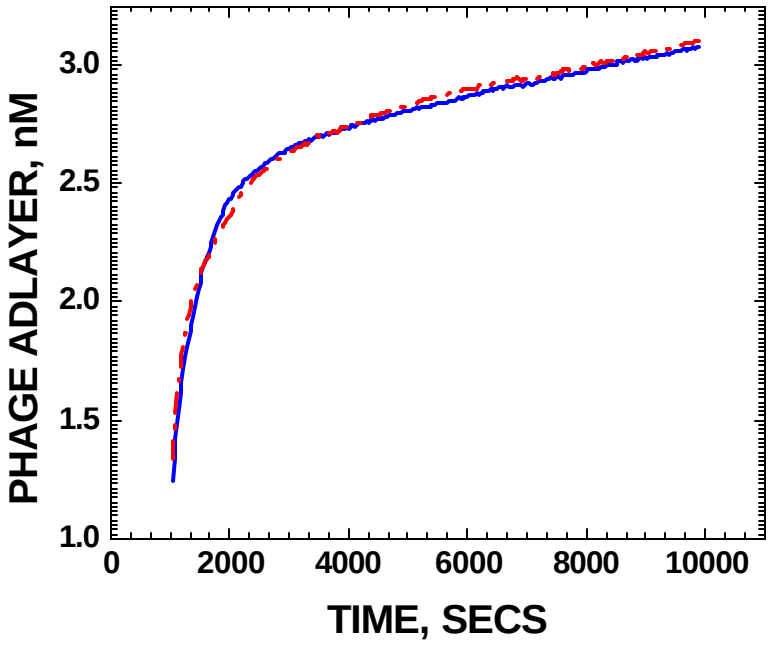

Fig 4.4: Graph shows a typical example of addition of 1G40 phage adlayer through physical adsorption using the flow through method as described. The two curves represent the two different working channels of the SPR sensor.

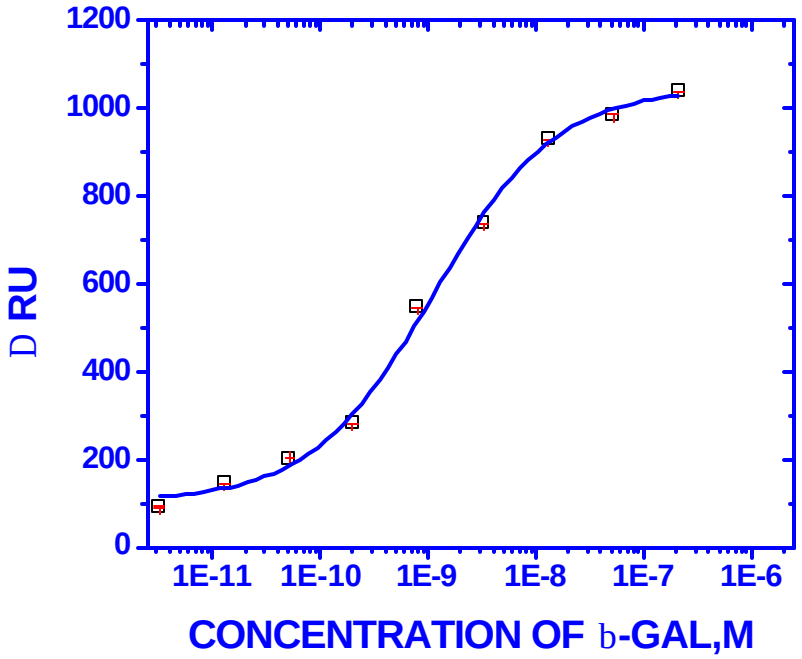

Fig 4.5 (A): A full range dose response curve. The smooth curve representing phage binding is the sigmoid fit to the experimental data (␣- c^2=3815 RU, R^2=0.99). Data points plotted are the mean of twenty experiments, each of which represents a steady state level of response-time curves.

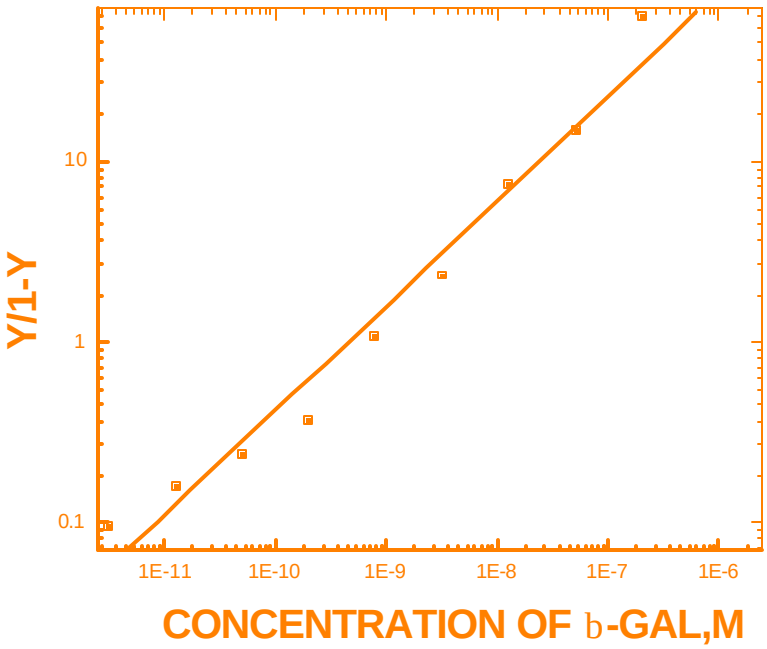

Fig 4.5 (B): Hill plots of binding isotherm showing the ratio of occupied and free phages as a function of ß-galactosidase concentrations. The Straight line is the linear least squares fit to the data (slope=0.59 ±0.04; R=0.99)

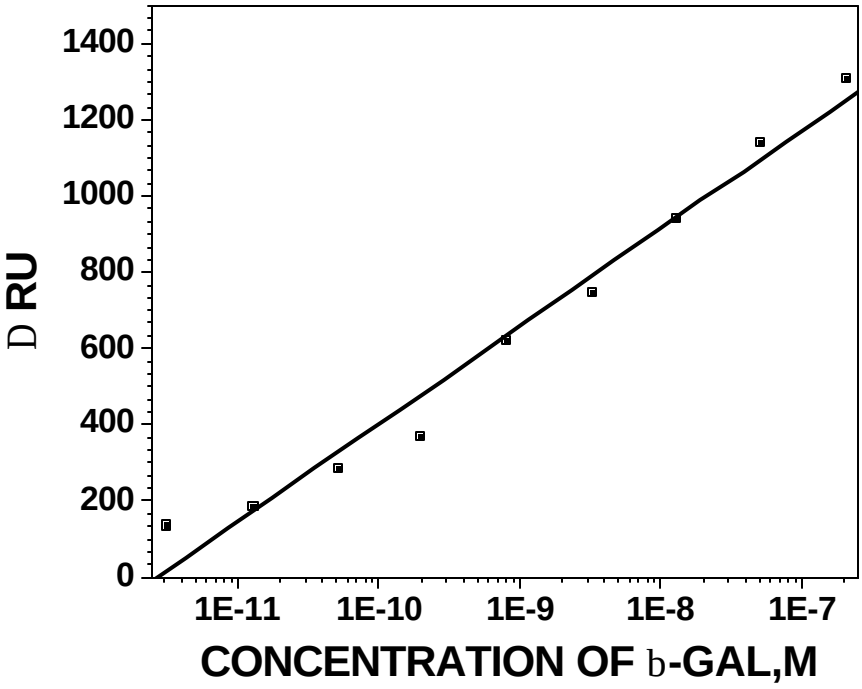

Fig 4.6: Typical binding mean responses of ß-galactosidase to phage immobilized on the gold surface using batch mode of delivery, repeated six times. The straight line is the linear least squares fit to the data (slope=2.6´ 10^{-4}±1.5 ´ 10^{-5}; R=0.99)

Formatted: Justified

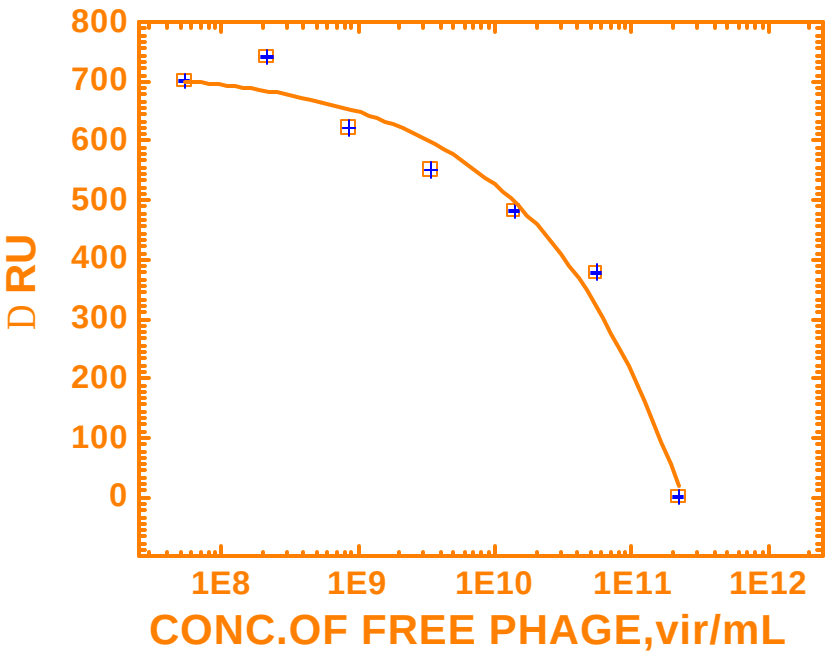

Fig 4.7 : *Specificity of phage*. Dose responses of the sensor to ß-galactosidase (22nM) incubated free phage (8.4×10^5 - 2.2×10^{11} vir/mL) prior to exposure. The smooth curve is the sigmoid fit to the experimental data (¦ - $c^2=3.5\,´\,10^{-9}$, $R^2=0.97$). Data points represent steady state level of response-time curves.

7. References:

1. V. Nanduri, A.Samoylov., V.Petrenko, V. Vodyanoy, A.L.Simonian, *Comparison of optical and acoustic wave phage biosensors.* 206th Meeting of The Electrochemical Society, 2004.
2. Petrenko, V.A. and V.J. Vodyanoy, *Phage display for detection of biological threat agents.* Journal of Microbiological Methods, 2003. **53**(2): p. 253-262.
3. Paul S.Mead, L.S., Vance DDietz, Linda F. McCaig, Joseph S.Breese, Craig Shapiro, Patricia M.Griffin and Robert V Tauxe, *Food-Related Inllness and Death in the United States.* Emerging Infectious Diseases, 1999. **5**(5): p. 607-625.
4. Petrenko, V.A., Smith, G.P., Gong, X., and Quinn, T, *A library of organic landscapes on filamentous phage.* Protein Engineering, 1996. **9**: p. 797-801.
5. Spangler, B.D., Wilkinson, Elisabeth A.,Murphy, Jesse T. and Tyler, Bonnie J., *Comparison of the Spreeta(R) surface plasmon resonance sensor and a quartz crystal microbalance for detection of Escherichia coli heat-labile enterotoxin.* Analytica Chimica Acta, 2001. **444**(1): p. 149-161.
6. Markgren, P.-O., Hämälainen, M. and Danielson, U.H., *Screening of compounds interacting with HIV-1 proteinase using optical biosensor technology.* Analytical Biochemistry, 1998. **265**: p. 340-350.
7. Green R.J., Frazier.A. R., Shakesheff K.M., Davies M.C., Roberts C.J., Tendler S.J.B., *Surface plasmon resonance analysis of dynamic biological interactions with biomaterials.* Biomaterials, 2000. **21**: p. 1823-1835.

8. Su, X. and J. Zhang, *Comparison of surface plasmon resonance spectroscopy and quartz crystal microbalance for human IgE quantification.* Sensors and Actuators B: Chemical, 2004. **100**(3): p. 311-316.

9. Laricchia-Robbio., Leopoldo Revoltella., Roberto P., *Comparison between the surface plasmon resonance (SPR) and the quartz crystal microbalance (QCM) method in a structural analysis of human endothelin-1*. Biosensors and Bioelectronics, 2004. **19**(12): p. 1753-1758.

10. Aleksandr L. Simonian, A.R., Jamers R. Wild, Jerry Elkind and Michael V. Pishko, *Characterization of oxidoreductase-redox polymer electrostatic film assembly on gtold by surface plasmon resonance spectroscopy and Fourier transform infrared -external reflection spectroscopy.* Analytica Chimica Acta, 2002. **466**: p. 201-212.

11. Alexei N. Naimushin, C.B.S., Scott D. Soelberg, Tobias Mann, Richard C Stevens, Timothy Chinowsky, Peter Kauffman, Sinclair Yee and Clement E. Furlong, *Airborne analyte detection with an aircraft-adapted surface plasmon resonance sensor system.* Sensors and Actuators B: Chemical, 2005. **104**(2): p. 237-248.

12. J. Melendez, R.C., D. U. Bartholomew, K. Kukanskis, J. Elkind, S. Yee, C. Furlong, R. Woodbury., *A commercial solution for surface plasmon sensing.* Sensors and Actuators B, 1996. **35**: p. 1-5.

13. Elkind, J.L., Stimpson, D. I.,Strong, Anita A.,Bartholomew, D. U.,Melendez, J. L *Integrated analytical sensors: the use of the TISPR-1 as a biosensor.* Sensors and Actuators B: Chemical, 1999. **54**(1-2): p. 182-190.

14. Wilson, P.K., Jiang, T.,Minunni, M.E.,Turner, A.P.F.,Mascini, M., *A novel optical biosensor format for the detection of clinically relevant TP53 mutations.* Biosensors and Bioelectronics, 2005. **20**(11): p. 2310-2313.

15. Jiang, T., Minunni, Maria.,Wilson, P.,Zhang, Jian.,Turner, A.P.F., and Mascini, Marco, *Detection of TP53 mutation using a portable surface plasmon resonance DNA-based biosensor*. Biosensors and Bioelectronics, 2005. **20**(10): p. 1939-1945.

16. Wang, R., Tombelli, Sara.,Minunni, Maria.,Spiriti, Maria Michela and Mascini, Marco, *Immobilisation of DNA probes for the development of SPR-based sensing.* Biosensors and Bioelectronics, 2004. **20**(5): p. 967-974.

17. Mannelli, I., Minunni, Maria., Tombelli, Sara., Wang, Ronghui., Michela, Spiriti Maria and Mascini, Marco., *Direct immobilisation of DNA probes for the development of affinity biosensors.* Bioelectrochemistry, 2005. **66**(1-2): p. 129-138.

18. Yu, J.C.C., Lai, Edward P. C and Sadeghi, Susan., *Surface plasmon resonance sensor for Hg(II) detection by binding interactions with polypyrrole and 2-mercaptobenzothiazole.* Sensors and Actuators B: Chemical, 2004. **101**(1-2): p. 236-241.

19. Petrenko, V.A. and G.P. Smith, *Phages from landscape libraries as substitute antibodies.* Protein Eng., 2000. **13**(8): p. 589-592.

20. Barbas, C.F., Dennis R. Barton, Jamie K. Scott, Gregg J. Silverman., eds. *Phage display: a laboratory manual*. 2001, Cold Spring Harbor Laboratory Press.: Cold Spring Harbor, NY.

21. Naimushin., Alexei N.Soelberg,Scott D.Nguyen, Di K.Dunlap, Lucinda Bartholomew, Dwight Elkind, Jerry Melendez, Jose and Furlong, Clement E., *Detection of Staphylococcus aureus enterotoxin B at femtomolar levels with a miniature integrated two-channel surface plasmon resonance (SPR) sensor.* Biosensors and Bioelectronics, 2002. **17**(6-7): p. 573-584.

22. Irwin H.Segel.,Arwin H.Segel., *Biochemical calculations.* 1976.

23. Linda S.Jung, Charles T. Campbell., Timothy M. Chinowsky, Mimi N. Mar and Sinclair S.Yee, *Quantitative Intterepretation of the Response of Surface Plasmon Resonance Sensors to Adsorbed Films.* Langmuir, 1998. **14**: p. 5636-5648.

24. Liedberg.B, Lundstorm.I and Stenber.E., *Principles of Biosensing with an extended coupling matrix and Surfce Plasmon Resonance.* Sensors and Actuators B, 1993. **11**: p. 63-72.

25. Lukosz.W, *Principles and sensitivities of integrated optical and surface plasmon sensors for direct affinity sensing and immunosensing.* Biosensors and Bioelectronics, 1991. **6**: p. 215-225.

26. Lukosz.W, *Integrated-optical and surface-plasmon sensors for direct affinity sensing. part II: Anisotropy of adsorbed or bound protein layers.* Biosensors and Bioelectronics, 1997. **12**(3): p. 175-184.

5. PHAGE AS A MOLECULAR RECOGNITION ELEMENT IN BIOSENSORS IMMOBILIZED BY PHYSICAL ADSORPTION

Abstract

An understanding of the interactions of the probe-analyte forms an essential part of the development of a specific and sensitive biosensor. As a part of a project for the development of a biosensor for the detection of biothreat agents, this work was done to determine if phage could be used as a probe on a sensor. As a model threat agent, ß-galactosidase (ß-gal) from *E.coli* was used in this study. Binding of the selected phage to ß-gal was characterized by enzyme linked immunosorbent assay (ELISA) and a thickness shear mode (TSM) sensor in which the phage were immobilized by physical adsorption on the plastic/gold surfaces of the ELISA wells and TSM/SPR sensors respectively and reacted with their antigens (ß-gal). The specificity and selectivity of the selected probe for ß-gal was also tested and established for both ELISA and TSM sensors. A mathematical derivation for the interaction of ß-gal with both free phage in solution and with immobilized phage on the TSM sensor surface was also obtained. The dissociation constant calculated for the acoustic wave sensor based on measurements of 6 repeats was 1.7 ± 0.5 nM, while 6 ELISA experiments gave the dissociation constant of 30± 0.6 nM. The difference in affinities can be attributed to the monovalent (in ELISA) and

multivalent (in sensor) interaction of the phage with β-galactosidase, as indicated by Hill plots. The results obtained indicate that physical adsorption of landscape phage to sensor surface may produce a sensor that compares well with the one made by Langmuir-Blodgett technique. Immobilization of the probe through physical adsorption is simple and economical. The sensor demonstrates high affinity, selectivity, and specificity.

1. Introduction

It has been shown that filamentous phage, a thread-like virus which attacks bacteria, can be modified so that a collection, or 'library' of phages can be generated each of which has on its' surface a different recognition peptide specific for different targets [1, 2]. By well-known means, phages, which bind to the desired target, can be selected, isolated, and rapidly reproduced in great numbers. Landscape phages have been shown to serve as bioprobes for various biological targets [3-8]. These phage probes have been used in ELISA and thickness shear mode (TSM) quartz sensors to detect bacterial and mammalian targets [5, 9]. The TSM acoustic wave sensor is proven to be an excellent analytical tool for the study of specific molecular interactions at the solid–liquid interface [10-17]. Furthermore, acoustic wave devices were shown to be quite specific immunosensors in complex biological media containing cells and human serum. Acoustic waves in TSM are excited by the generation of a radio frequency alternating voltage in the piezoelectric crystal. Changes in the resonance frequency are usually attributed to the effect of the added mass[13, 18] due to the binding at the solid–liquid interface[17]. Acoustic wave sensors with immobilized biological recognition molecules (biosensors) were utilized for the real-time study of the adsorption of biochemical macromolecules. In

the comparative ELISA/TSM study of phage-β-galactosidase binding monolayers containing biotinylated phospholipid were transferred onto the gold surface of an acoustic wave sensor using the Langmuir- Blodgett technique. Biotinylated phage was coupled with the phospholipid via streptavidin intermediates by molecular self-assembling. The detection by the phage-β-galactosidase interaction [19] shown to be sensitive, selective, and specific.

The direct physical adsorption of the phage to the surface is a much simpler method of a phage immobilization on the sensor surface. This method was previously successfully employed for immobilization a wide range of biological elements directly on piezoelectric electrodes, including anti-human serum albumin [20], IgG[21], goat anti-ricin antibody [22] anti-vibro cholera [23], African swine fever virus protein [24] , and recombinant protein fragments of HIV specific antibodies [25] . Protein molecules adsorb strongly and irreversible on gold surfaces due to hydrophobic actions [26]. The main goal of this work is to determine if physical adsorption of the phage to the gold surface of TSM sensor provides adequate detection properties for sensing of the model protein, β-galactosidase.

2. Materials and methods

2.1 Phage

Wild type phage f8-5 and the phage (phage 1G40) selected for binding to ß-Gal was affinity selected from a landscape library as described [27]. The total number of viral particles present in phage preparations was determined by spectrophotometer using the formula [28]: virions (vir)/ml = (A_{269} × 6 x 10^{16}) /number of nucleotides in the phage genome, where A_{269} is absorbance at 269 nm. For the recombinant phages used in this

work (9198 nucleotides), the formula: absorbance unit $(AU)_{269} = 6.5 \times 10^{12}$ vir/ml was used to determine the concentration of phage particles in a solution.

2.2 ß-galactosidase

Escherichia coli ß-galactosidase was obtained from Sigma Chemical Co. (G5635) as a lyophilized powder and was dissolved in Dulbecco's phosphate buffered saline (DPBS) at final concentration of 2.4 mg/ml.

2.3 Solutions and reagents

O-nitrophenyl-ß-D- galactopyranoside (ONPG) was obtained from Sigma Chemical Co. ONPG ELISA substrate solution was prepared at concentration of 1.1 mg/ml in Z buffer composed of 0.1M $NaPO_4$, 0.01M KCl, 0.001M MgSO4, 0.05 M ß-mercaptoethanol (Petrenko et al., 2000). Dulbecco's phosphate buffered saline solution [DPBS] was obtained from BioWhittaker Inc., (17-512F). Tris-buffered saline (TBS) was prepared from Tris crystallized free base; Fisher Scientific. BP 152-1;TBS-Tween [TBS containing 0.5% (v/v) Tween]. Bovine serum albumin (BSA) Fraction V; Sigma Chemical Co. A2153; 50 mg/ml stock was filter-sterilized and stored at 4°C. Anti-β-galactosidase antibodies, monoclonal, clone GAL-13, was obtained from Sigma Chemical Co. (G-8021).

2.4 Phage sensor preparation

The quartz TSM sensors were washed in 50% Nitric acid 48 hrs and rinsed in running Millipore water for 2 minutes, and then placed in Millipore water for 3 hours. The water was changed twice and between the changes of water, sensors were washed in running Millipore water, again, this time for 1 minute. Then the sensors were immersed in Millipore water, for another three hours. Sensors then were rinsed again in running

Millipore water for 1 minute and let to dry in ambient air. After drying sensors were placed in individual 35 mm Petri dishes and used for preparation of phage sensors. A gold surface of cleaned quartz TSM sensor was exposed to a phage suspension containing 2.3×10^{11} virions/mL for 1 hour. After incubation the sensor was rinsed in Millipore water and then it was placed in wet chamber at 4 °C for 24 hours before tests with β-galactosidase began.

2.5 b-galactosidase binding measurements

2.5.1 Acoustic wave device.

Measurements were carried out using a PM-740 Maxtek plating monitor with a frequency resolution of 0.5 Hz at 5 MHz. Voltage output of the Maxtek device was recorded and records were analyzed offline. The voltage output from the Maxtek device is directly related to the resonance frequency of the quartz crystal sensor. Changes in the resonance frequency of the quartz crystal sensor were used to monitor the binding of vesicles in tissue homogenates to the sensor surface. The observed changes are hypothesized to be due to viscoelastic changes of the film near surface fluid media and the mass change associated with binding of the protein molecules.

2.5.2 Binding measurements.

AT-cut planar quartz crystals with a 5 MHz nominal oscillating frequency were purchased from Maxtek Inc. Circular gold electrodes were deposited on both sides of the crystal for the electrical connection to the oscillatory circuit. The quartz crystal microbalance was calibrated by the deposition of well-characterized stearic acid monolayers [16]. The sensor with the immobilized phage was positioned in the probe arm of the instrument just before delivery of samples. Immediately after recording was

started, 800 µl phosphate buffer saline (DPBS) was delivered with a pipette to the sensor surface and voltage was recorded for 8 min. Then DPBS was removed carefully with a plastic pipette tip and a new recording was initiated. Solutions of β-galactosidase of different dilutions (0.0032 – 210 nM) were added sequentially to the sensor and the same measuring procedure was performed. Each experiment was replicated two to four times. The temperature of all samples was 25°C. The data were stored and analyzed offline. Approximately 480 data points taken once a second were collected during each 8-min run. The steady state portion of the recorded signal of about 200 data points were averaged and used as a value of respon se in dose response plots [14].

2.5.3 Specificity of binding

The specificity of 1G40 phage binding to β-galactosidase cells was examined in a blocking experiment in which free phage was incubated with the β-galactosidase solution prior to exposure of the biosensor with the immobilized phage. The phage sensor was prepared as described in section 2.4 and then treated with 0.1% BSA in TBS for 1 hour at room temperature. Then the sensor was exposed to phage suspensions (2.2×10^{12}-3.36×10^{7} vir/ml) incubated with 22 nM β-galactosidase prior to the exposure.

2.6 Enzyme-linked immunosorbent assay (ELISA) with ß-galactosidase

Wells of a polystyrene ELISA plate[Corning Incorporated.] were coated with 40-µl samples – either 1G40 or f8-5 filamentous phage at 5×10^{11} virions/ml in TBS [overnight at 4°C. The dish was then washed 5 times with TBS-Tween to block non-specific binding in a Bio-Tek EL_x405 auto plate washer (Bio-Tek Instruments Inc.). 45-µl samples of ß-galactosidase at concentrations ranging from 250 to 0.24 nM in 0.1M $NaPO_4$, 0.01M KCl buffer were added to wells and incubated on a rocker at room temperature for 1 hour.

After the plate was again washed 5 times with TBS-Tween the wells were filled with 90 µl of ONPG substrate solution and read on a kinetic plate reader as previously described [29]. The slope of color development was measured as a change in optical density per 1,000 min (mOD/min) using a EL808 Ultra Microplate Reader (Bio-Tek Instruments Inc.). Wild-type vector f8-5 served as a negative control for evaluation of nonspecific background binding. A separate experiment with phages replaced with anti-ß-galactosidase antibodies was used a positive control.

2.7 Binding equations

Quantification of binding was done as described [19]. In short the binding equations were applied to analyte-phage interactions. The ratio of occupied (Y) and free (1-Y) phages on the sensor surface can be determined as

$$\log(Y/(1-Y)) = \log K_b + n \times \log[C] \quad (1)$$

where, K_b is the association binding constant, C is a β-galactosidase concentration, and n is the number of molecules bound to a single phage.

A plot of the left-hand side of equation (1) versus log[C] is known as a Hill plot [30]. It gives an estimate of n from the slope, K_b from the ordinate intercept, and EC_{50} at the point when Y=1-Y.

In specificity experiments, when β-galactosidase binds first with a free phage in solution during pre-incubation and then free β-galactosidase (unbound with free phage) binds the immobilized phage on a surface of sensor. The reactions between analyte and free and immobilized phage can be schematically presented as

$$A + mP \rightleftharpoons AP_m \quad (2)$$

Where, m is a numbers of molecules of free and phages bound to a single molecule of analyte.

The association binding constant for interactions with free phages K_f can be defined using the mass action low [31]

$$K_f = [AP_m]/([A] \times [P]^m) \quad (3)$$

The total number of the analyte molecules is composed of the free and bound to free phages (we assume that number immobilized phages is much smaller that number of phages in suspension):

$$C_A = [A] + [AP_m] \quad (4)$$

Dividing both sides of Eq. (4) by C_A after rearranging we get:

$$[AP_m]/C_A = 1 - [A]/C_A \quad (5)$$

Combining Eqs. (3) and (4) we can determine the fraction of analyte bound to free phages:

$$X = [AP_m]/C_A = K_f[P]^m/(1 + K_f[P]^m) \quad (6)$$

The fraction of free analyte is equal to 1-X. Therefore, ratio of

$$X/(1-X) = [P]^m/K_f \quad (7)$$

When analyte that is not bound to free phage binds the phage immobilized on the sensor surface the mass of the sensor element increases due to the transfer of the analyte molecules from solution to the surface, which we denote Δm, and the maximal mass change is proportional to the total number of analyte molecules:

$$[A] \sim \Delta m \quad (8)$$

$$[C_A] \sim \Delta m_{max} \quad (9)$$

The fraction of analyte bound to the sensor can be expressed as

$$Y = [A]/C_A = \Delta m/\Delta m_{max} \quad (10)$$

Using Eqs (5) and (10) Eq. (7) can be written as following:

$$(1-Y)/Y = [P]^m/K_f \quad (11)$$

Taking the logarithm of both sides, of Eq. (11) we get

$$\log((1-Y)/Y)=m\times\log[P_f]-\log K_f \quad (12)$$

A plot of the left-hand side of Eq. (12) versus $\log[P_f]$ yields an estimate of m from the slope, K_f from the ordinate intercept, and EC_{50} from the point when Y=1-Y. If the plot analyzed by a linear regression y=a+bx, then m=b, $K_f = 10^{-a}$; $(K_f)_{apparent} = K_f^{1/b}$; $EC_{50}=10^{-a/b}$, and $K_f=(EC_{50})^b$.

3. Results and discussion

3.1. Specificity and selectivity of b-galactosidase binding

Binding of phages to β-galactosidase was initially analyzed by ELISA in which the phages were immobilized on the plastic surface of the ELISA wells and interacted with β-galactosidase in the presence and absence of BSA. Figure 5.1 shows results of ELISA experiments in which β-galactosidase reacted directly with immobilized peptide-bearing phages. The data demonstrate specific, dose-dependent binding of selected phage 1G40, while interaction with wild type phage, f8-5 produce no response. The results are consistent with those obtained by [32]. The presence of 10 µg BSA together with β-galactosidase produced a small change in the dose-response curve generated by β-galactosidase alone (Figure 5.1, ?). This indicated that the binding of the selected phage and β-galactosidase is selective. The selectivity of binding is further demonstrated by experiment in which phages were first immobilized in the wells of ELISA plate and then exposed to the mixture of 16nM ß galactosidase and BSA that varied in the range of 3.9 – 2000 µg/mL (Figure 5.1, Insert). If we assume that an average molecular weight of BSA is equal ~66429 Da [33] then the highest concentration of BSA was 30 µM. A marked

selectivity for β-galactosidase over BSA was observed in mixed solutions even when the concentration of BSA exceeded the concentration of β-galactosidase by the factor of ~2000.

When phages were immobilized on the surface of an acoustic wave sensor as described in the experimental section and exposed to β-galactosidase at different concentrations a typical dose response curve appeared as shown in Figure 5.2 A (upper curve labeled by ¦). The normalized mean values of steady-state output sensor voltages were plotted as a function of β-galactosidase concentrations. The binding dose-response curve had a typical sigmoid shape and the signal was saturated at the β-galactosidase concentration of about 200 nM. The ELISA dose-response curve plotted in the same graph (Figure 5.2 A, lower curve labeled by ?) looked similar but it is shifted towards higher concentration of β-galactosidase by ~6 nM and becomes steeper. The dissociation constant calculated for the acoustic wave sensor based on measurements of 6 repeats was 1.7 ± 0.5 nM, while 6 ELISA experiments gave the dissociation constant of 30± 0.6 nM. The difference in affinities can be attributed to the monovalent (in ELISA) and multivalent (in sensor) interaction of the phage with β-galactosidase, as indicated by Hill plots (Figure 5.2B). One or another mode of interaction probably depends on the conformational freedom of the phage immobilized to the solid surface. Binding of the phage to β-galactosidase on the sensor surface was very selective, because presence of 360-fold excess of bovine serum albumin in mixture with β-galactosidase reduces the biosensor signal only by 2%.The dissociation constant obtained with the phage bound by physical adsorption in

this work compares well with one obtained by Langmuir-Blodgett method[19]. This dissociation constant also compares well with one found for antibodies isolated from a phage display library [34].

Binding of the immobilized phage to β-galactosidase is quite specific because the biosensor response is reduced in dose-dependent manner if β-galactosidase is incubated with free phage prior to the exposure. Figure 3 shows the dose response of the sensor to β-galactosidase incubated with free phage before it was added to the sensor surface. The response is reduced by 65% if β-galactosidase is pre-incubated with 2.2×10^{11} vir/ml of free phage. The data shown in Figure 3 fit well with Eq. (12) in the whole examined range of free phage concentrations of 8.4×10^{5} – 2.2×10^{11} vir/mL. The apparent value of the dissociation constant of the interaction of free phage with β-galactosidase obtained from the linear fit ($k_{d(apparent)}$=9.1±0.9 pM) has appeared to be smaller compared with the one calculated for the bound phage (1.7 ± 0.5 nM). The difference could be explained by the higher degree of freedom and accessibility of free phage compared to one bound to the sensor surface.

These results show that physical adsorption of landscape phage to sensor surface may produce a sensor that compares well with the one made by Langmuir-Blodgett technique. The method of physical adsorption is simple and economical. The sensor demonstrates high affinity, selectivity, and specificity.

4. Figures

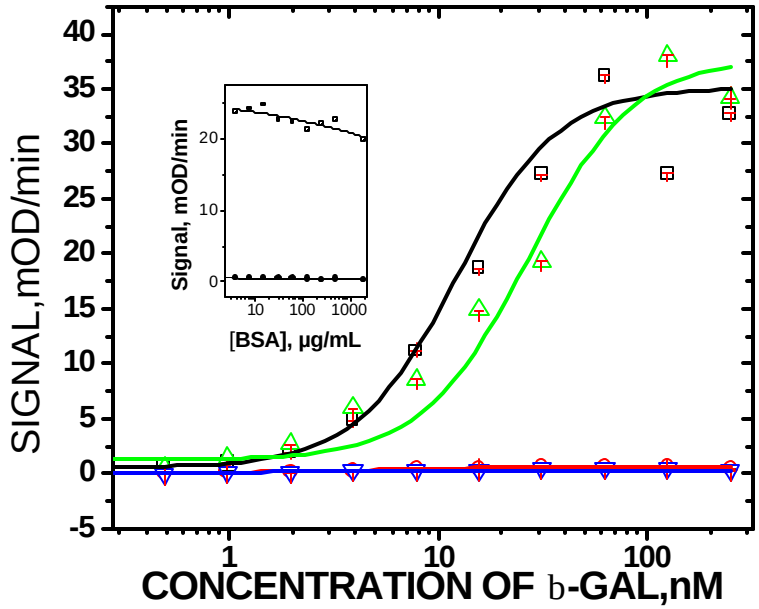

Figure 5.1. Dose-dependent binding of b-galactosidase to the phage immobilized to ELISA plate.

? -binding of 1G40 phage with β-galactosidase; ? - binding of 1G40 phage with β-galactosidase in the presence of 10 µg/ml of Bovine serum albumin (BSA); ? - binding of f8-5 wild type phage with β-galactosidase; ? -binding of f8-5 wild type phage with β-galactosidase at the presence of 10 µg/ml of Bovine serum albumin (BSA); Each experiment was replicated six times. The mean relative errors were as following: ? - 0.004; ? -0.002; ? - 0.002; ? -0.004.

Insert: Selectivity of binding of the phage to ß-galactosidase (ELISA). The selected phage, 1G40-A (upper curve) and a wild type phage, f8-5-B, (lower curve) were first immobilized in the wells of ELISA plate and then exposed to the mixture of 16 nM ß-galactosidase and BSA that varied in the range of 3.9 – 2000 µg/mL.). The upper curve was the sigmoid fit to experimental data (χ=0.94, R2=0.78); the lower data were smoothed by a linear fit (Signal = 0.57[BSA]-0.078; R2=0.91, p<0.0001). The mean relative errors were ¦ -0.04; ? -0.01

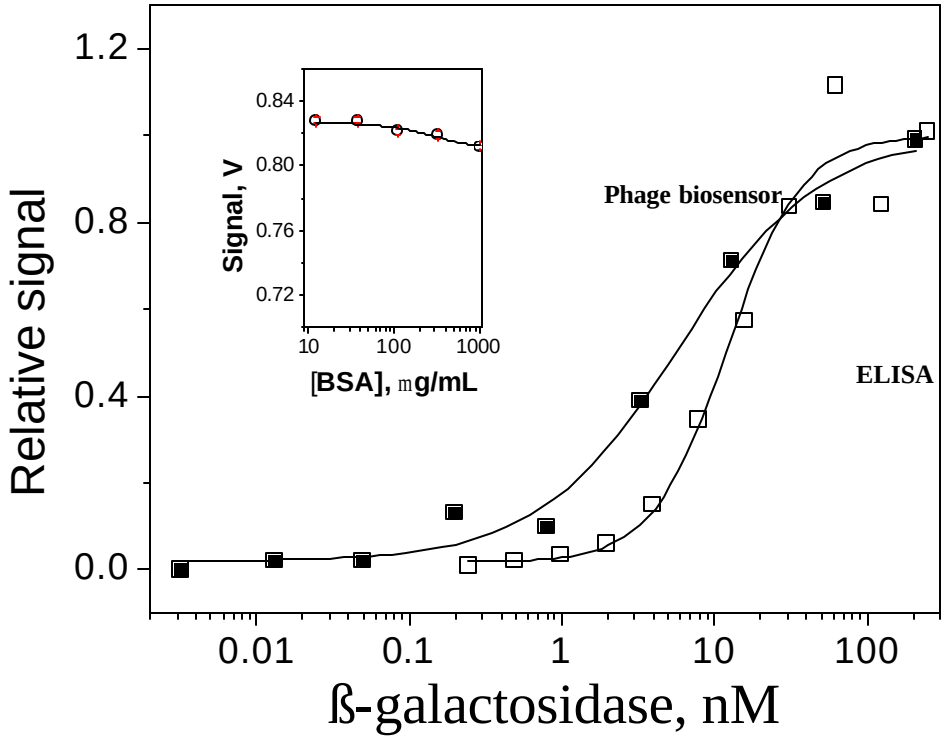

Figure 5.2 A. Dose-dependent binding of β-galactosidase to the 1G40 phage immobilized to ELISA plate and to the acoustic wave sensor. The upper curve represents the mean values of steady-state bound mass as a function of β-galactosidase concentrations measured by the phage biosensor. The biosensor signals were normalized at the maximal binding of 0.51 V. The smooth curve is the sigmoid fit to the experimental data ($\chi^2=5.9\times10^{-4}$, R^2 = 0.99). The mean relative error was 0.02. The lower line shows the dose-dependent binding measured by ELISA and normalized by a maximal signal of 47.35 mOD/min. The smooth curve is the sigmoid fit to the experimental data (($\chi^2=6.4\times10^{-4}$, R^2 = 0.98).

Insert: Selectivity of binding of the phage to ß-galactosidase (Biosensor). The phage, 1G40-A was first immobilized on the surface of the sensor and then exposed to the mixture of 50 nM of ß galactosidase and BSA that varied in the range of 10 – 1200 µg/mL.. The curve was the sigmoid fit to experimental data ($\chi=3.34$, $R^2=0.92$). The mean relative error was 0.0002.

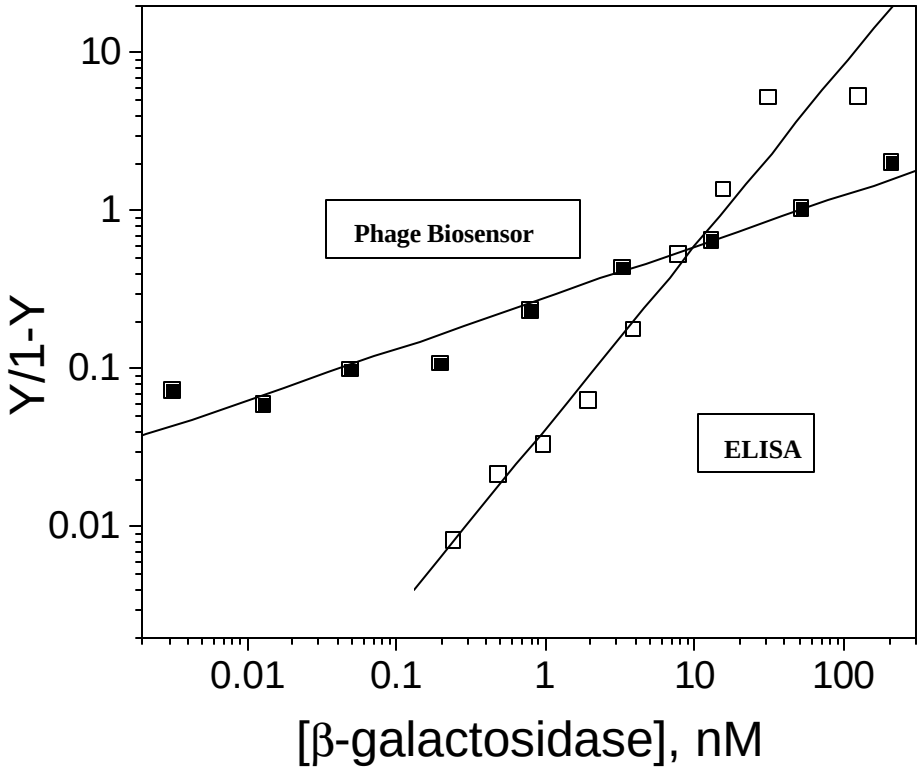

Figure 5.2 B. The Hill plots of binding isotherms had shown in **fig.2A**. The ratio of occupied and free phages is shown as a function of β-galactosidase concentrations measured by a phage biosensor and ELISA, respectively. The biosensor straight line is the linear least squares fit to the data (slope = 0.32±0.03; R=0.98, $p<0.0001$). The ELISA straight line is the linear least squares fit to the data (slope = 1.15± 0.08; R=0.98, $p<0.0001$).

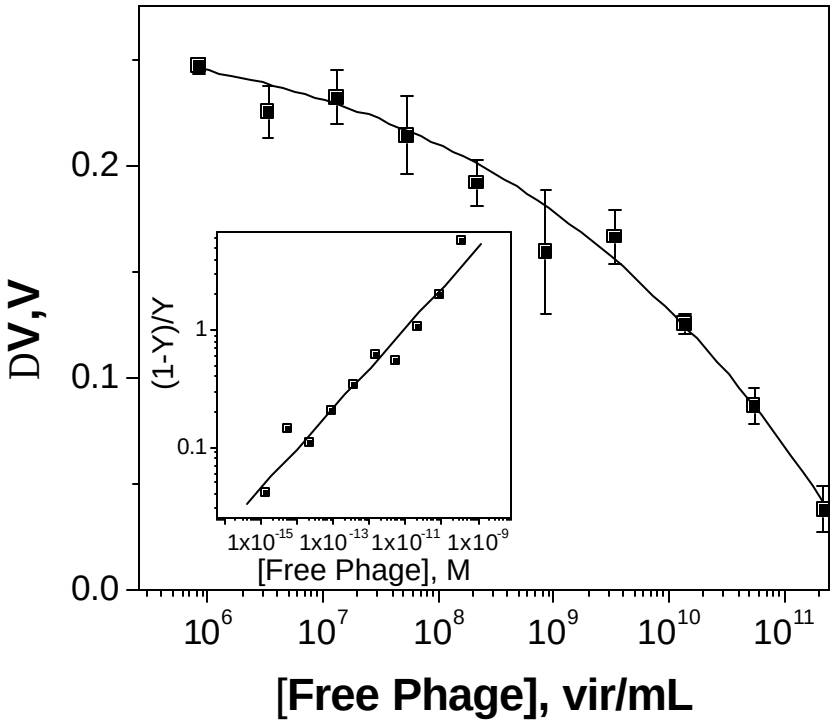

Figure 5.3. The specificity of β-galactosidase binding to the 1G40 phage immobilized to the gold surface of the sensor. The curve shows the dose response of the sensor to β-galactosidase incubated with free phage prior to the exposure. 22 nM β-galactosidase were incubated with phages at concentration range of 8.4×10^5 – 2.2×10^{11} vir/mL in DPBS for 1 hour. The smooth curve is the sigmoid fit to the experimental data (χ=0.57, R^2=0.99).

Insert: A plot of the left-hand side of Eq. (12) versus log [P_f]. The line represents the least square fit of Eq. (12) with a slope=0.34±0.03, R=0.98, p<0.0001; $k_d=1.72\times10^{-4}$ M, $k_{d(apparent)}=9.1\times10^{-12}$ M.

4. References

1. Petrenko, V.A., Smith, G.P., Gong, X., and Quinn, T, *A library of organic landscapes on filamentous phage.* Protein Engineering, 1996. **9**: p. 797-801.
2. Smith, G.P., Petrenko, V.A.,, *Phage display.* Chemical reviews, 1997. **97**: p. 391-410.
3. Romanov, V.I., D.B. Durand, and V.A. Petrenko, *Phage display selection of peptides that affect prostate carcinoma cells attachment and invasion.* Prostate, 2001. **47**(4): p. 239-251.
4. Legendre, D. and J. Fastrez, *Construction and exploitation in model experiments of functional selection of a landscape library expressed from a phagemid.* Gene, 2002. **290**: p. 203-215.
5. Petrenko, V.A. and G.P. Smith, *Phages from landscape libraries as substitute antibodies.* Protein Engineering, 2000. **13**(8): p. 589-592.
6. Petrenko, V.A., Smith, G.P.,Mazooji, M.M.,Quinn, T., *Alpha-helically constrained phage display library.* Protein Engineering, 2002. **15**(11): p. 943-950.
7. Samoylova, T.I., Petrenko, V.A., Morrison, N.E., Globa, L.P., Bekker, H.J.,Cox, N.R.,., *Phage Probes for Molecular Profiling of Malignant Glioma Cells.* Molecular Cancer Pharmaceuticals, 2003. **2**: p. 1-9.
8. Mount, Jane D., Samoylova, Tatiana I., Morrison, Nancy E., Cox, Nancy R., Baker, Henry J., Petrenko, Valery A., *Cell Targeted Phagemid Rescued by Pre-Selected Landscape Phage.* Gene, 2004.
9. Petrenko, V.A. and V.J. Vodyanoy, *Phage display for detection of biological threat agents.* Journal of Microbiological Methods, 2003. **1768**: p. 1-10.

10. Bunde, R.L.J., Eric J. Rosentreter, Jeffrey J., *Piezoelectric quartz crystal biosensors.* Talanta, 1998. **46**(6): p. 1223-1236.

11. O'Sullivan, C.K., Guilbault, G.G., *Commercial quartz crystal microbalances-theory and applications.* Bisoensors and Bioelectronics, 1999. **14**: p. 663-670.

12. Cavicacute, B.A., Hayward, G.L., Thompson, M.,, *Acoustic waves and the study of biochemical macromolecules and cells at the sensor-liquid interface.* Analyst, 1999. **124**: p. 1405- 1420.

13. Kaspar, M., Stadler, H., Weiss, T., Ziegler, C.,, *Thickness shear mode resonators ("mass-sensitive devices") in bioanalysis.* Fresenius' Journal of Analytical Chemistry, 2000. **366**: p. 602-610.

14. Pathirana, S.T., Barbaree, J.,Chin, B. A.,Hartell, M. G.,Neely, W. C.,Vodyanoy, V., *Rapid and sensitive biosensor for Salmonella.* Biosensors and Bioelectronics, 2000. **15**(3-4): p. 135-141.

15. Samoylova, T.I., Ahmed, Bushra Y.,Vodyanoy, Vitaly.,Morrison, Nancy E.,Samoylov, Alexandre M.,Globa, Ludmila P.,Baker, Henry J.,Co x, Nancy R., *Targeting peptides for microglia identified via phage display.* Journal of Neuroimmunology, 2002. **127**(1-2): p. 13-21.

16. Samoylov, A.M., Samoylova, T. I. Pathirana, S. T. Globa L. P. and Vodyanoy V.J., *Peptide biosensor for recognition of cross-species cell surface markers.* Journal of Molecular Recognition, 2002. **15**: p. 197-203.

17. Olsen, E.V., Pathirana, S. T.,Samoylov, A. M.,Barbaree, J. M.,Chin, B. A.,Neely, W. C.,Vodyanoy, V., *Specific and selective biosensor for Salmonella and its*

detection in the environment. Journal of Microbiological Methods, 2003. **53**(2): p. 273-285.

18. Muramatsu, H., Kajiwara, K.,Tamiya, E.,Karube, I., *Piezoelectric immuno sensor for the detection of candida albicans microbes.* Analytica Chimica Acta, 1986. **188**: p. 257-261.

19. Petrenko, V.A.V., Vitaly J., *Phage display for detection of biological threat agents.* Journal of Microbiological Methods, 2003. **53**(2): p. 253-262.

20. Muratsugu, M., Ohta, F., Miya, Y., Hosokawa, T., Kurosawa, S., Kamo, N. & Ikeda, H., *Quartz-Crystal Microbalance for the Detection of Microgram Quantities of Human Serum-Albumin - Relationship between the Frequency Change and the Mass of Protein Adsorbed.* Analytical Chemistry, 1993. **65**: p. 2933-2937.

21. Minunni, M., Skladal, P. & Mascini, M., *A Piezoelectric Quartz-Crystal Biosensor as a Direct Affinity Sensor.* Analytical Letters, 1994. **27**: p. 1475-1487.

22. Carter, R.M., Jacobs, M. B., Lubrano, G. J. & Guilbault, G. G., *Piezoelectric Detection of Ricin and Affinity-Purified Goat Anti-Ricin Antibody.* Analytical Letters, 1995. **28**: p. 1379-1386.

23. Carter, R.M., Mekalanos, J.J., Jacobs, M.B., Lubrano, G.J. & Guilbault, G.G., *Quartz crystal microbalance detection of Vibrio cholerae O139 serotype.* Journal of Immunological Methods, 1995. **187**: p. 121-125.

24. Uttenthaler, E., C. Ko[ss]linger, and S. Drost, *Characterization of immobilization methods for African swine fever virus protein and antibodies with a piezoelectric immunosensor.* Biosensors and Bioelectronics, 1998. **13**(12): p. 1279-1286.

25. Aberl, Franz., Wolf, Hans., Ko[ss]linger, Conrad., Drost, Stephan., Woias, Peter., Koch, Sabine., *HIV serology using piezoelectric immunosensors.* Sensors and Actuators B: Chemical, 1994. **18**(1-3): p. 271-275.

26. Horisberger, M., Vauthey, M., *Labeling of colloidal gold with protein.* Histochemistry, 1984. **80**: p. 13-18.

27. Petrenko, Valery A. Smith, George P., *Phages from landscape libraries as substitute antibodies.* Protein Eng., 2000. **13**(8): p. 589-592.

28. Barbas, C.F., III, Barton, D.R., Scott, J.K.,Silverman, G.J. (Eds.),Barbas, C.F., III, Barton, D.R., Scott, J.K.,Silverman, G.J. (Eds.)., *Phage display : a laboratory manual.* 2001, Cold Spring Harbor Laboratory Press.: Cold Spring Harbor, NY.

29. Yu, J., Smith, G.P.,, *Affinity maturation of phage-displayed peptide ligands.* Methods in Enzymology, 1996(267): p. 3-27.

30. Irwin H.Segel., *Biochemical calculations.* 1976.

31. Connors K.A., *Binding Constants. The Measurements of Molecular Complex Stability.* 1987.

32. Petrenko, V.A., Smith, G.P.,Mazooji, M.M.,Quinn, T., *{alpha}-Helically constrained phage display library.* Protein Eng., 2002. **15**(11): p. 943-950.

33. Wada, Y., *Primary Sequence and Glycation at Lysine-548 of Bovine Serum Albumin.* Journal of Mass Spectrometry, 1996. **31**: p. 263-266.

34. Vaughan, T.J., Williams, A.J., Pritchard, K., Osboum, J.K., Pope, A.R., Earnshaw, J.C., McCafferty, J., Hodits, R.A., Wilton, J., Johnson, K.S.,, *Human anitbodies with sub-nanomolar affinities isolated from a large non-immunized phage display library.* Nature Biotechnology, 1996. **14**: p. 309-314.

6. PHAGE BASED BIOSENSOR RESPONSES: A COMPARATIVE STUDY USING ELISA, THICKNESS SHEAR MODE SENSOR AND SPREETA™ SENSOR

Abstract

As a part of a project for environmental monitoring of biothreat agents, this work was done to determine if filamentous phage could be used as a recognition molecule on a sensor. ß -galactosidase (ß-gal) from *E.coli* was used as a model threat agent. Binding of ß–gal to the selected landscape phage [1] was characterized by enzyme linked immunosorbent assay (ELISA), thickness shear mode (TSM), surface plasmon resonance (SPR-SPREETA ™) sensors and the responses obtained were compared. The landscape phage was immobilized through physical adsorption [2]. The characteristics of the gold surfaces of both the TSM and SPR sensors were investigated using an atomic force microscope (AFM). The influence of the different diluents employed on the distribution of phage on a formvar, carbon coated copper grids was also studied using a transmission electron microscope (TEM).

1. Introduction

A sensitive and specific biosensor is essential in the early detection of any bio-threat agent. In order to achieve this, optimum configuration of the biosensor system using the most suitable recognition probe needs to be first characterized and its responsiveness on different platforms tested and compared. We have already reported the use of filamentous phage as a molecular recognition element using ELISA, TSM and SPR sensors. Landscape phages have been shown to be selective for various biological targets[3-6]. The TSM sensor has been proven successful for the study of specific molecular interactions at the solid–liquid interface [7-12]. Changes in the resonance frequency of the TSM sensors are usually attributed to the effect of the added mass[13] due to the binding at the solid–liquid interface[12] SPREETA™ has been used for the detection of analysis of biomolecular interactions with biomaterials [14]; *E. coli* enterotoxin [15]; structural analysis of human endothelin-1 [16] and characterization of thin film assembly [17]. Sample investigation through this platform can be achieved without any labeling; unlike other devices uses comparatively low volumes of reagents and can be used for the detection of biological warfare agents[18]. The simpler method of immobilization through physical adsorption was successfully employed for the immobilization of a wide range of biological elements ranging from anti-vibro cholera[19], African swine fever virus protein[20] and IgG [21]. Evidence of irreversible adsorption of protein molecules to gold surfaces due to hydrophobic actions was previously reported [22]. The viability of both TSM and SPR sensors for use a biosensors have been compared for the study of whole blood and plasma coagulation[23],

in the structural analysis of human endothelin-1[16] and study of DNA assembly and hybridization [24]. The chief goal of this work is to compare the responses obtained from ELISA, TSM and SPR sensors. AFM studies on average roughness changes due to the cleaning procedures employed are aslo studied. Images of the filamentous phage selected for ß-gal were also obtained using TEM in a bid to understand the orientation of phage. The real time measurements in these platforms are achieved by immobilizing the probe on the platform and allowing it to come into contact with the target analyte. The binding kinetics such as the association (K_a) and dissociation (K_d) constants determine the sensitivity of the probe-analyte complex. Sensitivity of such biosensors mainly depend on the efficiency of probe immobilization technique, the affinity of probe to the substrate and the surface nature of the sensor interface [25-27]. The surface topography of the gold substrate on which the probe is immobilized plays a vital role for providing an optimum orientation of the probe so as to bind to the analyte. Hence, the effect of the standard cleaning processes of the gold substrate of both the TSM and SPR sensors were investigated using the AFM.

2. Materials and methods

2.1 Phage

Wild type phage f8-5, with no sensitivity to ß-gal and the phage (phage 1G40) selected for binding to ß-Gal was affinity selected from a landscape library as described [3].

For the recombinant phages used in this work (9198 nucleotides), the formula:

$$\text{Absorbance unit (AU)}_{269} = 6.5 \times 10^{12} \text{ vir/ml}$$

was used to determine the concentration of phage particles in a solution.

2.2 ß-galactosidase

Escherichia coli ß-galactosidase was obtained from Sigma Chemical Co. (G5635) as a lyophilized powder and was dissolved in Dulbecco's phosphate buffered saline (DPBS) at final concentration of 2.4 mg/ml.

2.3 Materials

2.3a ELISA, TSM and SPR sensor

Polystyrene ELISA plate [Corning Incorporated]; Bio-Tek EL_x405 auto plate washer [Bio-Tek Instruments Inc]; EL808 Ultra Microplate Reader (Bio-Tek Instruments Inc); O-nitrophenyl-ß-D- galactopyranoside (ONPG) was obtained from Sigma Chemical Co. ONPG ELISA substrate solution was prepared at concentration of 1.1 mg/ml in Z buffer (composed of 0.1M NaPO4, 0.01M KCl, 0.001M MgSO4, 0.05M ß-mercaptoethanol) [3]. Dulbecco's phosphate buffered saline solution [DPBS] was obtained from BioWhittaker Inc., (17-512F). Tris-buffered saline (TBS) was prepared from Tris crystallized free base; Fisher Scientific, BP 152-1; TBS-Tween [TBS containing 0.5% (v/v) Tween]. Bovine serum albumin (BSA) Fraction V; Sigma Chemical Co. A2153; 50 mg/ml stock dissolved in Millipore water was filter-sterilized and stored at 4°C. O.64 mm (inner diameter) silicone tubing (Cole Parmer, cat #: 07625-22), 3mL latex syringes

(Becton and Dickinson) and 2 mL polypropylene cryogenic, round bottomed tubes cylinder (Corning, cat #: EW-44351-15)

2.3b Atomic force microscopy

The TSM AT-cut planar quartz crystals were obtained from Maxtek (Santa Fe Springs, CA). Circular gold electrodes were vapor deposited on both sides of the crystal. The sensing interface of the SPR sensors consisted of Gold-coated borosilicate glass slides (15×4×0.2 mm). Both the sensors were initially coated with chromium and then followed by gold. A *SPM-100*™ (Nanonics Imaging Ltd, Jerusalem Israel) NSOM & SPM System was used to study the distribution of phage particles on the surfaces of gold gilded, carbon coated formvar grids.

2.3c Transmission electron microscopy

Gold guilder formvar, carbon coated grids and formvar, carbon coated 300 mesh copper grids (Electron Microscopy Sciences, Hatfield, PA); 2% phosphotungstic acid (PTA) [Fischer Scientific Company, Fairlawn, New Jersey]; wetting agent (0.1% BSA) and Philips 301 Transmission Electron Microscope (TEM) [FEI Company Hillsboro, Oregon]

3. Phage immobilization on sensors

3.1 TSM sensor preparation

The quartz TSM sensors were washed in 50% Nitric acid for 48 hours, rinsed in running Millipore water for 2 minutes, and then placed in Millipore water for 3 hours. The water was changed twice and between the changes of water, sensors were washed in running Millipore water, again, this time for 1 minute. Then the sensors were immersed in Millipore water, for another three hours. Sensors then were rinsed again in running Millipore water for 1 minute and let to dry in ambient air, stored and used within 1 hour

of cleaning. The gold surface of cleaned quartz TSM sensors was exposed to a phage suspension containing 2.3×10^{11} virions/mL for 1 hour. After incubation the sensor was rinsed in Millipore water and then it was placed in wet chamber at 4 °C for 24 hours before tests with β-galactosidase began.

3.2 SPR sensor preparation

All SPR sensors were plasma cleaned in Argon using Plasmod ™ system (Manchester Inc) at 1 torr for 5 minutes prior to phage immobilization on the gold surfaces through physical adsorption for both flow through and batch mode of investigations. In the flow through mode, both the inlet and outlet silicone tubing were of uniform internal diameter (0.64 mm). Polypropylene tubes [Corning] of 2 ml capacity were used as both the inlet and outlet tubes in the flow system.

4. ß-galactosidase binding measurements

4.1 Enzyme-linked immunosorbent assay (ELISA)

Polystyrene ELISA plate wells were coated with 40 µl of either 1G40 or f8-5 filamentous phages at a concentration of 5×10^{11} virions/ml in TBS overnight at 4°C, following which the wells were washed five times with TBS Tween using a Bio-Tek EL_x 405 auto plate washer so as to ensure the prevention of non-specific binding. Following the wash, 45µl of ß-gal samples ranging in concentrations from 0.0032-210 nM in 0.1M $NaPO_4$, 0.01M KCl buffer was added to the wells and incubated in a rocker at room temperature for one hour. This was followed with another five washes with TBS Tween as described before, following which 90µl of ONPG substrate solution was added and kinetic readings were obtained as previously described [28]. The slope of color development was measured as a change in optical density (OD) over a period of 1hour, with readings at every 3 minute

intervals using an EL808 Ultra Microplate Reader. Wild type phage f8-5 served as a negative control for the evaluation of non-specific background binding.

4.2 Acoustic wave device.

A PM-740 Maxtek plating monitor with a frequency resolution of 0.5 Hz at 5 MHz was used to carry out the acoustic wave sensor measurements. Voltage output changes were recorded via a computer interface card and analyzed using Origin software. The voltage output from the Maxtek device is directly related to the resonance frequency of the quartz crystal sensor. The observed changes are hypothesized to be due to viscoelastic changes of the film near surface fluid media and the mass change associated with binding of the protein molecules.

4.2.1 Binding measurements.

5 MHz nominal oscillating frequency, AT cut crystals [Maxtek Inc.] deposited on both sides with gold electrodes to enable connection to the oscillatory circuit were used for this study. The crystals were calibrated as described [29]. To the sensor with the immobilized phage 800 µl of DPBS was delivered via a pipette onto the sensor surface and voltage readings were recorded for 8 minutes. After this, the solution was pipetted out and sequential addition of solutions (0.0032-210 nM) of the analyte (β-gal) was added onto the crystal, starting with the lowest concentration and the voltage changes were recorded. All experiments were conducted at room temperature (25°C). All data were collected and analyzed offline using *Mircocal Origin* software. The steady portion of the recorded signals were averaged and this was used as a value for plotting the dose response curves [9].

4.3 Surface plasmon resonance (SPREETA™) sensor

SPREETA™, a dual channel miniature sensor (Texas instruments) that belongs to the class of SPR sensors that use angle interrogation was used in this study. The various components of the device and the flow cell and their different functions are as described[30]. The wavelength of the light employed for interrogation of the angle change is 830 nM and the approximate flow rate of all solutions was set at 150µl/min.

4.3.1 SPR binding measurements.

A cleaned, gold surface of the sensor was exposed to a phage suspension at a concentration of 3.2×10^{11} virions/mL until saturation was achieved in flow through experiments (in approximately 3 hours) and followed by washing with Dulbecco's phosphate buffered saline (DPBS). Bovine serum albumin (2 mg/mL) was utilized to block the uncovered sensor surface. The sensor was then exposed to graded concentrations of ß-gal solutions with intermediate washes of DPBS, and the changes in refractive units were recorded.

4.4 Atomic force microscopy

4.4.1 AFM Imaging

AFM studies were conducted using a *The SPM-100*™ (Nanonics Imaging Ltd, Jerusalem Israel) NSOM & SPM System. The system uses a piezoelectric flat scanner (thickness 7 mm) with a scan range of 70 µm Z-range and 70 µm XY-range. Cantilevered, pulled fiberglass probes with a tip size of 20 nm were used for scanning the samples. The scan area for all samples was uniform (3×1.5 µm). Unless otherwise mentioned, all samples were scanned using tapping mode in 4 sub steps with a reference force of 486.690 nN and with a sample delay of 10 ms. All samples were measured at room temperature.

4.4.2 Surface roughness calculation

The average surface roughness of the samples was calculated using the Quartz software (provided by the manufacturer). The determined value for surface topography is R_q (average roughness), the root mean square (RMS) which denotes the standard deviation of all values in z direction for the scanned area (3×1.4 µm). R_q is derived from the equation

$$Rq = \sqrt{\frac{1}{N\sum(Z_n - Z)^{-2}}}$$

Where N is the number of points in the defined area; z_n, is the z values within the scanned area and z, the current z value.

4.4.3 Preparation of samples for AFM imaging

The two sensors (TSM, and SPR samples) were subjected to two different treatment procedures. For each type of sensor, a control set (untreated) was set aside. After drying sensors/ gold coated glass slides were placed in individual 35 mm Petri dishes and used for preparation of AFM imaging. While the SPR sensors samples were subjected to plasma cleaning in Argon using Plasmod ™ system (Manchester Inc) at 1 torr for 5 minutes, the TSM sensor surfaces were subjected to cleaning with HNO_3, as described in *materials and methods*. The surface characteristics of all samples were studied the same day they underwent treatment processes.

4.5 Transmission electron microscopy

4.5.1 Negative staining

Formvar carbon coated /copper grids/formvar carbon gold guilder grids were incubated on 20 µl drops of 3.18×10^{11} vir/mL of phage solution for 20 minutes, membrane side

down. The grids were then rinsed in a drop of 2% PTA so as to aid in the removal of excess non-adhered material and then placed in a second drop of the same stain preparation for 2 minutes. The grids were dried before examination under a Philips 301 TEM at 60 Kv. Representative fields were photographed at an original magnification of 71,000, magnified 2.75 times giving us a final magnification of 195,250.

4.52 Phage loading procedures

Two procedures were employed:

Bulk: A 20µl droplet was put on a strip of parafilm and the grids were incubated atop the phage droplet for 20 minutes after which they underwent a process of drying and negative staining and drying again, following which they were examined under the Philips 301 TEM at different magnifications

***Atomized*:** In this procedure, the phage solution was loaded atop the grids after a fine uniform spray of Millipore water was applied onto the grids using a standard atomizer container.

5. Results and discussion

5.1 ELISA and TSM sensor

Dose response plots from ELISA and TSM sensor experiments are shown in fig 1. Curve A represents the responses from TSM sensor experiments in volts, as a function of increasing ß-gal concentrations. The signals were normalized at a maximal value of 0.35 volts. The smooth curve is the sigmoid fit to the experimental data ($?^2=1.4\times10^{-3}$, $R^2=0.99$). Curve B represents the mean values in mOD/min values as a function of increasing ß-gal solutions. The signal was normalized at a maximal value of 47.35 mOD/min. The smooth curve is the sigmoid fit to the experimental data ($?^2=1.2\times10^{-4}$,

R^2=0.99). Dose response curves indicated a stronger binding on a biosensor than that seen in ELISA. Hill plots obtained from binding isotherms [1] for both the ELISA and TSM sensors are shown in fig 2, which shows the ratio of occupied and free phages as a function of ß-gal concentrations. The upper straight line is the linear least squares fit to the TSM sensor data (R=0.99, slope=0.47±0.02). The bottom straight is the linear least squares fit to the ELISA data (R=0.99, slope=0.57±0.01).

5.2 SPR and TSM sensor

Dose response plots from SPR and TSM sensor experiments are shown in Fig 3. Curve A represents the mean values of steady state refractive indices change as a function of increasing concentrations of ß-gal obtained from an SPR sensor. The signals were normalized at the maximal refractive index change of 3.6×10^{-5}. The smooth curve is the sigmoid fit to the experimental data ($?^2=8.2\times10^{-4}$, R^2=0.99). Curve B represents the mean values of steady-state output voltages as a function of increasing concentrations of ß -gal obtained from a TSM sensor. The smooth curve is the sigmoid fit to the experimental data ($?^2=2.3\times10^{-3}$, R^2=0.99). The signals were normalized at the maximal voltage change of 0.43 Volts. Hill plots obtained from binding isotherms for a SPR and TSM sensors are shown in Fig 4. The ratio ofoccupied and free phages is shown as a function of ß -gal concentrations. The upper straight line is the linear least squares fit to the SPR sensor data (R=0.99, slope=0.73±0.03). The bottom straight line is the linear least squares fit to the TSM sensor data (R=0.98, slope =0.32 ±0.03).

5.3 Atomic force microscopy

Pilot studies showed that the TSM sensors which were subjected to harsher cleaning procedures showed a marked difference when compared to the control set as opposed to

less significant topographical changes observed on the SPR sensors. While the control set showed an R_q of 45.9 ±0.001 nm, the treated TSM samples showed an R_q of 31.2 ±0.003 nm. The values obtained from the SPR sensors on the other hand, showed a much smaller difference in R_q values .Figs 5a (I) , b (I) and 6a (I), b (I) exemplify typical surface changes before and after treatment of a TSM sensor and SPR sensors respectively. Table 6T.1 shows the RMS values for the control and treated TSM and SPR sensors

5.4 Transmission electron microscopy

As mentioned in materials and methods, different types of grids and loading conditions were used for TEM. Fig 6.7a and b shows the images obtained as a result of phage loaded atop formvar-Carbon coated grids using no wetting and wetting agent respectively. 0.1% BSA was used as the wetting agent. The former shows aggregation of phage as bundles while the latter shows a more uniform spread of phage particles with a number of broken off particles, which maybe due to the drying process that is involved. Fig 6.8 is a representative image obtained as a result of loading phage using bulk method, prior to which the gold gilded carbon grids were treated with a fine spray of Millipore water so as to wet the grid surface. No wetting agent (BSA) was used. The image shows a uniform dispersal of phage particles on the grid's surface with individual phage particles seen clearly. Fig 6.9 was also obtained in a similar manner using copper grids, devoid of a gold gild. In this image, phage bundles are uniformly aligned and spaced. This maybe due to the fact that phage solution used to load on the grids was diluted from the parent stock in Millipore water instead of DPBS, which is usually the diluent. This would have lowered the salt content in the phage solution and maybe responsible for the arrayed alignment of phage particles. The blobs seen invariably in all the images are the gilded

gold/carbon coat peeling off due to high temperatures generated as a result of the intensity of the rays generated by the TEM.

6. Conclusions

Experiments conducted showed that phage could be used as sensitive probe to specified target analyte for effective detection in the picomolar range. Binding studies indicate that although ELISA is useful, in establishing preliminary protocols for selection and characterization of probe-analyte that needs to be tested; sensitive and effective detection is achieved using both the TSM and SPR sensor platforms. The sensitivity of both SPR and QCM sensor show similarities. For both Platforms, the detection limit of binding to ß-gal 13 pM *(Fig: 6.3)*. The binding valences were 3.1 and 1.4 for the TSM and SPR sensor respectively. EC_{50} for the SPR sensor is about 5 times smaller than that for the TSM sensor, while effective dissociation constants (K_d) are not significantly different. Although commercially available compact TSM sensor variations allow effective deployment in the field, the SPREETA™ SPR sensor is more compact and versatile than the TSM sensor.

7. Figures

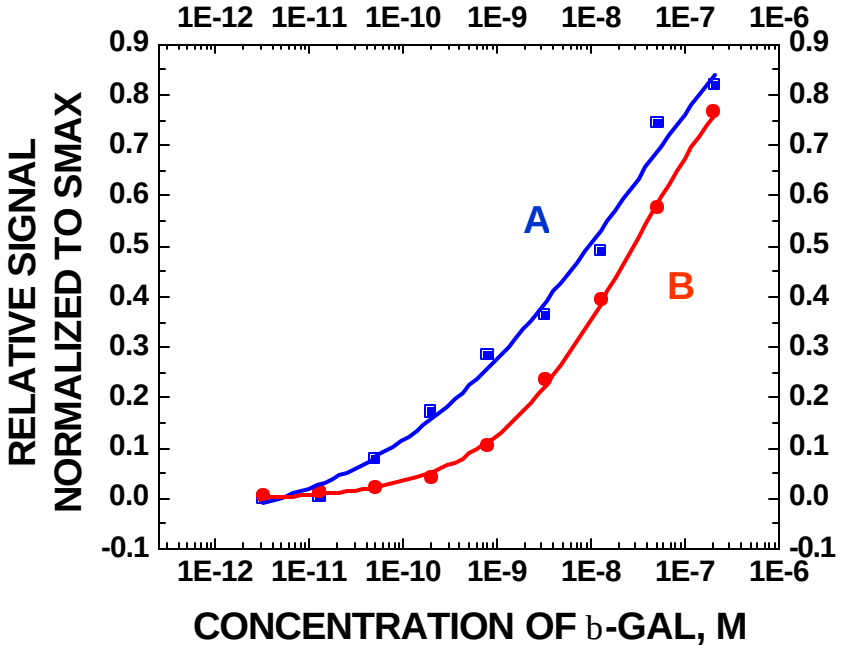

Fig 6.1: Dose response plots from ELISA and TSM sensor experiments are shown. Curve A represents the mean values of steady-state output voltages as a function of increasing concentrations of ß-gal obtained from a TSM sensor. The smooth curve is the sigmoid fit to the experimental data (-?^{2}=1.4×10^{-3}, R^2=0.99). The signals were normalized at a maximal value of 0.35 volts. Curve B represents the mean values in mOD/min values as a function of increasing ß-gal solutions. The signal was normalized at a maximal value of 47.35 mOD/min. The smooth curve is the sigmoid fit to the experimental data (-?^{2}=1.2×10^{-4}, R^2=0.99).

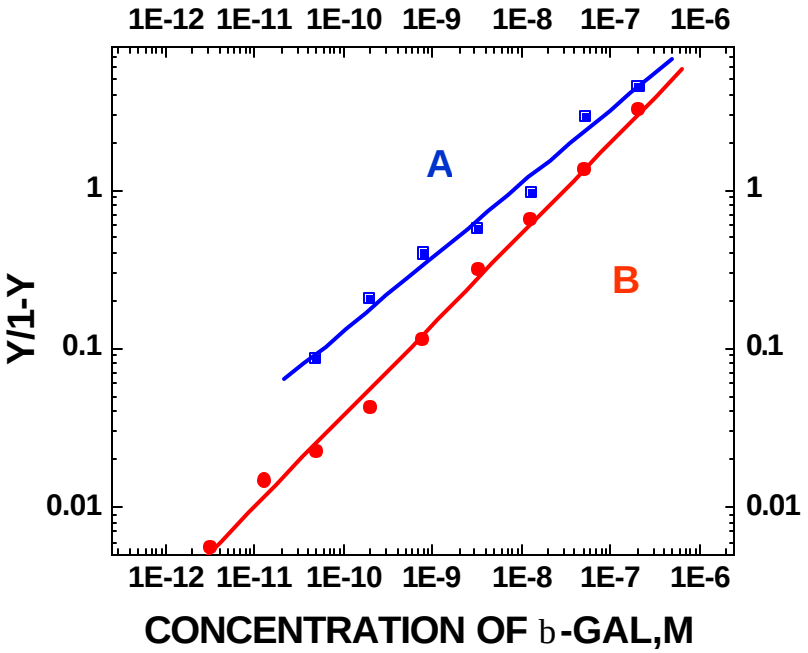

Fig 6.2: Hill plots of binding isotherms showing the ratio of occupied and free phages as a function of ß-galactosidase concentrations. The upper straight line (A) is the linear least squares fit to the TSM sensor data (R=0.99, slope=0.47±0.02). The bottom straight line (B) is the linear least squares fit to the ELISA data (R=0.99, slope=0.57±0.01).

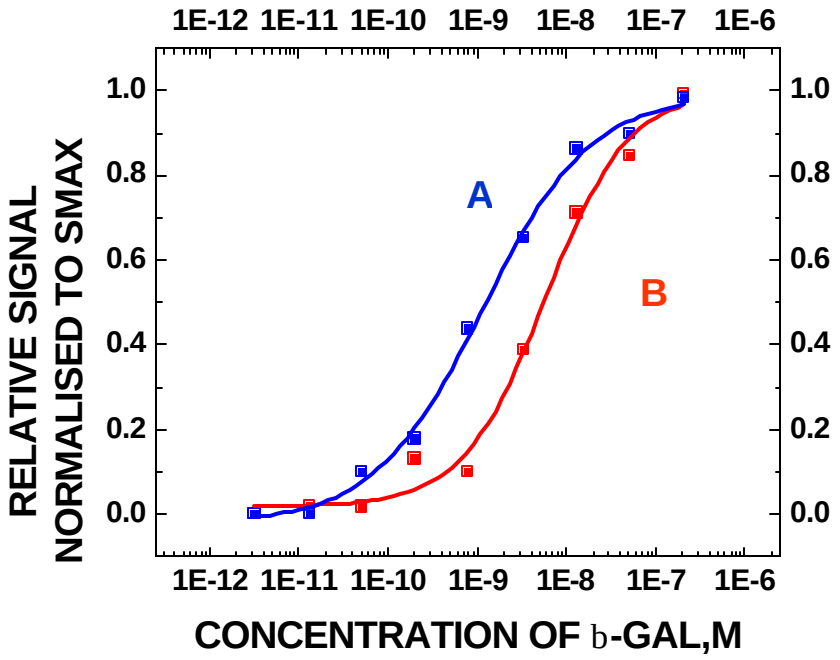

Fig 6.3 : Dose response plots from SPR and TSM sensor experiments are shown. Curve A represents the mean values of steady state refractive indices change as a function of increasing concentrations of ß-gal obtained from an SPR sensor. The signals were normalized at the maximal refractive index change of 3.6×10^{-5}. The smooth curve is the sigmoid fit to the experimental data (- $?^2=8.2 \times 10^{-4}$, $R^2=0.99$). Curve B represents the mean values of steady-state output voltages as a function of increasing concentrations of ß-gal obtained from a TSM sensor. The smooth curve is the sigmoid fit to the experimental data (- $?^2=2.3 \times 10^{-3}$, $R^2=0.99$). The signals were normalized at the maximal voltage change of 0.43 Volts.

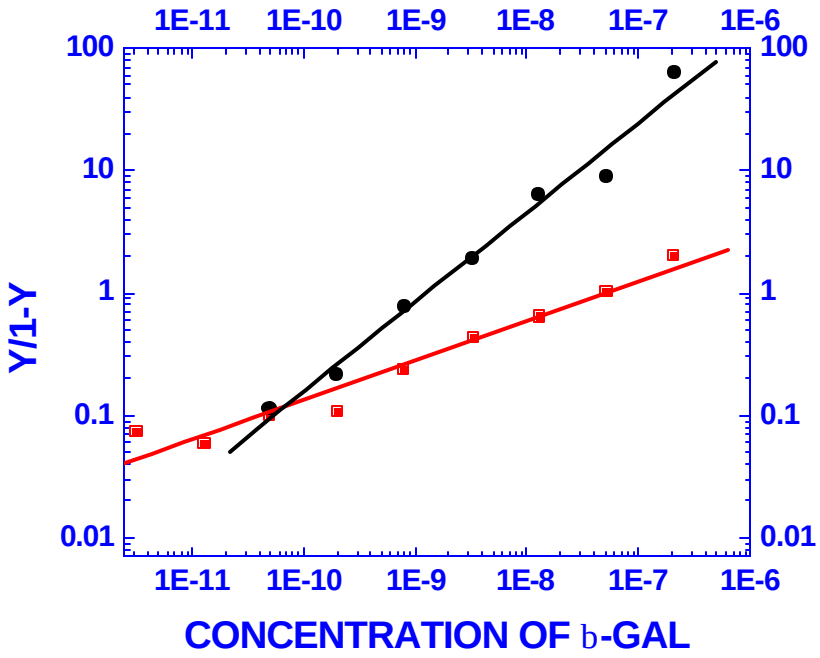

Fig 6.4: Hill plots of binding isotherms showing the ratio of occupied and free phages as a function of ß-galactosidase concentrations. The ratio of occupied and free phages is shown as a function of ß –gal concentrations. The upper straight line is the linear least squares fit to the SPR sensor data (R=0.99, slope=0.73±0.03). The bottom straight line is the linear least squares fit to the TSM sensor data (R=0.98, slope =0.32 ±0.03).

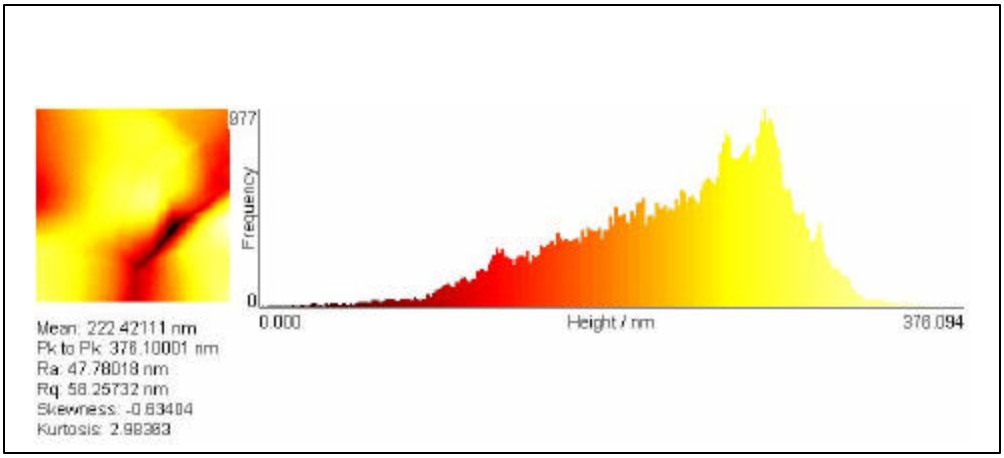

Fig 6.5a (I): The figure on the left shows the surface topography of the scanned area (3×1.5 µm) and the surface roughness (R_q= 58.25 nm) of a TSM sensor before it goes through the cleaning processes as described in *materials and methods.* The figure on the right shows us the frequency of distribution of the heights of the scanned area with a P_k to P_k value of 376 nm.

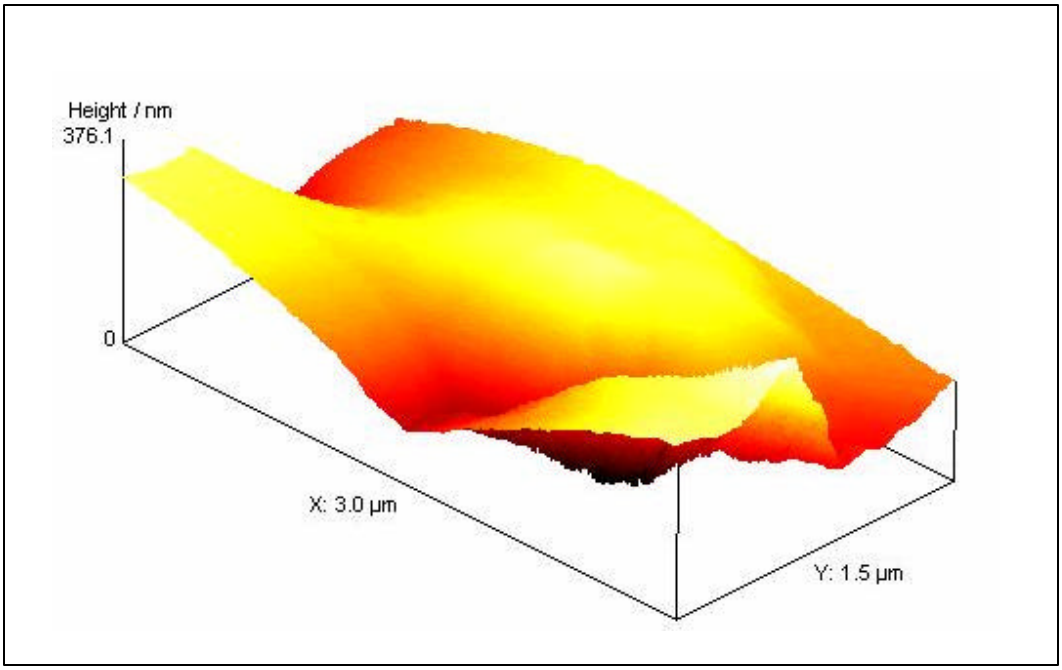

Fig 6.5 a (II): The figure shows the three dimensional features in X, Y and Z directions of the scanned area (3×1.5 µm) and the mean height in nm of a typical surface of a TSM sensor before it goes through the cleaning processes as described in *materials and methods.*

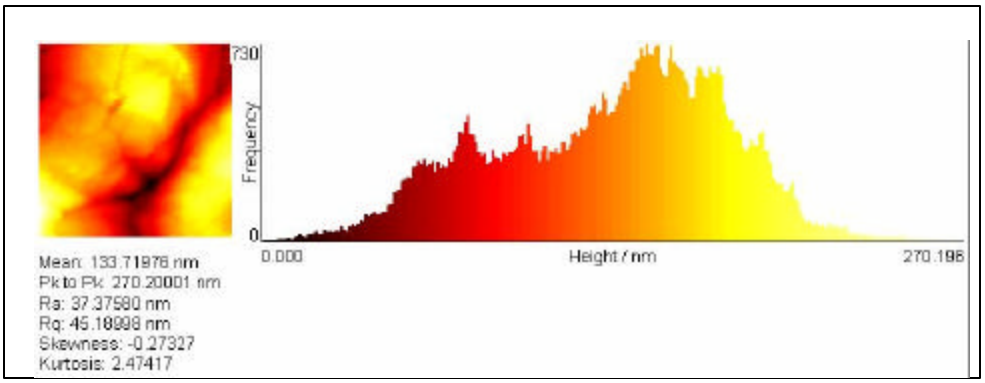

Fig 6.5b (I): The figure on the left shows the surface topography of the scanned area (3×1.5µm) and the surface roughness (R_q=45.2) typical surface of a TSM sensor after it goes through the cleaning processes as described in *materials and methods* with a P_k to P_k value of 270nm. The figure on the right shows us the frequency of distribution of the heights of the scanned area.

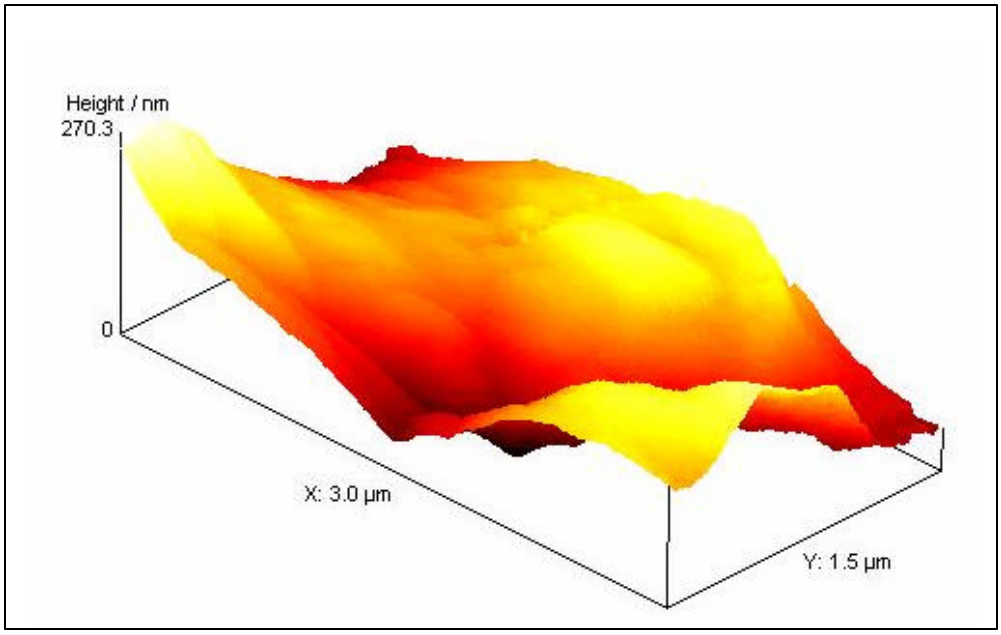

Fig 6.5b (II): The figure shows the three dimensional features in X, Y and Z directions of the scanned area (3×1.5µm) and the mean height in nm of a typical surface of a TSM sensor after it goes through the cleaning processes as described in *materials and methods.*

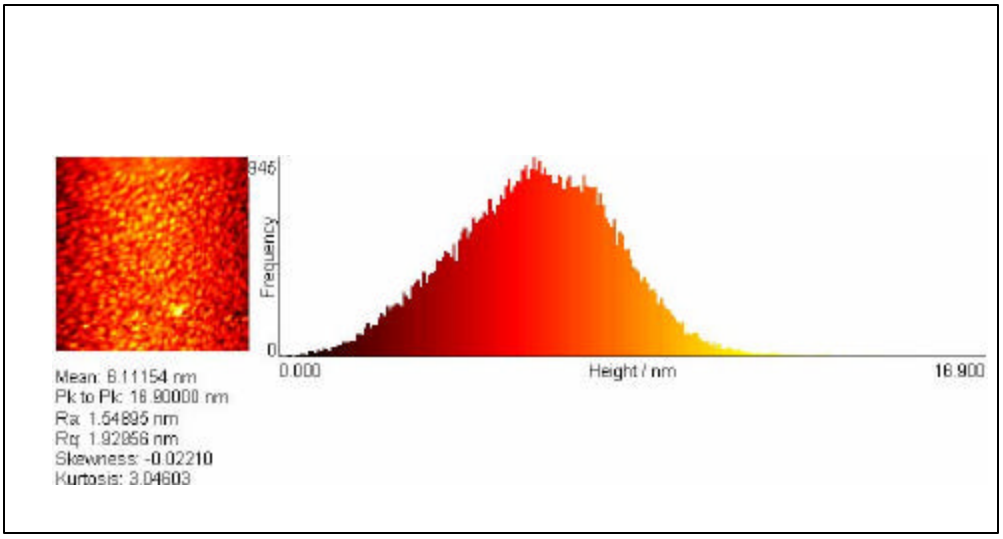

Fig 6.6a (I): The figure on the left shows the surface topography of the scanned area (3×1.5 µm) and the surface roughness (R_q= 1.9 nm) of an SPR sensor before it goes through the cleaning processes as described in *materials and methods.* The figure on the right shows us the frequency of distribution of the heights of the scanned area with a P_k to P_k value of 16.9 nm.

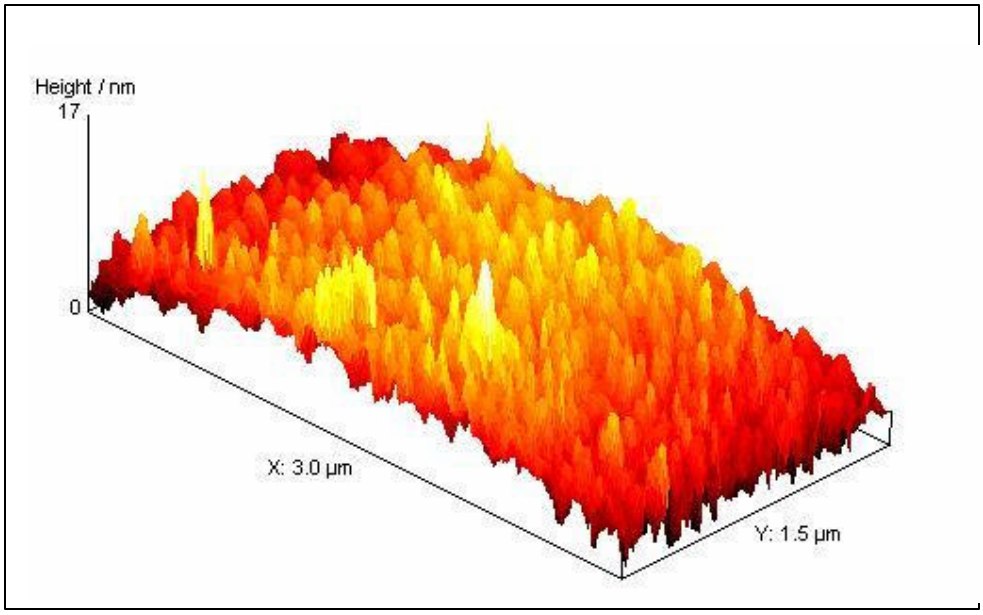

Fig6.6a (II): The figure shows the three dimensional features in X, Y and Z directions of the scanned area (3×1.5µm) and the mean height in nm of a typical surface of an SPR sensor before it goes through the cleaning processes as described in *materials and methods.*

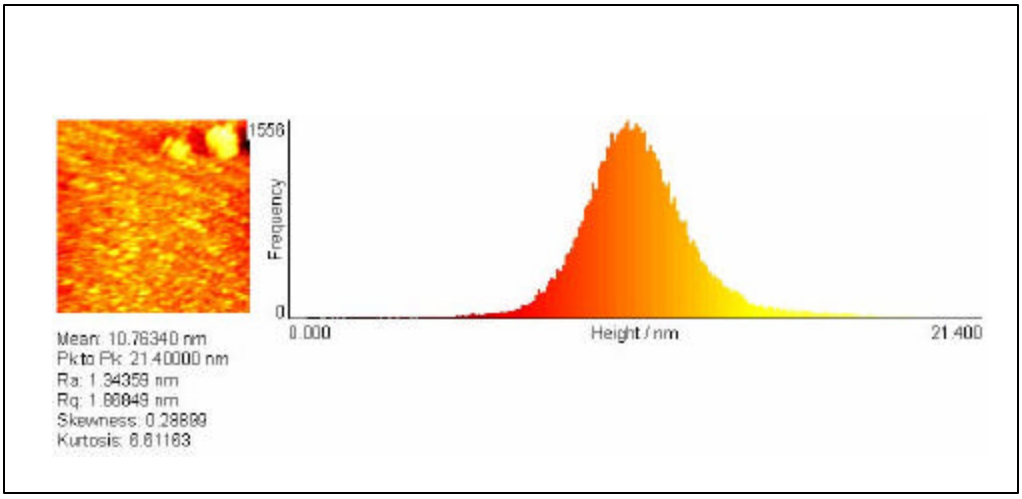

Fig 6.6b (I): The figure on the left shows the surface topography of the scanned area (3×1.5 µm) and the surface roughness ($R_{q=}$1.86) typical surface of a SPR sensor after it goes through the cleaning processes as described in *materials and methods* with a P_k to P_k value of 21nm. The figure on the right shows us the frequency of distribution of the heights of the scanned area.

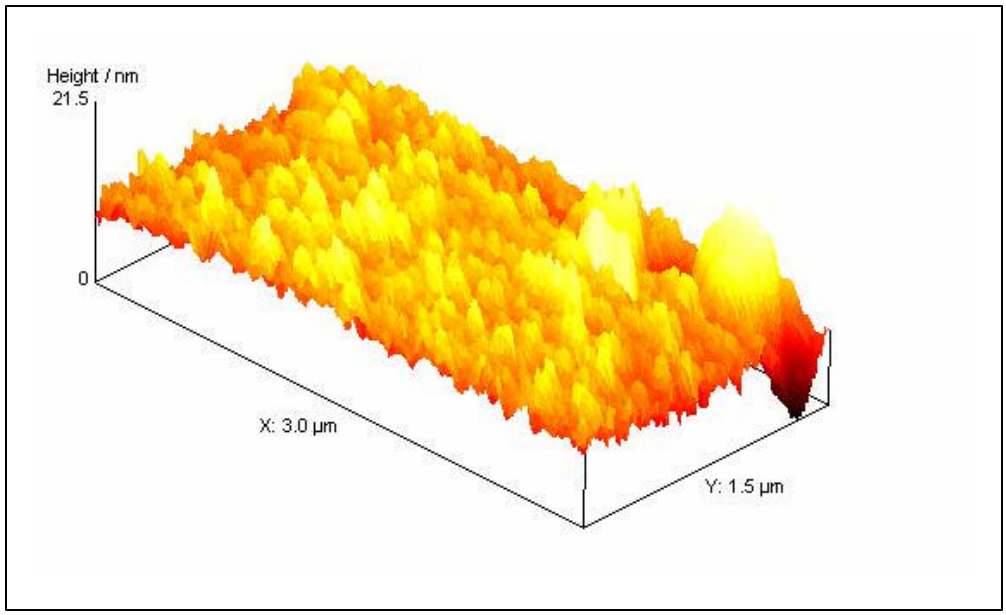

Fig 6.6b (II): The figure shows the three dimensional features in X, Y and Z directions of the scanned area (3×1.5µm) and the mean height in nm of a typical surface of a SPR sensor after it goes through the cleaning processes as described in *materials and methods.*

Sample type	R_q (nm)
TSM control	45.9
TSM treated	31.2
SPR control	2.1
SPR treated	1.7

Table 6 T.1: The above table shows the mean surface roughness (R_q) values of the scanned surfaces of the control and treated TSM and SPR sensors respectively. The mean values were obtained from six repeats of each of the categories shown above.

Method	EC_{50} nM	Hill Coefficient	K_d, nM	t , min
TSM SENSOR	5.8 ±1.4	0.32± 0.03	1.7 ±0.5	22
SPR SENSOR	1.2 ± 0.2	0.73± 0.05	1.1 ±0.2	45

Table 6 T.2: The above table shows the EC_{50} and effective K_d in nM; Hill Coefficient obtained from binding isotherms using the Hill plot and the time constants (t) of signal responses obtained from each of the categories

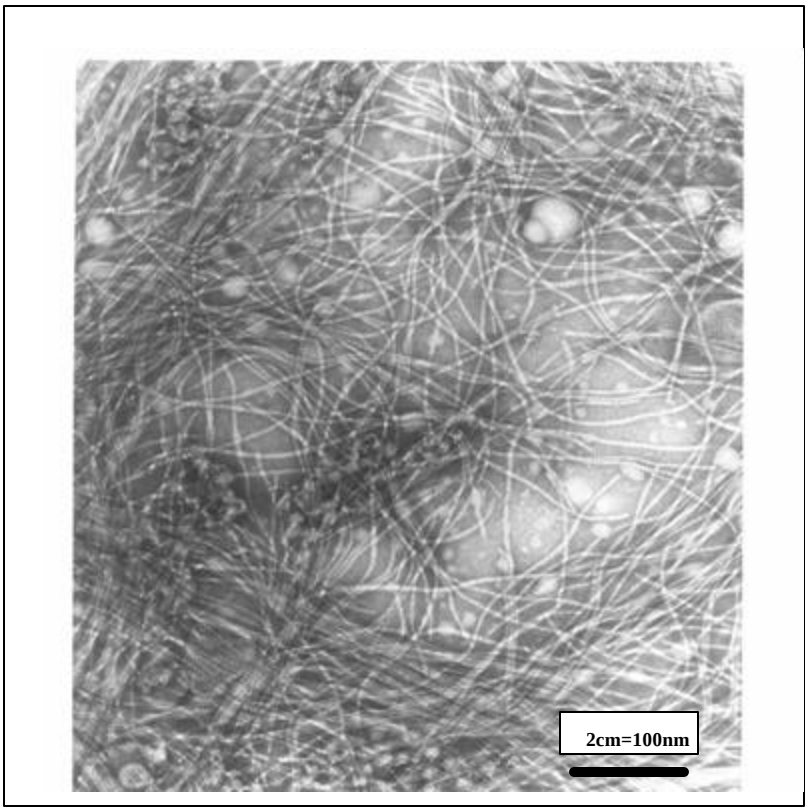

Fig 6.7a: TEM image of the phage 1G40 on a formvar, carbon coated grid of 300 mesh size using a wetting agent (0.1% BSA). The phage particles have aggregated as bundles on the gridwhich maybe due to the effect of the wetting agent used.

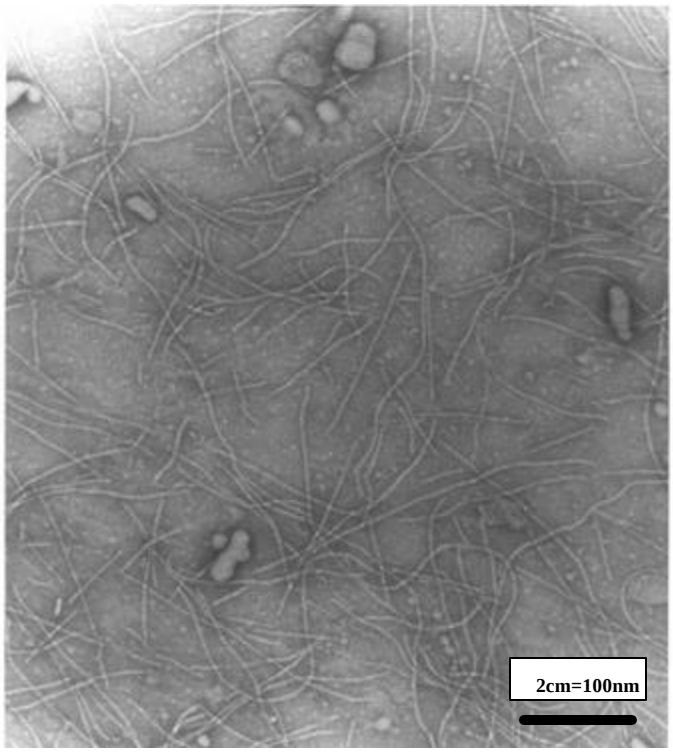

Fig 6.7b: TEM image of the phage 1G40 on a formvar, carbon coated grid of 300 mesh size using no wetting agent (0.1% BSA). The phage particles are more evenly spread out on the grid.

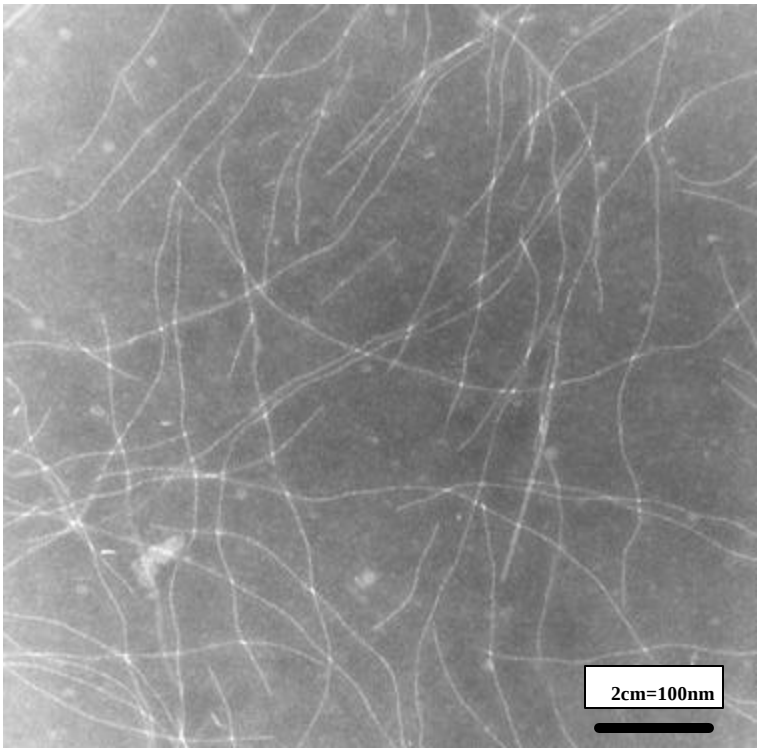

Fig 6.8: TEM image of the phage 1G40 on a gold gilded carbon coated grids using no wetting agent. The surface of the grid was treated with a fine spray of Millipore water to enhance the adhesion of phage particles on the grid prior to bulk loading of phage solution as described in *materials and methods.*

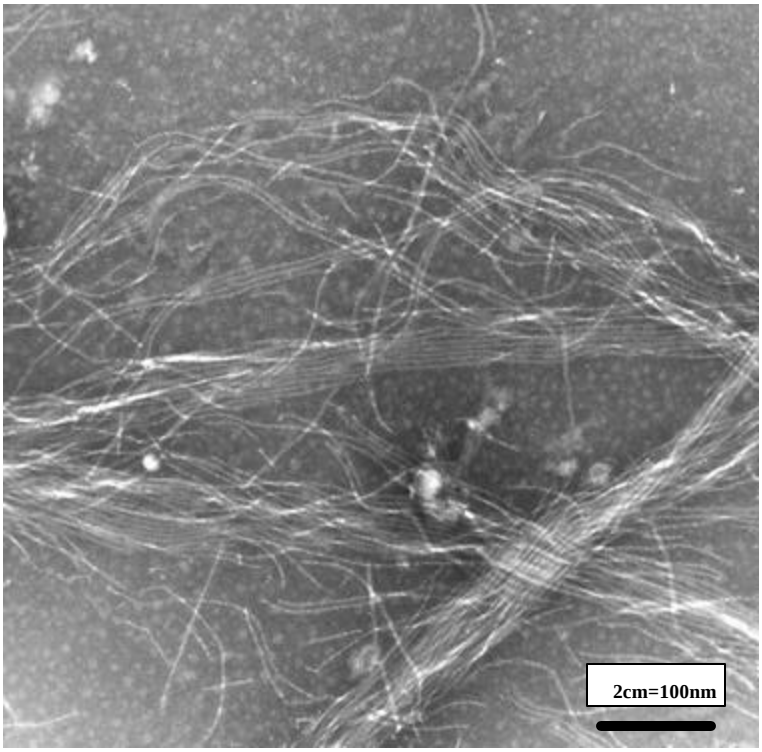

Fig 6.9: TEM image of the phage 1G40 on a formvar, carbon coated copper grids using no wetting agent. The surface of the grid was treated with a fine spray of Millipore water to enhance the adhesion of phage particles on the grid prior to bulk loading of phage solution as described in *materials and methods.* The phage solution used in this sample was diluted from the parent stock in Millipore water.

8. References

1. Petrenko, V. A., V, Vitaly J., *Phage display for detection of biological threat agents.* Journal of Microbiological Methods, 2003. **53**(2): p. 253-262.
2. V. Nanduri, A.Samoylov., V.Petrenko, V. Vodyanoy, A.L.Simonian, *Comparison of optical and acoustic wave phage biosensors.* 206th Meeting of The Electrochemical Society, 2004.
3. Petrenko, V.A., Smith., *Phages from landscape libraries as substitute antibodies.* Protein Eng., 2000. **13**(8): p. 589-592.
4. Romanov, V.I., Durand, D.B.,Petrenko, V.A.,, *Phage display selection of peptides that affect prostate carcinoma cells attachment and invasion.* Prostate, 2001. **47**: p. 239-251.
5. Petrenko, V.A., Smith, G.P.,Mazooji, M.M.,Quinn, T., *{alpha}-Helically constrained phage display library.* Protein Eng., 2002. **15**(11): p. 943-950.
6. Samoylova, T.I., Petrenko, V.A., Morrison, N.E., Globa, L.P., Bekker, H.J.,Cox, N.R.,, *Phage Probes for Molecular Profiling of Malignant Glioma Cells.* Molecular Cancer Pharmaceuticals, 2003. **2**: p. 1-9.
7. Bunde, R.L.J., Eric J. Rosentreter, Jeffrey J., *Piezoelectric quartz crystal biosensors.* Talanta, 1998. **46**(6): p. 1223-1236.
8. Cavicacute, B.A., Hayward, G.L., Thompson, M.,, *Acoustic waves and the study of biochemical macromolecules and cells at the sensor-liquid interface.* Analyst, 1999. **124**: p. 1405- 1420.

9. Pathirana, S.T., Barbaree, J.,Chin, B. A.,Hartell, M. G.,Neely, W. C.,Vodyanoy, V., *Rapid and sensitive biosensor for Salmonella.* Biosensors and Bioelectronics, 2000. **15**(3-4): p. 135-141.

10. Samoylov, A.M., Samoylova, Tatiana I.,Hartell, Mark G.,Pathirana, Suram T.,Smith, Bruce F.,Vodyanoy, Vitaly, *Recognition of cell-specific binding of phage display derived peptides using an acoustic wave sensor*. Biomolecular Engineering, 2002. **18**(6): p. 269-272.

11. Samoylova, T.I., Ahmed, Bushra Y.,Vodyanoy, Vitaly.,Morrison, Nancy E.,Samoylov, Alexandre M.,Globa, Ludmila P.,Baker, Henry J.,Cox, Nancy R., *Targeting peptides for microglia identified via phage display.* Journal of Neuroimmunology, 2002. **127**(1-2): p. 13-21.

12. Olsen, E.V., Pathirana, S. T.,Samoylov, A. M.,Barbaree, J. M.,Chin, B. A.,Neely, W. C.,Vodyanoy, V., *Specific and selective biosensor for Salmonella and its detection in the environment*. Journal of Microbiological Methods, 2003. **53**(2): p. 273-285.

13. Muramatsu, H., Kajiwara, K.,Tamiya, E.,Karube, I., *Piezoelectric immuno sensor for the detection of candida albicans microbes.* Analytica Chimica Acta, 1986. **188**: p. 257-261.

14. Green R.J., Frazier.A. R.., Shakesheff K.M., Davies M.C., Roberts C.J., Tendler S.J.B., *Surface plasmon resonance analysis of dynamic biological interactions with biomaterials.* Biomaterials, 2000. **21**: p. 1823-1835.

15. Spangler, B.D., Wilkinson, Elisabeth A.,Murphy, Jesse T. and Tyler, Bonnie J., *Comparison of the Spreeta(R) surface plasmon resonance sensor and a quartz*

crystal microbalance for detection of Escherichia coli heat-labile enterotoxin. Analytica Chimica Acta, 2001. **444**(1): p. 149-161.

16. Laricchia-Robbio, L. and R.P. Revoltella, *Comparison between the surface plasmon resonance (SPR) and the quartz crystal microbalance (QCM) method in a structural analysis of human endothelin-1*. Biosensors and Bioelectronics, 2004. **19**(12): p. 1753-1758.
17. Aleksandr L. Simonian, A.R., Jamers R. Wild, Jerry Elkind and Michael V. Pishko, *Characterization of oxidoreductase-redox polymer electrostatic film assembly on gtold by surface plasmon resonance spectroscopy and Fourier transform infrared -external reflection spectroscopy*. Analytica Chimica Acta, 2002. **466**: p. 201-212.
18. Alexei N. Naimushin, Charles B. Spinelli., Scott D. Soelberg, Tobias Mann, Richard C. Stevens, Timothy Chinowsky, Peter Kauffman, Sinclair Yee and Clement E. Furlong, *Airborne analyte detection with an aircraft-adapted surface plasmon resonance sensor system.* Sensors and Actuators B: Chemical, 2005. **104**(2): p. 237-248.
19. Carter, R.M., Mekalanos, J.J., Jacobs, M.B., Lubrano, G.J. & Guilbault, G.G., *Quartz crystal microbalance detection of Vibrio cholerae O139 serotype*. Journal of Immunological Methods, 1995. **187**: p. 121-125.
20. Uttenthaler, E., C. Ko[ss]linger, and S. Drost, *Characterization of immobilization methods for African swine fever virus protein and antibodies with a piezoelectric immunosensor*. Biosensors and Bioelectronics, 1998. **13**(12): p. 1279-1286.

21. Minunni, M., Skladal, P. & Mascini, M., *A Piezoelectric Quartz-Crystal Biosensor as a Direct Affinity Sensor*. Analytical Letters, 1994. **27**: p. 1475-1487.

22. Horisberger, M., Vauthey, M., *Labeling of colloidal gold with protein.* Histochemistry, 1984. **80**: p. 13-18.

23. Vikinge, Trine P.,Hansson, Kenny M.,Sandstrom, Par.,Liedberg, Bo.,Lindahl, Tomas L.,Lundstrom, Ingemar.,Tengvall, Pentti.,Hook, Fredrik., *Comparison of surface plasmon resonance and quartz crystal microbalance in the study of whole blood and plasma coagulation.* Biosensors and Bioelectronics, 2000. **15**(11-12): p. 605-613.

24. Su, Xiaodi.,Wu, Ying-Ju., Knoll, Wolfgang., *Comparison of surface plasmon resonance spectroscopy and quartz crystal microbalance techniques for studying DNA assembly and hybridization.* Biosensors and Bioelectronics, 2005. **In Press, Corrected Proof**.

25. Piehler, J., Brecht, Andreas., Geckeler, Kurt E., Gauglitz, Gunter, *Surface modification for direct immunoprobes.* Biosensors and Bioelectronics, 1996. **11**(6-7): p. 579-590.

26. Polzius, R., Schneider, Th.,Biert, F. F.,Bilitewski, U.,Koschinski, W., *Optimization of biosensing using grating couplers: immobilization on tantalum oxide waveguides.* Biosensors and Bioelectronics, 1996. **11**(5): p. 503-514.

27. Johnson, J.C., Nettikadan, Saju R.,Vengasandra, Srikanth G.,Henderson, Eric, *Analysis of solid-phase immobilized antibodies by atomic force microscopy*. Journal of Biochemical and Biophysical Methods, 2004. **59**(2): p. 167-180.

28. Yu, J., Smith, G.P., *Affinity maturation of phage-displayed peptide ligands.* Methods in Enzymology, 1996(267): p. 3-27.

29. Samoylov, A.M., Samoylova, T. I. Pathirana, S. T. Globa L. P. and Vodyanoy V.J., *Peptide biosensor for recognition of cross-species cell surface markers.* Journal of Molecular Recognition, 2002. **15**: p. 197-203.

30. Naimushin, Alexei., N.Soelberg., Scott D.Nguyen., Di K.Dunlap., Lucinda Bartholomew., Dwight Elkind., Jerry Melendez., Jose and Furlong, Clement E., *Detection of Staphylococcus aureus enterotoxin B at femtomolar levels with a miniature integrated two-channel surface plasmon resonance (SPR) sensor.* Biosensors and Bioelectronics, 2002. **17**(6-7): p. 573-584.

7. CONCLUSIONS

This research was conducted in order to study the binding properties of the probe-analyte system that could later, facilitate the development of sensitive, specific and a rapid biosensor. This research also established the use of a filamentous phage as a probe in a biosensor using a simple method of immobilization viz., ***physical adsorption.*** The direct physical adsorption of the phage to the surface is a very simple method of a phage immobilization on the sensor surface.

Results obtained from this research showed the validity of the selected probe to the target antigen, ß -galactosidase through ELISA. Binding studies indicate that ELISA is useful, in establishing preliminary protocols for selection and characterization of probe-analyte that needs to be tested. Specificity and selectivity of the phage binding ß-galactosidase were also determined. The dissociation constant of 30± 0.6 nM and an affinity valency of 0.86±0.01 SD were determined from ELISA.

The conditions for binding of the selected probe on the gold platform of the TSM sensor through ***physical adsorption*** were defined and the binding parameters such as K_d and valency of binding were determined. It appeared that careful preparing and multiple washing and cleaning of a sensor surfaces before deposition of the phage were very important for preparation of a successful sensor. Atomic force photographs showed strong effects of chemical treatment on the sensor surface topography. The specificity

and selectivity of the selected probe were determined for the gold platform of the TSM sensor. Binding of the phage to β-galactosidase on the sensor surface was very selective and specific. The dissociation constant calculated for the acoustic wave was 1.7 ± 0.5 nM. The apparent value of the dissociation constant of the interaction of free phage with β-galactosidase was found to be 9.1±0.9 pM). These results show that physical adsorption of landscape phage to sensor surface may produce a sensor that compares well with the one made by Langmuir-Blodgett technique. The method of physical adsorption is simple and economical. The sensor demonstrates high affinity, selectivity, and specificity.

The binding conditions for the probe-analyte interaction on a SPR platform were also carried out and the selectivity and specificity of the probe to ß-galactosidase was also determined using the SPR platform. The binding parameters using both batch and flow through mode were also concluded. Also, the binding parameters obtained from the three platforms viz., ELISA, TSM and SPR sensors were compared. Dynamic range, detection limit, EC_{50}, Hill coefficient, apparent dissociation constant, and time constant for TSM sensors were found to be respectively: 0.0032-210 nM, ~13 pM, 5.8±1.4 nM, 0.32±0.03, 1.7±0.5 nM, and 22 min. The same parameters for SPR sensor were found to be quite similar and they are respectively as following: 0.0032-210 nM, ~13 pM, 1.2±0.2 nM, 0.73±0.05, 1.1±0.2 nM, and 45 min.

The influence of the cleaning processes on the topographical changes of the gold surfaces of both TSM and SPR sensors were investigated using AFM. We found that the original roughness of the gold surfaces of TSM sensors (R_q=45.9) is much larger than one for SPR sensors (R_q=2.1). We found also that for both devices a cleaning process

significantly reduced a roughness of the surfaces (32% and 20% reduction for TSM and SPR respectively).

The visualization of the phage 1G40 on formavar/Cu grids was carried out by using a TEM. We found that the phage particles have aggregated as bundles on the grid when the wetting agent (0.1% BSA) for pre-treating of the microscopic grids. We found also that pretreatment of grids with Millipore water enhances the adhesion of the phage particles and prevents their aggregation.

Results obtained from the TSM sensor platform showed that the binding dose-response curve had a typical sigmoid shape and the signal was saturated at the β-galactosidase concentration of about 200 nM. The ELISA dose-response curve looked similar but it is shifted towards higher concentration of β-galactosidase by ~6 nM and becomes steeper. The difference in affinities between ELISA and TSM sensors can be attributed to the monovalent (in ELISA) and multivalent (in sensor) interaction of the phage with β-galactosidase, as indicated by Hill plots. One or another mode of interaction probably depends on the conformational freedom of the phage immobilized to the solid surface. Binding of the phage to β-galactosidase on the sensor surface was very selective, because presence of 360-fold excess of bovine serum albumin in mixture with β-galactosidase reduces the biosensor signal only by 2%. Binding of the immobilized phage to β-galactosidase is quite specific because the biosensor response is reduced in dose-dependent manner if β-galactosidase is incubated with free phage prior to the exposure. The response is reduced by 65% if β-galactosidase is pre-incubated with 2.2×10^{11} vir/ml of free phage. The apparent value of the dissociation constant of the interaction of free

phage with β-galactosidase obtained from the linear fit has appeared to be smaller compared with the one calculated for the bound phage. The difference could be explained by the higher degree of freedom and accessibility of free phage compared to one bound to the sensor surface.

Surface Plasmon Resonance studies also establish that phage can be used as the sensing layer for the specific and sensitive detection of ß-gal. Employing the flow through mode gives us a sensor of higher sensitivity in comparison to that obtained through batch mode studies. On the other hand, the binding valences however, were higher in the batch mode studies as opposed to the flow through mode. This was possibly due to divalent interaction of phage-ß-gal which could be as a result of

d) The thin nature of the phage adlayer which could in turn, increase the flexibility of the phage layer making more binding sites available to ß-gal
e) Due to the stabilization of the phage layer prior to being interacted with ß-gal
f) Or the combination of both the above factors.

Experiments conducted showed that phage could be used as sensitive probe to specified target analyte for effective detection in the picomolar range. Binding studies indicate that although ELISA is useful, in establishing preliminary protocols for selection and characterization of probe-analyte that needs to be tested; sensitive and effective detection is achieved using both the TSM and SPR sensor platforms. The sensitivity of both SPR and QCM sensor show similarities. Although commercially available compact TSM sensor variations allow effective deployment in the field, the SPREETA™ SPR sensor is more compact and versatile than the TSM sensor.